

Functional and kinetic characterization of the human post-proline cleaving enzyme
prolyl oligopeptidase

Dissertation
for the obtainment of the academic degree of
doctor rerum naturalium (Dr. rer. nat)

Submitted to the

Faculty of Natural Sciences I
-department of Biochemistry/Biotechnology-
of the Martin-Luther-Universität Halle-Wittenberg

by the graduated in biochemistry Mr. David Ruiz Carrillo
Born the 17th of May of 1974 in Figueres (Spain)



Referees:

- 1.- Prof. Dr. Milton T. Stubbs (University Martin-Luther Halle-Wittenberg)
- 2.- Prof. Dr. Hans U. Demuth (Hochschule Koethen)
- 3.- Prof. Dr. Dietmar Schomburg (Technical University of Braunschweig)

Halle an der Saale on June 30th. 2009

a mis amados padres
(to my beloved parents)

1.0 Introduction.....	1
1.1 Aim of the work.....	1
1.2 The amino acid proline.....	1
1.3 The amino acid proline and its influence on the structure of proteins.....	2
1.3.1 The amino acid proline and its importance on protein secondary structure... 2	2
1.4 The amino acid proline and its relevance on the function of proteins.....	3
1.5 The proteases cleaving proline-containing peptides.....	5
1.6 Prolyl oligopeptidase.....	5
1.7 Prolyl oligopeptidase closely related enzymes.....	6
1.8 Prolyl oligopeptidase gene, PREP.....	7
1.9 Human tissue distribution of prolyl oligopeptidase.....	7
1.10 Prolyl oligopeptidase brain distribution.....	7
1.11 Subcellular localization of prolyl oligopeptidase.....	8
1.12 Prolyl oligopeptidase tertiary structure.....	9
1.13 Substrate selectivity of prolyl oligopeptidase.....	11
1.14 Prolyl oligopeptidase catalytic mechanism.....	11
1.15 Kinetic characterization of prolyl oligopeptidase.....	15
1.16 Biological relevance of prolyl oligopeptidase.....	16
1.17 Prolyl oligopeptidase inhibitors.....	19
2.0 Materials and methods.....	23
2.1 Cloning of the human prolyl oligopeptidase coding sequence.....	23
2.2 Site directed mutagenesis.....	26
2.3 Expression of the recombinant human prolyl oligopeptidase.....	26
2.4 Purification of the recombinant human prolyl oligopeptidase.....	27
2.5 Dialysis and ultrafiltrations.....	29
2.6 Protein content determination.....	30
2.7 Enzymatic activity measurement.....	30
2.7.1 Kinetic measurements.....	31
2.7.2 Michaelis-Menten constant, K_m	32
2.7.3 Turnover constant, k_{cat}	32
2.7.4 Specificity constant, k_{cat}/K_m	33
2.7.5 Inhibition constant, K_i	33
2.7.6 IC_{50} constant.....	34
2.7.7 Slow-tight binding Inhibition.....	34
2.7.8 Rate constants temperature dependence. Arrhenius and Eyring plots.....	35
2.8 Mass spectrometry.....	36
2.9 SDS-PAGE.....	37
2.10 pH dependence of rate constants.....	38
3.0 Results.....	39
3.1.0 Prolyl oligopeptidase. cloning, expression and purification.....	39
3.1.1 Prolyl oligopeptidase cloning.....	39
3.1.2 Prolyl oligopeptidase expression.....	39
3.1.3 Prolyl oligopeptidase purification.....	41
3.2 Recombinant human prolyl oligopeptidase kinetic characterization.....	43
3.2.1 Wild type recombinant prolyl oligopeptidase catalyzed hydrolysis of AMC derivatives.....	43
3.2.2 Wild type recombinant prolyl oligopeptidase catalyzed hydrolysis of FRET derivatives.....	44
3.2.3 Temperature and pH dependencies of prolyl oligopeptidase catalyzed substrate hydrolysis.....	45
3.3.0 Recombinant human prolyl oligopeptidase arginine 643 variants.....	47
3.3.1 Recombinant human prolyl oligopeptidase alanine 643 variant.....	48
3.3.2 Recombinant human prolyl oligopeptidase lysine 643 variant.....	49
3.4.0 Recombinant human prolyl oligopeptidase tryptophan 595 variants.....	50
3.4.1 Recombinant human prolyl oligopeptidase alanine 595 variant.....	50

Index

3.4.2 Recombinant human prolyl oligopeptidase phenylalanine 595 variant.....	51
3.4.3 Recombinant human prolyl oligopeptidase tyrosine 595 variant.....	52
3.5.0 Recombinant human prolyl oligopeptidase phenylalanine 173 variant.....	53
3.5.1 Recombinant human prolyl oligopeptidase alanine 173 variant.....	53
3.6.0 Recombinant human prolyl oligopeptidase methionine 235 variants.....	53
3.6.1 Recombinant human prolyl oligopeptidase alanine 235 variant.....	54
3.6.2 Recombinant human prolyl oligopeptidase isoleucine 235 variant.....	54
3.7.0 Recombinant human prolyl oligopeptidase cysteine 255 variant.....	55
3.7.1 Recombinant human alanine 255 prolyl oligopeptidase variant.....	55
3.8.0 Characterization of prolyl oligopeptidase inhibitors.....	56
3.8.1 Slow-tight binding ammonium methyl ketone inhibitor.....	56
3.8.2 Competitive irreversible heteroarylketone inhibitor.....	57
3.8.3 Competitive diketone inhibitor.....	57
3.8.4 Inhibitors derivatization.....	58
3.8.4.1 Ammonium methyl ketones inhibitor derivatization.....	58
3.8.4.2 Heteroaryl ketones inhibitor derivatization.....	59
3.8.4.3 Diketones inhibitor derivatization.....	60
3.8.4.4 Slow-tight binding inhibitors, k_{on} and k_{off} rate constants characterization.....	61
3.9.0 MALDI-TOF-MS characterization of the prolyl oligopeptidase activity.....	61
4.0 Discussion.....	68
4.1 Expression and purification of the recombinant human prolyl oligopeptidase variants.....	68
4.2 Recombinant wild type prolyl oligopeptidase.....	69
4.3 Recombinant human prolyl oligopeptidase Arg ⁶⁴³ variants.....	78
4.4 Recombinant human prolyl oligopeptidase Trp ⁵⁹⁵ variants.....	80
4.5 Recombinant human prolyl oligopeptidase Phe ¹⁷³ variant.....	82
4.6 Recombinant human prolyl oligopeptidase Met ²³⁵ variants.....	83
4.7 Recombinant human prolyl oligopeptidase Cys ²⁵⁵ variant.....	84
4.7 Inhibitors binding pattern.....	86
4.8 Inhibitors derivatization.....	88
4.9 Slow-tight binding inhibitors characterization.....	91
4.10 MALDI-TOF-MS characterization of prolyl oligopeptidase hydrolysis pattern...	93
4.11 Summary (Zusammenfassung).....	99
5.0 References.....	102
6.0 Appendix.....	116
6.1 Buffers and mediums.....	116
6.1.1 Cloning.....	116
6.1.2 E. Coli expression.....	116
6.1.3 Activity measurements.....	116
6.1.4 Substrates and Inhibitors.....	116
6.1.5 Protein purification.....	117
6.1.6 Protein characterization.....	117
6.1.7 MALDI-TOF-MS.....	117
6.2 Mathematical equations.....	118
6.3 Chemicals.....	120
6.4 Vectors.....	120
6.5 Chromatograms of the prolyl oligopeptidase purification.....	121
6.6 List of oligoprimers.....	122
6.7 Molecular structure of the ammonium methyl ketone analogue molecules.....	123
6.8 Molecular structure of the heteroaryl ketone analogue molecules.....	124
6.9 Molecular structure of the diketone analogue molecules.....	125
6.10 Miscellaneous.....	126

Abbreviations

	Miscellaneous
AMC	7-amido-methylcoumarin
AMK	ammonium methyl ketone
APS	ammonium persulfate
bp	basepair
BRIJ	polyoxyethyleneglycol dodecyl ether detergent
BSA	bovine serum albumina
BT	benzothiazole
cDNA	complementary Deoxy Ribonucleic Acid
Dabcyl	4-(4dimethylaminophenyl-azo)benzoyl
DFP	diisopropylfluorophosphate
DK	diketone
DNA	desoxyribonucleic acid
DMSO	dimethyl sulfoxide
dNTP	desoxyribonucleosidetriphosphate
DTT	dithiothreitol
E. coli	<i>Escherichia coli</i>
EC	enzyme number
Edans	5-[(2-Aminoethyl)amino]naphtalene-1-sulfonic acid
EDTA	ethylenediaminetetraacetic acid
FPLC	fast performance liquid chromatography
FRET	fluorescence resonance energy transfer
GnrH	gonadotropin-releasing hormone
GSP	gene especific primers
H ₂ O	water
HAK	heteroaryl ketone
Hepes	4-(2-hydroxyethyl)-1-piperazineethanesulfonic acid
His _{x6}	hexahistidine tag
HN	humanin peptide
IMAC	immobilized metal affinity chromatography
IP	inositol phosphate
IP ₃	inositol triphosphate
IP ₅	inositol pentaphosphate
IPTG	isopropyl-β-D-thiogalactopyranosid
IUBMB	international union of biochemistry and molecular biology
kbp	kilobasepair
k _{cat}	turnover rate constant
k _{cat} /K _m	specificity constant
K _i	inhibitor-enzyme complex dissociation constant
K _m	Michaelis-Menten constant
k _{off}	inhibitor first order rate constant
k _{on}	inhibitor second order rate constant
LB	Luria Bertani medium
m/z	mass/charge ratio
MALDI-TOF-MS	matrix assisted laser desorption-ionization time of flight mass spectrometry
mRNA	messenger ribonucleic acid
N.A.	not available
N.D.	not detected
NAP	NAP peptide
NEB	New england biolabs
OD ₆₀₀	optical density measured at 600nm wave length
P	phenyl sepharose
PAGE	polyacrylamide gel electrophoresis
PCR	polymerase chain reaction

Abbreviations

PDB	protein data bank		
pI	isoelectric point		
PMSF	phenylmethylsulfonyl fluoride		
pNA	4-paranitroaniline		
P _x	substrate residue		
Q	q sepharose		
rATP	ribose adenosine triphosphate		
RFU	relative fluorescence units		
rhPEP	recombinant human prolyl oligopeptidase		
RNA	ribonucleic acid		
RT-PCR	reverse transcriptase polymerase chain reaction		
SDS	sodium dodecyl sulphate		
S _x	Enzyme's active center subsite		
TFA	trifluoroacetic acid		
TRH	thyrotropin-releasing hormone		
Tris	tris(hydroxymethyl)aminomethane		
U	enzymatic activity units		
UV	ultraviolet light		
V _{max}	enzymatic initial maximal velocity		
www	world wide web		
Units			
°C	celsius degree		
Å	angstrom		
cal	calorie		
h	Hour		
kJ	kilojoule		
K	kelvin degree		
kDa	kilodalton		
M	Molarity (mole/liter)		
mg	milligram		
min	minutes		
mol	Mole		
ml	milliliters		
nm	nanometer		
l	liter		
psi	pound force per square inch		
rpm	revolutions per minute		
xg	unit of gravitation force		
φ	phi peptide N-C _α torsion angle		
ψ	psi peptide C _α -CO torsion angle		
Enzymes			
EcoRI	endonuclease		
NdeI	endonuclease		
Pfu	<i>Pyrococcus furiosus</i> polymerase		
SuperScript-RT	<i>Moloney Murine Leukemia Virus</i> reverse transcriptase		
SrfI	endonuclease		
T4	DNA Ligase		
Taq	<i>Thermophilus aquaticus</i> polymerase		
Amino acid names with the three and one letter codes			
Alanine: Ala/A	Glutamine: Gln/Q	Leucine: Leu/L	Serine: Ser/S
Arginine: Arg/R	Glutamic acid:Glu/E	Lysine: Lys/K	Threonine: Thr/T
Asparagine: Asn/N	Glycine: Gly/G	Methionine: Met/M	Tryptophan: Trp/W
Aspartic acid: Asp/D	Histidine: His/H	Phenylalanine:Phe/F	Tyrosine: Tyr/Y
Cysteine: Cys/C	Isoleucine: Ile/I	Proline: Pro/P	Valine: Val/V

1.0 Introduction.

1.1 Aim of the work.

Prolyl oligopeptidase (PEP) has attracted special attention of the scientific community since it was discovered on the early seventies. At first its enzymatic specificity caught the interest of many studies. It appeared to be relevant that the specialization achieved to perform the post-proline cleavage could indicate for this enzyme a key regulatory role. Most of the studies were faced in order to clarify the role of different residues directly implicated on the enzyme catalytic mechanism. Additionally, the correlation of the enzyme inhibition with memory and learning disorders was afterwards confirmed. To this, the attainment of the crystal structure of the enzyme shed the necessary light in order to clarify basic questions of the enzyme specificity, but also it prompted new questions about the relevance of some other non-catalytic residues implicated in the architecture of the enzyme's active site.

The coding sequence of the human PEP was cloned in a bacterial expression system and the heterologous protein could be purified to homogeneity in a soluble form. Herein this scheme was further applied to unveil the relevance of non-catalytic active site related residues, namely Arg⁶⁴³, Trp⁵⁹⁵, Met²³⁵, Cys²⁵⁵ and Phe¹⁷³. The kinetic characterization of the wild type and its active site related variants was accomplished. On the one hand, a full kinetic profiling of the human PEP was achieved. On the other hand, the relevance of the above mentioned non-catalytic residues could be additionally elucidated and justified.

Moreover, little it is yet known about the influence of the substrates P_n' residues over the enzyme catalysis. A MALDI-TOF approach was followed in order to determine whether the lack of well defined electron density maps on existing PEP crystal structures indeed correlates with a catalytic irrelevance of such substrate residues.

Finally, three different inhibitor scaffolds were used to profile the enzyme's active site main features. On the one hand, the enzyme variants inhibition profiling, and on the other hand, a full inhibitor derivatization strategy were implemented in order to characterize the major determinants that are driving the binding of those small molecules to PEP's active center.

1.2 The amino acid proline.

The amino acid proline outstands among the rest of protein building unit-blocks because of its structural features. The propyl side-chain of the proline residue is bound back to the amide nitrogen of the amino acid's amino group, thus generating a secondary amide and the pyrrolidine ring structure. Proline is then the only natural

amino acid with its amino group doubly substituted, and therefore it is rather an imino acid than an amino acid.

The main consequence of this structural particularity is that the phi torsion angle (ϕ), defined for the the N-C α bond, of proline residues in *trans* configuration is seriously restricted to a mean value of $-63^\circ(\pm 15)$ [1]. In addition, the pyrrolidine structure increases the intrinsic probability of adopting the *cis* rather than the *trans* conformation within the preceding peptide bond, between 0.1 and 0.3 [2], while other amino acids are showing a probability around 10^{-3} [3]. These higher probabilities are also supported by the activation energy barrier measured for the *cis/trans* isomerization. This energetic barrier is lower in the case of proline, 13 kcal/mol, compared to other amino acids which show values of 20 kcal/mol [1]. Proline is therefore playing a central role in the structural conformation of proteins and in their underlying functions.

1.3 The amino acid proline and its influence on the structure of proteins.

In peptide chains, studying the influence of prolines over the dihedral angles conformation of their preceding amino acids, one can see how, for example, for alanine the region $-180^\circ < \psi < +60^\circ$ of the Ramachandran plot is completely prohibited when this amino acid is preceding proline [4]. Even glycine shows a significant constriction in its conformational freedom when is preceding proline. Thus, it has been found how the glycine-proline pair forms conformational clusters around the Ramachandran plot region $\psi = 180^\circ \pm 30^\circ$ in the 77% of the studied cases, compared to the only 30% of the glycines that were occupying such region when they were not followed by proline [1].

1.3.1 The amino acid proline and its importance on protein secondary structure.

In spite of such a clear influence of proline over its neighbouring residues in the protein chains, this amino acid has not been particularly restricted to any particular secondary structure. Thus, out of a studied sample with 963 proline residues it was found that about 38% of these residues were placed in loops and in random coils, 26% in helices, predominantly in their amino terminal first turn, 23% in turns and the rest, 13%, in β -strands [1].

Proline has a preferential tendency to be placed within the first amino terminal turn of helices, a fact that can be explained on the basis of the missing amide hydrogen. The initial position in the helices, actually only up to the fourth residue, would exempt proline in such secondary structures from hydrogen bonding requirements [1]. Nevertheless, this residue has been also detected along of helices, where it is often

promoting a “helix kink” characterized by a theta angle, θ , with a mean value of $26(\pm 5)^\circ$ [5].

The behaviour of prolines in the β -sheets was found, otherwise, to be less distinctive as the one observed in helices. In principle, in parallel and in antiparallel β -sheets, proline used to appear frequently between the widely spaced bond pairs, without making any contribution with its carbonyl oxygen to the hydrogen bonding network [1]. It is worth to point out how the β -bulges, that are β -sheet singularities in which two consecutive hydrogen bonds involve two residues in one strand and a single one in the opposed strand, are responsible for the intensification of the strands bending, a role that is able to carry out as well on its own proline [6]. It is as well noticeable how frequently proline residues appear immediately after the carboxy terminus of both main secondary structures, helices and β -Sheets [1].

Finally, one needs to mention the β -turns. The importance of such structures is revealed by the fact that in all proteins an average of the 25% of their residues are involved in β -turns [7]. The most radical assumptions gave to the β -turns a main role in protein folding processes [8], however this issue still remains controversial. Proline, compared to the rest of amino acids, has the fourth-fold higher global potential to be placed in β -turns, following glycine, asparagine and aspartic acid respectively. This potential is the highest value if proline is regarded to be placed in the defined as $i+1$ position of a β -turn [9].

1.4 The amino acid proline and its relevance on the function of proteins.

As it has been basically described above, one can not underestimate the capacity of proline to structurally influence, in protein chains, its immediate residues. It might be argued whether this influence has a significant meaning on proteins functionality. The mutual influence, between the structural and the dynamic roles, that proline is exercising in proteins can be synthesized in the case of the α -helical transmembrane section of many integral membrane proteins, where this residue appears with certain frequency [10]. Thus, for example, the class A and D of the superfamily of G-protein-coupled receptors are holding in their transmembrane helices 6 and 7 highly conserved, and functionally essential, prolines [11]. The point mutation of those highly conserved prolines in the rat m3 muscarinic G protein-coupled receptor demonstrated that they play an important role in the expression levels, ligands affinity and modulation of the receptor [12].

In the same sense, it could be characterized the influence of proline on the behaviour of ion channels. The superfamily of voltage gated sodium channel proteins are

generically formed by a pore of α -subunits, containing four homologous domains of six transmembrane helices. It has been demonstrated by whole-cell voltage-clamp experiments how the chimeric insertion of prolines in such voltage gated sodium channels dramatically influenced the functionality of the pore channel. Interestingly the adequate proline exchange yielded transformed channels. Compared to the depolarization-activated wild type channels the insertion of proline in their sequences generated chimeric hyperpolarization-activated channels [13], that is the completely opposite pumping driving force. Additionally, it has been demonstrated, for example, on the 5-HT₃ receptor how a proline *cis/trans* isomerization participates directly in the control of its pore opening mechanism [14].

One basic aspect that is gaining strength and interest is to discern the way biological macromolecules, such as proteins, interact. It has been concluded that many of such intermolecular associations are the result of interactions within very short amino acid regions of one of the binding partners, usually less than 10 amino acids [15]. Proline is a residue that plays a central role in the binding properties of many ligands to their receptors, as it can be seen for the presence of the constrained amino acid in many primary sequences of ligands recognized by SH3, WW and other proline rich binding motifs [15]. The reason of the active participation of proline in the ligands binding sites motif could be found in the fact that such polyprolines sequences adopt preferentially a PII helix structure, which is the scaffold that builds a three residues per turn helix. Thus, for example in the SH3 ligand core, PxxP, both prolines are placed in the same face of this PII helix, forming a hydrophobic stripe with the backbone carbonyls in position to generate ideal hydrogen bonding sites, being both conformationally restricted and electronically enriched [15].

Peptide hormones are also influenced by the amino acid proline. Interestingly, proline is particularly conserved in the amino terminal sequence of many cytokines and growth factors [16]. There might be two reasons for this phenomenon, first, the presence of prolines might play a direct role in the affinity of such peptides for their receptors, and second, proline might serve as one of the key regulatory signals that controls the lifetime and degradation rates of peptides and proteins [16;17]. Thus, Neuropeptide Y is a 36 amino acid long peptide which is involved, among other functions, in the control of the Luteinizing hormone secretion [18]. Due to its content of prolines, Neuropeptide Y is able to build a tertiary structure which shows a type II proline helix at its amino terminus [19]. Furthermore, the presence of proline in the hormone's peptidic chain might act as a protecting nucleus against unspecific proteolysis [20;21], and in parallel, as a key regulatory mechanism of the peptide function [22], as it modulates the selectivity of the peptide towards its various receptors [23].

1.5 The proteases cleaving proline-containing peptides.

Enzymes have been classified according to the reaction they are able to perform. Thus, enzymes are classified into the following: oxidoreductases, transferases, hydrolases, lyases, isomerases and ligases [24]. The hydrolase enzymes, with the EC number 3, catalyze the hydrolysis of covalent bonds. A water molecule is tightly implicated in the catalytic mechanism, hence the definition as hydrolases. The peptide bond is the scissile bond processed by peptidases, all of them with a 3.4 EC number. Thus, if the scissile peptide bond is at the terminus of a substrate, one, two or three amino acid residues away from the amino or carboxy terminus of the substrate chain, the peptidase is referred as exopeptidase. Likewise, peptidases cleaving a peptide bond within a substrate are called endopeptidases [24]. The specificity of peptidases is understood, following the Schechter and Berger nomenclature, as the amino acid residue better accepted in a defined as S_1 active center enzyme pocket [25].

As a result of its structural idiosyncrasy and considering all arguments noted above, proline is a residue which accommodation is only accepted by a relative low number of peptidases. Regarding the Merops peptidase database [26] only 70 peptidase identifiers, out of a total of 2067, have been characterized with the putative post-proline peptidase ability. It is worthwhile to note that in humans the proline accepting peptidases are solely found in families of the peptidase SC clan and in the M24B subfamily of the MG clan [27]. This fact is denoting the high degree of specialization achieved, and required, in order to hydrolyze a proline containing peptide bond. Specifically in the clan SC of serine peptidases are grouped a set of enzymes which were classified as S9 family. Characteristically, most of the members of this peptidase family act preferentially on proline, accepting these residues as their main specificity. The S9 family is further classified in the S9a subfamily, which representative enzyme is prolyl oligopeptidase (EC 3.4.21.26).

1.6 Prolyl oligopeptidase.

Prolyl oligopeptidase was first described by Walter *et al.* [28] as an oxytocin leucylglycinamide releasing peptidase activity isolated from human uterus. Since then, the enzyme has received different nomenclatures, like for example, post-proline cleaving enzyme, post-proline endopeptidase, TRH-deaminase, brain-kinase B and prolyl endopeptidase. Finally the recommended IUBMB name was prolyl oligopeptidase with a given enzyme number EC 3.4.21.26 [24]. Prolyl oligopeptidase is an enzyme with a broad distribution among superkingdoms. It can be found either in eukaryotic, prokaryotic or archaea sources, although it has not been found in some kingdoms such as like in fungi [29]. The direct isolation of the enzyme from various

tissues and organisms has been achieved. Examples include mice [30], the Pacific herring fish [31], porcine muscle [32], bovine testis and brain [33;34] as well as human lymphocytes and brain [35;36]. However, higher yields and more readily reproducible purification standards have been achieved when the *Escherichia coli* system was used for expression purposes. The enzyme's gene has been cloned and expressed with coding sequences coming from various sources. Thus, several genes of bacterial origin can be found in the literature, like *Sphingomonas capsulata* [37], *Aeromonas hydrophila* [38], *Aeromonas punctata* [39] and *Flavobacterium meningosepticum* [40;41]. Similarly, a large number of eukaryotic sources have been used in order to clone their prolyl oligopeptidase gene. Thus for example, the human gene [42;43], the mouse gene [44], a porcine coding sequence [45], a rat cDNA [46], a brain bovine sequence [47] and the gene from the fly *Sarcophaga peregrina* [48]. Finally, an archaea genome, such as the *Pyrococcus furiosus* [49], was as well a suitable template to isolate and express the coding sequence of the enzyme prolyl oligopeptidase.

1.7 Prolyl oligopeptidase closely related enzymes.

Prolyl oligopeptidase is the main enzyme in the S9a subfamily of the S9 family of serine peptidases. This family also includes the representative enzymes dipeptidyl peptidase 4 in the S9b subfamily, acylaminoacyl peptidase in the S9c subfamily and the glutamyl peptidase in the S9d subfamily. In addition to prolyl oligopeptidase, other proline specific enzymes are present in the S9 family, although as well other members of this family have either no demonstrated catalytic activity, like for example dipeptidyl peptidase 6 in the S9b subfamily, or have a complete different enzymatic specificity, like for example oligopeptidase B in the S9a subfamily [26].

Regarding the proline specific enzymes, prolyl oligopeptidase shares a relatively low primary sequence homology with the other members of the family, but in contrast, and together with its enzymatic specificity, it shares a high structural three dimensional homology. Nevertheless, the highest sequence homologies between prolyl oligopeptidase and the rest of the members of the S9 family are achieved always within the carboxy terminal segment of these proteins [50]. On the other hand, and in contrast to for example dipeptidyl peptidase 4 and other members of the S9b subfamily, prolyl oligopeptidase is a monomer whereas the formers are dimers. Finally, to mention that noteworthy these enzymes do not have zymogens, they are synthesized as active enzymes, and that their molecular weight is relatively large, over 80 kDa [50].

1.8 Prolyl oligopeptidase gene, PREP.

The human gene of prolyl oligopeptidase, PREP, has been mapped and localized in the chromosome 6q22 [51]. Lately, the structure and localization of the mouse prolyl oligopeptidase gene was as well accomplished [52]. The mouse gene spans over 91.9 kilobases of DNA and includes 15 exons [52]. Exons 13th and 15th are holding the coding sequences for the catalytic Ser⁵⁵⁴ and the Asp⁶⁴¹ and His⁶⁸⁰, respectively.

The mouse prolyl oligopeptidase transcription promoter has a "housekeeping" structure lacking TATA and CAAT boxes, but with functional GCTCC(C/G) motifs, known as multiple start site element, MED-1. This G+C rich regions, 77% between the gene region -68 and +377, contain potential binding sites for several transcription factors such as Sp1, Ap2 and E4TF [52].

The comparison between 28 different prolyl oligopeptidase genes showed how the highest conserved gene regions were found in the corresponding coding sequences for the carboxy terminus section of the enzyme with 17.8% of the amino acids with a 100% similarity [29]. Importantly, the amino acids forming the defined as S₁ pocket, and the three residues of the catalytic triad show 100% similarity and almost 100% identity among the 28 characterized prolyl oligopeptidase sequences [29].

1.9 Human tissue distribution of prolyl oligopeptidase.

In addition to the wide expression found among different organisms, the broad prolyl oligopeptidase tissue expression has been investigated, particularly in humans. It could be found, for example, in prostate, lung, spleen, rectum, lymphocytes, testis, renal cortex [53], skeletal muscle, kidney, pancreas, uterus, liver, thymus and stomach [54;55]. In contrast, the lowest levels of prolyl oligopeptidase activity were found in body fluids such as plasma, urine, seminal plasma and serum [53;55].

1.10 Prolyl oligopeptidase brain distribution.

Because of the correlation between the prolyl oligopeptidase activity and its impairment in certain psychologic pathologies [56], a main endeavor has been focused on the characterization of the prolyl oligopeptidase enzyme in brain. The regional distribution of human prolyl oligopeptidase in brain has been determined. The highest enzyme activities were found in the frontal, parietal and occipital cortices, followed by moderate activities in the striatum, the hypothalamus, the hippocampus and the amygdala, see figure 1. In contrast, the lowest activity levels were detected in the cerebellum [57]. A similar distribution was confirmed by *Kato et al.* who quoted the frontal cortex as the region with the highest prolyl oligopeptidase activity, followed by nucleus caudatus, pulvinar, locus coeruleus, thalamus, pallidum and hypothalamus, respectively [55].

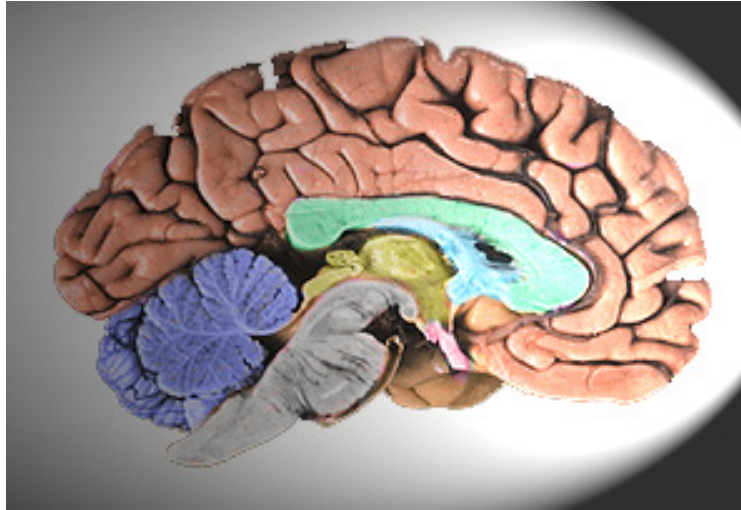


Figure 1 Sagittal section of a human brain. From the forebrain to the innerbrain, in red were coloured the Cortices, in green the Corpus Callosum and Septum, in yellow Thalamus and Hypothalamus, in grey Pons, Medulla Oblongata and Spinal Cord, in blue the Cerebellum and in pink the pituitary gland.

However, the activity profile of prolyl oligopeptidase appears to be specie-dependent, as different distribution profiles have been reported in human, rat and rabbit [55]. For example, comparing rat and human brain tissues, the prolyl oligopeptidase activity distribution among different studied rat brain areas showed no significant differences, while the regional distribution in human brain was found to be in contrast well differentiated [57]. On the other hand, a very detailed study of the prolyl oligopeptidase mRNA expression in rat brain shown how the highest transcription levels of the enzyme's gene were characterized in hypothalamus and cerebellum, quantified as 2- to 2.5-fold higher than the ones found in the occipital cortex. The prolyl oligopeptidase mRNA levels were found to be similar in occipital cortex, amygdala, hippocampus, thalamus, pontine nuclei and pituitary. In turn, the lowest prolyl oligopeptidase mRNA transcription levels were found in the substantia nigra, the medulla oblongata and the spinal cord [58].

1.11 Subcellular localization of prolyl oligopeptidase.

The subcellular localization of prolyl oligopeptidase was determined in rabbit brain homogenates to be intracellular and cytosolic [59], although evidences exist indicating a differential subcellular localization during cell development [60]. However, other authors went a step further and suggested a concrete localization in the perinuclear space in human neuroblastoma and glioma cell lines [61]. Additional studies using the *Sarcophaga peregrina* fly also located the enzyme in the cell nucleus [62]. In spite of its indubitable soluble and cytosolic localization some authors have argued the existence

of a membrane related form of the enzyme associated to synaptosomal membranes [63;64]. A later comparative kinetic and immunological characterization between the putative membrane bound and the soluble prolyl oligopeptidase did not show major differences, thus indicating the possible existence of a post-translationally modified version of the enzyme [65]. Furthermore, some authors even claimed the existence of a secreted form of the enzyme which has been characterized in bovine serum [66].

1.12 Prolyl oligopeptidase tertiary structure.

The three dimensional crystal structure of the porcine prolyl oligopeptidase was the first to be determined [67]. A 97% homology between the porcine and the human protein sequences allows to establish precise extrapolations and parallelisms between both proteins. The structure is defined by two main domains, an α/β -hydrolase and a β -sheet containing propeller domain, as shown in figure 2A. The α/β -hydrolase domain [68] includes residues 1 to 72 and the carboxy terminal segment 428-710, while the remaining peptidase chain, residues 73 to 427, comprises the β -propeller domain [69]. The prolyl oligopeptidase α/β -hydrolase domain is built with a significantly twisted eight-stranded β -sheet that has a parallel topology with the exception of the second strand which is aligned in an antiparallel manner. This central β -sheet is respectively surrounded by two α -helices at one side and six more α -helices on its opposite face. The β -propeller domain, as shown in figure 2B, also referred as non-catalytic domain, is constructed with a seven-fold repetition of a four stranded antiparallel β -sheet. The β -sheets are arranged radially around a central axis. The β -sheets are packed face-to-face, stabilizing their global tertiary domain structure by hydrophobic interactions. In the most of the cases, the β -propeller domains have evolved closing their cylindrical structure. Thus, two ways have been used to achieve this ring closure, either building an extense intradomain hydrogen bond network between the first and last β -strands of the propeller defined as a velcro motif, or directly building disulfide bridges [70]. The prolyl oligopeptidase β -propeller exhibits an unusual permanently stable open conformation, in which the above defined velcro or disulfide bridges closures are lacking [70].

The α/β -hydrolase domain is defined as the catalytic domain as it contains the residues responsible for the protein enzymatic activity. These residues are the Ser⁵⁵⁴, Asp⁶⁴¹ and His⁶⁸⁰ which are grouped and defined as the catalytic triad, shown in figure 2C. The catalytic triad is exposed to the interface region between the two domains, lying on the base of the inner cavity of the β -propeller. The Ser⁵⁵⁴ is placed in a very sharp turn, His⁶⁸⁰ is placed in the middle of a non-ordered loop, so that the imidazol ring is accessi-

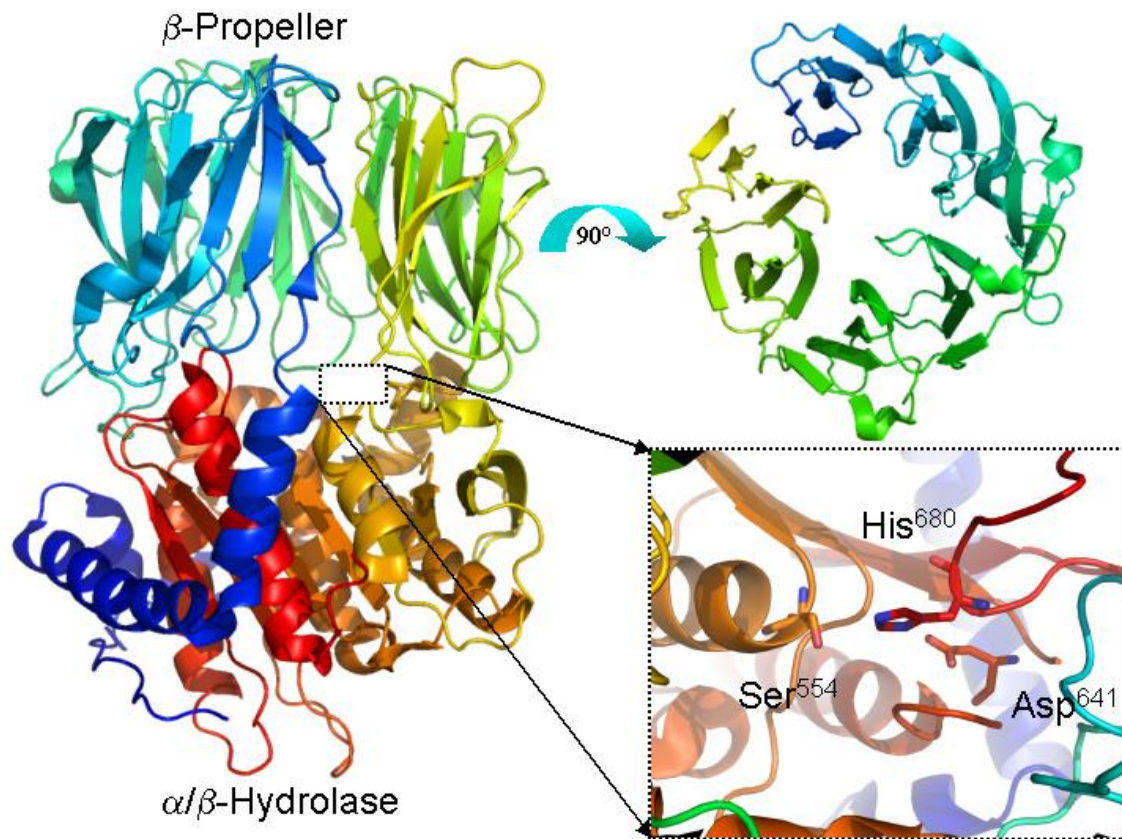


Figure 2 Representation of the three dimensional structure of the porcine prolyl oligopeptidase (PDB id: 1qfs). A) On the left side, cartoon representation of the structure, with the β -propeller domain on the top and the α/β -hydrolase domain at the bottom. On the right side. B) Axial view of the unclosed β -propeller domain. C) Detail of the catalytic triad residues are highlighted .

-ble from one side to the Ser⁵⁵⁴ side-chain hydroxyl moiety and from the other side to the oxygens of the Asp⁶⁴¹ carboxylate side-chain. The co-crystallization of the prolyl oligopeptidase enzyme with an inhibitor allowed to make a model of the active center subsites. Thus, following the nomenclature established by Schechter and Berger [25], the S₁ subsite is a hydrophobic pocket lined by the side-chains of the residues Trp⁵⁹⁵, Phe⁴⁷⁶, Val⁶⁴⁴, Val⁵⁸⁰ and Tyr⁵⁹⁹. Furthermore, in terms of the active site area singularity, the S₂ pocket is not so well defined as it is the S₁ subsite. Hence, the only contribution to the S₂ subsite is made by the residue Arg⁶⁴³. The S₃ pocket is built with the non-polar side-chains of the residues Phe¹⁷³, Met²³⁵, Cys²⁵⁵, Ile⁵⁹¹ and Ala⁵⁹⁴ [67]. Thus, structurally the S₁-S₂-S₃ subsites, see figure 8, are defining the main restrictions regarding the enzyme substrate specificity. Beyond them, only the S₁'-S₂' subsites might make a certain minor contribution configuring the substrate specificity of the enzyme [67].

The crystal structures of three additional proteins belonging to the S9 family have been solved, namely dipeptidyl peptidase 4 [71], fibroblast activated protein [72] and

dipeptidyl peptidase 6 [73]. Noteworthy, all they share a high structural homology with the one described above for prolyl oligopeptidase.

1.13 Substrate selectivity of prolyl oligopeptidase.

Prolyl oligopeptidase is cleaving the peptide bond at the carboxy side of proline residues. One significant feature of the substrate selectivity of prolyl oligopeptidase, together with its proline specificity, is its limitation to accept oligopeptides no longer than thirty amino acid residues [32;74]. The narrow entrance on top of the β -propeller domain of approximately 4 Å of diameter and the lack of any cleft-like side opening, present otherwise in other members of the S9 family, do not clarify a possible substrate access pathway to the buried active site. The β -propeller domain has been pointed to be the main substrate size selector by acting as a gating filter during the catalysis [75]. Nevertheless, the hyperthermophilic *Pyrococcus furiosus* prolyl oligopeptidase differs from its mesophilic counterparts in that it is able to hydrolyze proteins, not only oligopeptides, like azocasein [49]. In that sense, it was shown that the prolyl oligopeptidase from *Trypanosoma cruzi* was as well able to degrade large substrates like fibronectin or native collagen [76]. In order to explain the substrate size exclusion mechanism, it was suggested that the hyperthermophilic enzyme could have a hinge-like motion, where the two domains are moving apart from each other, enabling the access of the substrate to the active site [77]. In principle, this assumption should not be discarded for the mammalian enzyme [75]. Actually, the crystal structure of the *Sphingomonas capsulata* prolyl oligopeptidase has confirmed this principle since it is showing an enzyme with an open conformation, product of a hinge-like motion [78]. All this correlates with the fact that for the catalysis of the porcine prolyl oligopeptidase the rate limiting step has been associated with an enzyme conformational change rather than with a chemical reaction step [79].

1.14 Prolyl oligopeptidase catalytic mechanism.

Prolyl oligopeptidase, as already mentioned above, is a serine peptidase. The very first and basic premise is that any peptidase will carry out the breakage of the stable amide bond. The non-enzymatic hydrolysis of the peptide bond, although possible, is a rather very slow phenomenon which can be enzymatically accelerated by a factor of approximately $2 \cdot 10^6$ [80]. Peptidases then, have the biological responsibility of an efficient control of the cleavage of the peptide bond in proteins. Basically, the enzymes responsible to perform the cleavage of the peptide bond have been classified in function of the group responsible to carry out a nucleophilic attack over the peptide bond that ends with its hydrolysis. Thus, eight different peptidase families have been

classified: aspartic, cysteine, metallo, serine, glutamic, threonine, mixed type and unknown type [81]. The serine peptidases, classified because of their catalytic serine residue, represents the largest group of peptidases. The serine peptidase family has been further classified regarding structural specificities. Thus, the subfamilies with chymotrypsin (EC 3.4.21.1) and subtilisin (EC 3.4.21.62), as representative members, have been taken often as a reference of the serine peptidases as they have been extensively characterized.

As schematically depicted in figure 3, the chemical reaction performed by these peptidases consists in an initial weakening of the peptide bond as a result of a nucleophilic attack carried over the peptidic carbonyl moiety. This generates a displacement of the electron densities that ends up building a tetrahedral intermediate centered in the attacked substrate carbonyl carbon by bearing in one of its fourth substitutions an oxyanion. The nucleophilic attack is enhanced by a general base mechanism which accepts the proton released by the nucleophile group. The unsteady tetrahedral intermediate is stabilized with the contribution of a hydrogen bond pair formed between the oxyanion and the appropriate hydrogen-electrophile atoms moieties. It follows the liberation of the amine leaving group, promoted with an acid based mechanism that yields the breakage of the C-N bond through the reduction of the amide moiety. The remainder peptidic carboxy group stays bonded to the protein as an ester-enzyme intermediate. This is now reversed with the participation of water molecule. A promoted general base attack allows the nucleophilic attack of a water molecule over the acyl-enzyme intermediate. For a second time an unstable tetrahedral intermediate is generated, figure 3. The system collapses to the ground state by a new general acid mechanism that yields the reconstitution of the hydroxyl nucleophilic serine side-chain moiety giving a free enzyme and a leaving carboxy moiety [82]. The prolyl oligopeptidase catalytic mechanism fits properly into the above general description of serine peptidases catalytic mechanism, figure 3, although it is noteworthy to point out some specificities.

In the human prolyl oligopeptidase, the residues Ser⁵⁵⁴, Asp⁶⁴¹ and His⁶⁸⁰ have been identified to constitute the catalytic triad of the enzyme. It is important to note how the arrangement of the primary sequence of these catalytic residues does not follow the same order found for the termed classical serine peptidases. Thus, for chymotrypsin (EC 3.4.21.1) the arrangement of the catalytic triad is His⁵⁷, Asp¹⁰² and Ser¹⁹⁵, while the one found in the subtilisin enzyme (EC 3.4.21.62) is Asp¹³⁷, His¹⁶⁸ and Ser³²⁵.

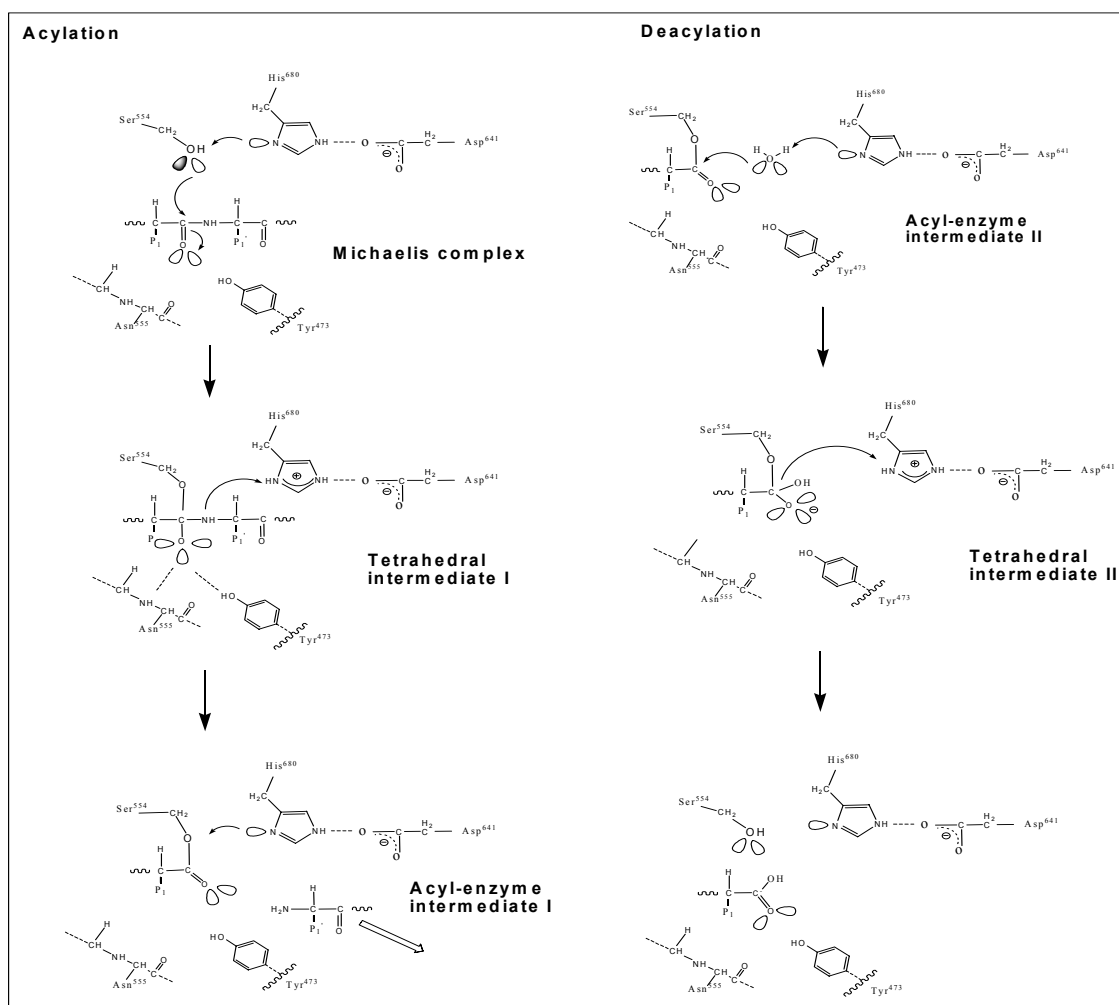


Figure 3 Schematic representation of the catalytic mechanism followed by prolyl oligopeptidase. The events follow the sequence Michaelis complex, Tetrahedral intermediate I, Acyl-enzyme intermediate I, Acyl-enzyme intermediate II and Tetrahedral intermediate II.

In prolyl oligopeptidase the active Ser⁵⁵⁴, responsible to initiate the reaction, is framed in the primary sequence by four glycines (GlyGlySer⁵⁵⁴AsnGlyGly). The motif, GX SXG, is known as a nucleophile elbow and it is a representative motif of the α/β -hydrolases in which the nucleophilic serine stands on the vertex of a sharp turn, as shown in figure 2C. This nucleophilic elbow is responsible to give to the reactive serine the appropriate accessibility and conformation in order to be approached by the other enzyme and substrate reactive groups [68].

Following the primary sequence the next catalytically relevant residue is the Asp⁶⁴¹. The contribution of the aspartate to the enzymatic mechanism of the serine peptidases is still in some extent controversial. At first, it was suggested that the catalytic aspartate plays a role in a putative charge-relay system within the catalytic triad [83], where the acidic residue would have acted as a proton acceptor. This assumption was not further

corroborated as it seemed chemically unlikely that its carboxylic side-chain would be able to act as a base at neutral pH [84]. This extreme has been completely discarded with NMR studies of the serine peptidase subtilisin (EC 3.4.21.62) [85]. The latest proposals suggested that the aspartate would act during the tetrahedral intermediate formation either as a stabilizer of the imidazolium group of the histidine or would simply participate in the proper orientation and positioning of the histidine side-chain in order to facilitate its interaction with the reactive serine [86]. In prolyl oligopeptidase the exchange of the catalytic Asp⁶⁴¹, either for asparagine or for alanine residues, produced variants with similar impaired catalytic characteristics. Regarding the authors this would support the idea that the reactive aspartate has a role as imidazolium stabilizer in the tetrahedral intermediate state to the detriment of the orientation role [87]. In other cases, like in the serine peptidase trypsin (EC 3.4.21.4), similar exchanges brought the authors to a different conclusion, namely the one of an incorrect tautomer histidine formation [88].

The His⁶⁸⁰ is the residue that completes the triumvirate, defined as catalytic triad, that governs the enzyme catalysis in prolyl oligopeptidase. In contrast to the aspartate, the role played by histidine is less controversial. The side-chain imidazol of the His⁶⁸⁰ is pivoting the whole enzymatic mechanism, as shown in figure 3. This residue with a pKa value of 6.2 [89] enables the proton transfers, thanks to an ambivalent general acid-base behaviour, that allows sequentially, both, to accept and to donate protons [82;86]. The generation of the acyl-enzyme adduct during the acylation or the free enzyme in the deacylation enzymatic pathways, figure 3, is achieved after the energetically unstable tetrahedral intermediate collapses. The way to stabilize the transition state associated to the formation of the tetrahedral intermediate is solved in serine peptidases with the construction of a hydrogen bond network centered on the negatively charged oxyanion atom [90]. Two main chain NH groups in the chymotrypsin-type and an amide side-chain of an asparagine residue together with a main chain NH moiety in the subtilisin-type serine peptidases are the respective representative oxyanion hole builders. In that sense, again prolyl oligopeptidase distinguishes itself from the established motifs found in the classical serine peptidases. Prolyl oligopeptidase is generating its oxyanion hole with the participation of a main chain NH moiety of the Asn⁵⁵⁵ and with the hydroxyl moiety of the side-chain of the Tyr⁴⁷³ [67]. The tyrosine side-chain hydroxyl is much more acidic than the main chain NH or the amide NH₂, therefore it might be a more suitable way to stabilize the tetrahedral intermediate in prolyl oligopeptidase [91].

1.15 Kinetic characterization of prolyl oligopeptidase.

The kinetic characterization of the enzyme began at the moment that its discoverers characterized in human uterus an oxytocin leucylglycinamide releasing activity [92]. Afterwards this activity was confirmed to be related to prolyl oligopeptidase [93]. The proline specificity of the enzyme was then the earliest established. Later an alanine specificity was additionally added, although with an up to 1/1000 decreased rate in comparison to the proline specificity [94]. In addition, it was found that the stereospecificity of the enzyme's active site is not enabling processing substrates with either P₁ or P₂ D-proline or D-alanine amino acid stereoisomers [95].

The pH-rate profile of an enzyme correlates the specificity constants, k_{cat}/K_m , with their measured pH. The classical serine peptidases exhibit a simple sigmoid bell shaped profile that denotes the relevance of ionisation of a group with a pK_a of 7 for the catalysis, this group is the imidazol side-chain of the catalytic histidine [96]. The porcine prolyl oligopeptidase, once again in contrast to the classical serine peptidases, showed more complex pH-rate profiles. The proline specific enzyme has a doubly sigmoid bell-shaped catalytic pH dependence that is denoting the existence of two active forms of the enzyme, one being present at pH 6 and the other at pH 8, with the presence of an unknown ionisable group in the active site that would influence the catalytic histidine [97;98]. This pH dependence complexity was as well characterized in the hyperthermophilic *Pyrococcus furiosus* prolyl oligopeptidase [77].

In the classical serine peptidases the acylation and deacylation steps proceed slower in deuterium oxide than in water by a factor of 2 to 3. This has been defined as the solvent effect and emphasizes the fact that the general acid/base catalysis of the catalytic histidine is the rate limiting step of the reaction. Prolyl oligopeptidase, however, has shown the solvent effect only for the low pH active form mentioned above, but not for the high pH form [99]. That would suggest that at physiological pH a conformational protein change would be the rate limiting step of the enzymatic reaction. In contrast, the hyperthermophilic *Pyrococcus furiosus* prolyl oligopeptidase has shown a stable deuterium isotope effect over the whole range of measured conditions demonstrating that the proton transfer is in the archeon prolyl oligopeptidase the catalytic rate limiting step [77].

Furthermore, an additional difference between the classical serine peptidases and prolyl oligopeptidase is the influence of ionic strength on the enzyme catalysis. Thus, the former are not affected by ionic strength, whereas the last experiences a linear increase of the second order rate constant parallel to the increase of the salt up to 0.5M NaCl concentration [99]. This result was also corroborated by the hyperthermophilic *Pyrococcus furiosus* prolyl oligopeptidase, which showed an ionic

strength dependence of the specificity constant, k_{cat}/K_m , but not of the single turnover constant, k_{cat} , suggesting that the catalytic improvement was the result of a more efficient substrate binding rather than any other catalytic changes [77]. This salt activating effect has been related in an enzyme such as Angiotensin converting enzyme to the influence of the halide atoms [100], however, prolyl oligopeptidase is equally activated by different type of salts such as NaCl, KCl, NaNO₃ and NaH₂PO₄ [98]. The favouring salt effect on the activity of prolyl oligopeptidase has been opposed by the deleterious effect on the enzyme activity by some other metal ions, like Hg²⁺, Cu²⁺ and Zn²⁺ [36;101].

As noted above, proline as a consequence of its special idiosyncrasy has a higher tendency to adopt *cis* configuration within the precedent residue in polypeptide chains. Prolyl oligopeptidase is only processing substrates which hold their proline residues in a *trans* conformation, a feature that was earlier confirmed with the bacterial *Flavobacterium meningosepticum* enzyme [102], and afterwards with the mammalian porcine prolyl oligopeptidase [99].

Another factor that influences the catalysis of prolyl oligopeptidase is the redox state of the medium where it reacts. Thus, it was confirmed in cell culture experiments that as a result of a temperature stress shock, intracellular redox changes led to the inactivation of the enzyme [103]. This phenomenon was also confirmed in experiments with the recombinant enzyme. A site directed mutagenesis approach demonstrated that the residue Cys²⁵⁵ was the responsible for the redox inactivation of the enzyme. A complete enzyme inhibition was obtained when the wild type enzyme was treated with the N-ethylmaleimide thiol blocking reagent, but not when the C255A prolyl oligopeptidase variant was equally treated [104].

1.16 Biological relevance of prolyl oligopeptidase.

The biological role played by prolyl oligopeptidase is still controversial. It is commonly said that this enzyme is involved in the metabolism of neuropeptides and peptide hormones [22], but this is certainly a so wide statement that it actually does not contribute to clarify the biological relevance of this enzyme. It suits as starting point to know which are the substrates that actually the enzyme is processing *in vitro*. The list is large and includes, for example, hormones like oxytocin, angiotensin II, bradykinin, thyroliberin, beta-endorphin, substance P, neurotensin and arginine-vasopressin [50;105;106]. However, none of them, so far, could be characterized as a natural prolyl oligopeptidase substrate. The main problem to assign them as putative endogenous substrates of the enzyme is their preferential extracellular localization.

A clarifying insight of the physiological role of prolyl oligopeptidase arose because of the use of its specific inhibitors. The most significant progress in that sense probably became when scopolamine induced amnesia models were successfully reversed with the use of specific prolyl oligopeptidase inhibitors [107]. Scopolamine is a secondary plant metabolite that acts as antagonist of muscarinic receptors. Scopolamine is used to generate in animals, or even in humans, experimental models of amnesia [108]. Several works have investigated the relationship between memory and learning disorders and prolyl oligopeptidase. Thus, *Yoshimoto et al.* [107] showed for a first time that in scopolamine pretreated rats prolyl oligopeptidase specific inhibitors were able to prolong *in vivo* a phenomenon defined as a Retention of the Passive Avoidance Response (RPAR), which is a test for long-term memory in rodents. Experimentally, rats were trained to avoid a behavior, to leave the platform of a cage, by an electric-shock punishment. This learned behaviour lasted so long as the control animals had defined. In that sense, scopolamine treatment shortened the time window whereas the prolyl oligopeptidase inhibitors were able to retain in scopolamine treated animals the defined control time. These results attracted immediately the interest of the pharmaceutical industry, so far that new highly specific inhibitors even underwent preclinical studies [109]. These preclinical studies demonstrated again the memory and learning enhancement features of the prodrug S17092, illustrated in table 1, a prolyl oligopeptidase inhibitor, in different cognitive tests in animal models. Moreover, these preclinical studies emphasized an *in vivo* relationship between increased Substance P immunoreactivities levels and prolyl oligopeptidase inhibition. Indeed, Substance P has been shown to be a peptide with enhancing cognitive capabilities by activating the dopamine neurons in cerebral areas such as *nucleus accumbens* and the mesolimbic dopamine system [110]. Nevertheless, it is necessary to underline that there is yet no evidence that the released endogenous Substance P has, even, a physiological or functional role in the studied cognitive processes, mainly because of the weak evidences concerning the site and mechanism of action of this neuropeptide [110]. Then, if the putative prolyl oligopeptidase substrate has yet not been clearly, and non-ambiguously, related to the above mentioned cognitive physiological processes, it would be premature to implicate the peptidase itself. The same might be argued for the rest of putative neuropeptides characterized as mnemonic enhancers like TRH, vasopressin, somatostatin and neurotensin.

Nevertheless, lately an interesting work dissociated the biological relevance of the enzyme from its catalytic activity, highlighted rather the relevance of prolyl oligopeptidase interactions with cytosolic proteins as the main issue on the protein relevance [111]

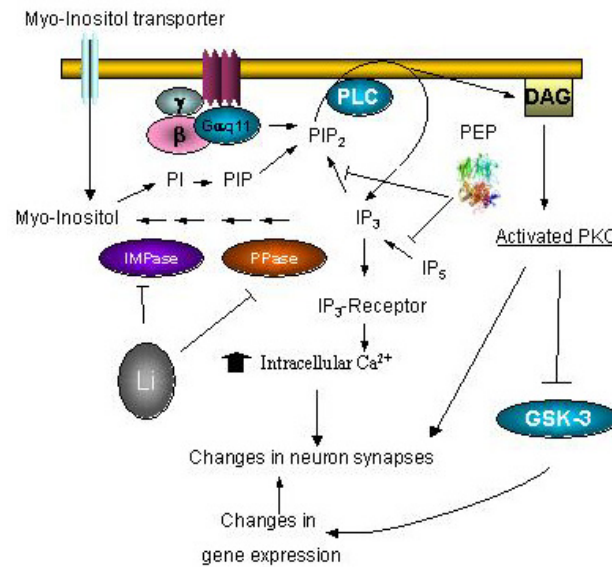


Figure 4 Cellular pathways were prolyl oligopeptidase have been indicated to be implicated. Adapted from [112] and [113]. Main actors of the pathways are GSK-3 that stands for glycogen synthetase kinase, IMPase for inositol monophosphatase, DAG for diacylglycerol, PLC for phospholipase C, Li for lithium and the different phosphorylated versions of inositol: IP₅, IP₃, PI, PIP and PIP₂.

Another useful approach in order to establish the biological significance of a protein might be the generation of a transgenic organism. Thus for example, gene knock-out models, where the absent target protein is producing in the best of the cases a new phenotype that might be investigated and compared to the one found within the wild type organism. Unfortunately, in the case of prolyl oligopeptidase only one example in the literature is following this approach. The *Dyctyostelium discoideum* amoeba was used in order to generate lithium resistant mutants, as this organism is sensitive to this chemical element [114]. Among the selected mutants, one could be found in which prolyl oligopeptidase gene was ablated, with the consequent lack of the endogenous enzyme in the studied organism [113]. Interestingly, in this case the derived phenotype was characterized with increased levels of inositol triphosphate, IP₃. This connection was independently supported with siRNA antisense experiments in the U343 astrocytoma cell line [115] which as well showed an intracellular increase of the basal levels of IP₃ in impoverished prolyl oligopeptidase cells, figure 4. All that was clearly suggesting the association between prolyl oligopeptidase activity and the maintenance of the basal levels of IP₃. In the *Dyctyostelium discoideum* prolyl oligopeptidase knock-out the dephosphorylation breakdown of IP₅ was indicated to be the process causing the IP₃ accumulation. The post-proline peptidase enzyme might participate in this process [113], discarding then the classical pathway for IP₃ generation which implicates phospholipase C, figure 4. This underlines a specific and single pathway on the IP₃

accumulation which was reported to be present also in higher mammals [116]. In addition, abnormal low activity levels of prolyl oligopeptidase have been characterized in plasma of patients with bipolar disorders [117]. The inhibition of prolyl oligopeptidase also reversed the effect of mood stabilizers, like lithium, which at the end is targeting the inositol phosphate-signalling pathway, figure 4. All these data support the idea that the prolyl oligopeptidase might be implicated in the regulation of IP₃ intracellular concentration [113].

In addition, although dispersedly, some other biological phenomena have been characterized where prolyl oligopeptidase was suggested to play a role. For example, PEP was implicated in mouse sperm motility [118]. It was also related to the DNA synthesis as a result of investigations in the Swiss 3T3 mouse fibroblast cell line [44]. The participation of the enzyme in differentiation processes of the imaginal discs of the *Sarcophaga peregrina* fly has been also suggested [119]. Furthermore, it has been described an enzymatic regulation of rat pituitary and hypothalamic GnRH hormone levels through a feedback control by one of the resulting sub-products of the prolyl oligopeptidase degradation [120]. In addition depressed enzyme activity levels were described in an inflammatory response to *in vivo* sensitization of guinea pig skin [121]. Moreover, an active role of prolyl oligopeptidase was suggested in the invasiveness processes of mammalian cells by the parasite *Trypanosoma cruzi* [76].

Finally, additional research has focused on the relationship between prolyl oligopeptidase plasma activity levels and various psychiatric diseases. Thus, they have been measured abnormal plasma levels of prolyl oligopeptidase activity in children with autistic disorders [122], lower plasma levels of prolyl oligopeptidase in depression [123;124], bulimia, anorexia [125] and fibromyalgia patients [126], but higher levels in patients suffering from post-traumatic stress disorders [127].

1.17 Prolyl oligopeptidase inhibitors.

In the early stages of characterization the inhibition of the enzyme was achieved with diisopropylfluorophosphate, DFP, but not with phenylmethanesulfonyl fluoride, PMSF, both general irreversible serine protease and acetyl cholinesterase inhibitors [99]. Additionally, carbobenzoxy-Gly-Pro-chloromethyl ketone and p-chloromercuribenzoate, general cysteine peptidase inhibitors, were found to inhibit successfully prolyl oligopeptidase [101]. The indications that prolyl oligopeptidase could be implicated in processes of pharmacological relevance triggered the interest to produce specific inhibitors against this enzyme. The Z-pro-prolinal inhibitor, illustrated in table1, was the first approach which showed inhibitory K_i constants in the nanomolar range [128]. Z-pro-prolinal is an aldehyde based inhibitor that acts by forming a hemiacetal adduct

with the active Ser⁵⁵⁴ which resembles the tetrahedral intermediate [129]. Later on, it was demonstrated how this molecule is acting as a competitive slow-tight binding inhibitor [130]. The mode of action is then, in this case, a rapid enzyme-inhibitor complex formation characterized with a k_{on} rate constant of $1.6 \cdot 10^5 \text{ M}^{-1}\text{s}^{-1}$. Once the complex with the inhibitor is formed, the diffusion from the active site is a very unlikely event characterized with a k_{off} rate constant of $4 \cdot 10^{-5} \text{ s}^{-1}$ [130]. It is likely that the presence of the reactive aldehyde moiety is responsible for this slow-tight binding behaviour. The substitution of the aldehyde group for an alcohol moiety, then Z-pro-prolinol, entailed a change in the inhibitory behaviour that was obeying a rather rapid competitive mechanism [130]. Interestingly, the introduction of sulfur atoms in the pyrrolidine rings of Z-pro-prolinal, that generated the Z-thiopropylthiaprolinol derivative, improved the K_i by two orders of magnitude [131]. In contrast, large extensions of the prolinal inhibitor towards the P_3 and P_4 positions did not improve at all the efficacy of the former molecule [132]. A large number of the inhibitors that have been developed afterwards have been derived from the Z-pro-prolinal scaffold. Some of them have been used in clinical studies such as for example ONO 1603 [133] and JTP-4819 [134], see table 1.

Another family of inhibitory prolyl oligopeptidase compounds were based on the derivatization of the pyrrolidinecarbonyl function, like SUAM-1221 in table 1. This pyrrolidinecarbonyl moiety occupies the P_1 position, whereas it is escorted by a central proline like ring that is accommodated in the S_2 pocket and by an alkylaryl amino terminal group that has to interact with the S_3 pocket [135]. Also in this case, exchanging the pyrrolidine group for thiazolidine moieties by insertion of a sulfur atom in the pyrrolidine ring improved the selectivity of the inhibitors [136].

Furthermore, methyl ketone derivatives of substrate analogues were assayed as potential inhibitors. Interestingly, the *modus operandi* of such molecules were found to depend on the peptidic moiety of the inhibitor. Thus, Z-ProPro- $\text{CH}_2\text{N}^+(\text{CH}_3)_3/\text{Cl}^-$ was found to be a slow-tight binding inhibitor while Boc-PhePro- $\text{CH}_2\text{N}^+(\text{CH}_3)_3/\text{Cl}^-$ was found to behave like a simple competitive inhibitor [137].

Another successful group of prolyl oligopeptidase inhibitors were developed on the basis of peptidyldiazomethanes, illustrated in table 1. Originally, the diazomethane derivatives were considered as inhibitors formulated for the specific inactivation of cysteine peptidases by the alkylation of their active cysteines. Otherwise, this kind of molecules were rarely able to inhibit the classical serine peptidases [138]. Interestingly, prolyl oligopeptidase, again in contrast to the classical serine peptidases, was inhibited by peptidyldiazomethanes compounds [138]. The mode of action of these compounds is working again through a competitive slow-tight binding mechanism in which the

diazomethane molecule establishes interaction with active Ser⁵⁵⁴ and not with the Cys²⁵⁵ [138]. As noted above, the enzyme was found to be inhibited by p-chloromercuribenzoate, a general inhibitor of cysteine peptidases. Initially, this caused some doubts about the chemical category of the enzyme [129]. However, it was later solved by the results obtained from smaller thiol modifying reagents. Thus, in comparison to p-chloromercuribenzoate and N-ethylmaleimide, other reagents, such as iodoacetamide, were not able to block completely the enzyme activity, suggesting that the modified cysteine was only an active site related residue, actually the Cys²⁵⁵ [98]. Some efforts have been made to take profit of the reactivity of Cys²⁵⁵ in order to produce prolyl oligopeptidase specific inhibitors.

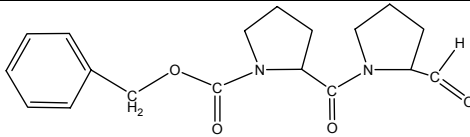
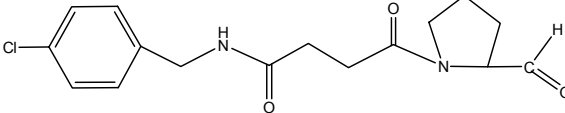
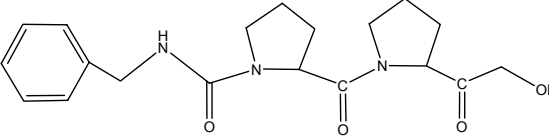
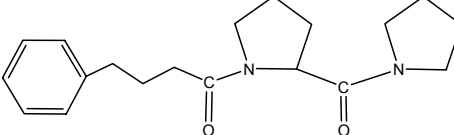
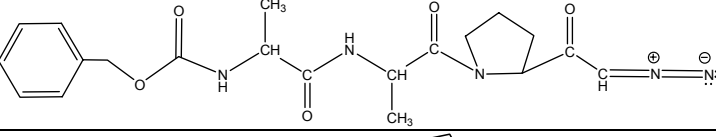
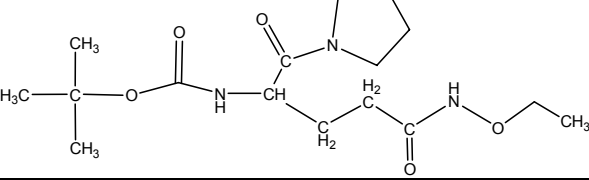
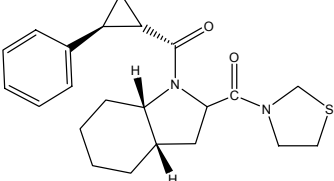
Name	Molecular structure	Ki (nM)	Ref.
Z-pro-prolinal		14	[128]
ONO-1603		12	[133]
JTP-4819		0.045	[134]
SUAM-1221		30	[136]
Diazomethane derivative		169	[138]
Hydroxylamine derivative		30	[139]
S17092		8.3	[140]

Table 1 Table summarizing the molecular structure of the most relevant synthetic prolyl oligopeptidase inhibitors. Ref. stands for reference.

It is known that N-peptidyl-O-acyl hydroxylamines can be effective and selective inhibitors of thiol-dependent enzymes [141]. The diacyl hydroxylamines derivatives are flexible to the variation on the N-acyl (R_1) and O-acyl (R_2) molecule arms, R_1 -CO-NH-O-CO- R_2 , allowing the selective control of their affinity and selectivity towards a studied enzyme. A substrate analogue of prolyl oligopeptidase was synthesized using the O-acyl hydroxylamine moiety, Boc-Glu(NH-O-Ac)pyrrolidide, illustrated in table 1. The mechanism of action was found to show a time dependent pattern. The recovery of the activity of a previously inhibited enzyme demonstrated the reversibility of such process, thus demonstrating that the catalytic triad was not affected. The inability of newly added inhibitor to depress the activity of an enzyme previously inhibited by O-acyl hydroxylamine, suggested that the active site related cysteine was actually the target of the inhibitor modification [139] and therefore the inhibitor had been processed by the enzyme as it had been a substrate.

Additionally, some molecules have been isolated from several biological sources which were found to act as prolyl oligopeptidase inhibitors. The microbial Eurystatin A and B are such examples. These are molecules obtained from the *Streptomyces eurythermus* that are composed of a 13-membered cyclic peptide core with an ornithine attached beta unsaturated fatty acid. Their mechanism is competitive towards the prolyl oligopeptidase from *Flavobacterium meningosepticum* [142]. Like Z-pro-prolinal, Eurystatin A and B were able to reverse the scopolamine-induced amnesia in rats [143].

Furthermore, methanolic extracts from roots of the *Rhodila sachalinensis* plant uncovered the prolyl oligopeptidase inhibition of five monoterpenoid molecules in addition to a structurally variety of twenty-two other molecules [144]. The inhibitory action tested on the recombinant *Flavobacterium meningosepticum* prolyl oligopeptidase usually showed non-competitive patterns. It is possible to find in that sense many other examples in literature. Such isolated inhibitors have generally a rather strong lipophilic character that might disturb the three-dimensional structure of the enzyme to such extent that they might inactivate it by a uncompetitive inhibition.

2.0 Materials and methods.

2.1 Cloning of the human prolyl oligopeptidase coding sequence.

To initiate the cloning, total RNA was isolated from cultured U343 astrogloma cells. For that TRIzol[®] reagent from GibcoBRL was used proceeding as indicated on the instructions manual. The spliced mature mRNA was immediately converted to a more stable pool of cDNA by means of reverse transcriptase polymerase chain reaction. For that invitrogen[®] Super Script[™] II Reverse transcriptase kit was used. The manufacturer recommendations, with minor modifications, were followed. Obtaining of the cDNA pool was achieved as it is schematically described in table 2.

Synthesis of the primary cDNA pool	
Reaction mixture	procedure
1 μ l 100 μ g/ml Oligo (dT) ₂₀ 1 μ l dNTP Mix 5 μ l 200 μ g/ml total RNA 6 μ l Sterile distilled water	heated up to 65°C for 5 minutes and immediately chilled on ice.
4 μ l 5X First-Strand Buffer 2 μ l 0.1M DTT	Incubation at 42°C for 2 minutes.
1 μ l SuperScript [™] II RT polymerase	Incubation at 42°C for 60 minutes.
Enzyme inactivation by incubation at 70°C for 20 minutes.	
1 μ l RNase H	Incubation at 37°C for 30 minutes.

Table 2 Schematic summary of the reagents, times and temperatures used for the synthesis of the cDNA pool. The reaction mixture describes the volumes of the respective reagents added subsequently up to a final 20 μ l reaction volume. On the right boxes are described the time and incubation temperatures applied during each step.

As shown in table 2 the synthesis of the cDNA began with the addition of 1 μ l SuperScript[™] II RT polymerase (200 units). Then, an incubation at 42°C lasted for 60 minutes. Finally, the reaction was inactivated by heating the mixture at 70°C for 20 minutes. The RNA-cDNA hybrid was subsequently removed by adding 1 μ l of endoribonuclease Rnase H (2 units) and incubating the mixture at 37°C for 30 minutes. This cDNA pool was a suitable biological material in order to amplify the coding sequence of the target enzyme. Therefore, gene specific primers (GSP) were used in order to specifically amplify the sought prolyl oligopeptidase coding sequence. For that a PCR reaction was performed. The reaction was performed in a PCR thermocycler programmed as detailed below in table 3.

PCR mixture	Thermocycler programm	Cycles
1.0 µl cDNA		
2.5 µl 10X pfu buffer	[d] 95°C 5 minutes	1X
0.5 µl dNTPs	[d] 95°C 45 seconds	} 30X
0.5 µl GSP hPEPEcoRI3'	[a] 60°C 45 seconds	
0.5 µl GSP hPEPNdeI5'	[p] 75°C 4 minutes	
0.5 µl Pfu polymerase	[p] 75°C 10 minutes	1X
19.5 µl Sterile bidistilled water		

Table 3 Amplification of the coding sequence of the prolyl oligopeptidase gene by PCR. On the left box are summarized the different mixed reagents. Thermocycler programm is summarized in the right box. It describes the followed cyclic set of temperatures and times. nX stands for the number of times that the noted temperature/time cycle was repeated. The parenthesis denotes that the set of temperatures constitute a single cycle of three different steps. The letters between squared parenthesis stand for, d, denaturation, a, annealing and p, polymerization.

As a result of the PCR reaction described above, table 3, a strong single band was visible in an 0.8% (w/v) agarose electrophoresis gel. This single band was standing at the height of 2.1 kba in comparison to the DNA ladder. Several parallel PCR reactions like the one described above in table 3 were performed. The obtained single bands were finally gel extracted from a preparative 0.8% (w/v) agarose gel by means of a silica based column chromatography, a kit purchased to Genomed. The quality and integrity of the extracted band were controlled in a new analytic 0.8% (w/v) agarose gel. Afterwards, the isolated DNA fragments were pooled and precipitated overnight as described in table 4.

DNA precipitation
1 volume DNA fragment
1/10 volume 3M Sodium Acetate
3 volumes 100% (v/v) Ethanol
Incubation overnight at -20°C
DNA pellet in a top-table microcentrifuge 1 hour at 13'000 rpm at 4°C
Discard the supernatant
Wash pellet with a prechilled 70% (v/v) ethanol solution
DNA pellet in a top-table microcentrifuge 3 minutes at 13'000 rpm and 4°C
Discard the supernatant
Air dry the DNA pellet for 20 minutes at room temperature
Finally redissolve the DNA in 10µl tridestilled sterile water

Table 4 Schematic description of the established protocol for DNA precipitation.

The precipitated DNA was then sub-cloned into the commercial pPCR-Script Cam SK(+) vector, see appendix table 39. The commercial PCR-Script® Cam cloning kit (Stratagene) was used following the provider recommendations in order to sub-clone the precipitated DNA, see table 5. The new obtained construct was finally transformed

in DH5 α competent cells (Invitrogen). The selection of the positive clones was made following a blue/white colony screening [145].

Sub-cloning reaction mixture	
1.0 μ l pPCR-Script Cam SK(+) cloning vector 1.0 μ l PCR-Script 10X reaction buffer 0.5 μ l 10 mM rATP 5.5 μ l blunt-ended prolyl oligopeptidase DNA fragment 1.0 μ l Srf I endonuclease 1.0 μ l T4 DNA ligase	1hour incubation at room temperature

Table 5 Cloning reaction performed following the recommendations indicated on the protocol of the pPCR-Script[®] Cam cloning kit (Stratagene).

Out of several clones one clone was selected for DNA sequencing in order to confirm the identity and quality of the cloned sequence. Thus, the first stable plasmid construct, pDRC1, was obtained.

The next was to clone the enzyme sequence into a bacterial expression vector. For that the commercial pET-28a(+) vector (Novagen) was chosen. Both, the pDRC1 construct and the empty pET-28a(+) vector were produced in large amounts by culturing their *Escherichia coli* clones for DNA Midiprep plasmid isolation (Genomed). Both isolated plasmids were handled in parallel for a direct cloning. The plasmids were digested with the Nde-I and EcoR-I endonucleases, as described in table 6.

Plasmid restriction	
18.0 μ l plasmid (pET-28a(+) or pDRC1) 2.5 μ l 10X BSA 2.5 μ l buffer n°4 from NEB 1.0 μ l NdeI endonuclease 1.0 μ l EcoRI endonuclease	Incubation at 37°C for 3 hours

Table 6 Plasmid restriction reaction used for the direct cloning of the prolyl oligopeptidase coding sequence into the commercial vector pET-28a(+). On the left box are detailed the reagents mixture used to accomplish the DNA digestion. On the right box are described the used temperatures and times conditions.

The restricted plasmid fragments were isolated from 0.8% (w/v) agarose gels. A 2.1 kba fragment for the prolyl oligopeptidase and a 5.4 kba fragment for the vector were selected. The DNA fragments were precipitated as described in table 4 and afterwards they were ligated following the reaction mixture described in table 7. This allowed us to obtain the plasmid pDRC3 as appropriate expression construct.

The two main features of the resulting construct (see appendix table 39) ought to have the cloned enzyme sequence in frame with an amino terminal hexahistidine tag and to

have, furthermore, a T7 RNA polymerase promoter that controls the expression of the non-native protein mRNA.

Ligation	
5 μ l NdeI/EcoRI digested prolyl oligopeptidase coding sequence	Ligation overnight at 12°C
3 μ l NdeI/EcoRI digested pET-28a(+) vector	
1 μ l T4 ligase	
1 μ l 10X T4 buffer	

Table 7 Ligation reaction of the DNA fragments for the direct cloning of the prolyl oligopeptidase coding sequence into the commercial vector pET-28a(+).

2.2 Site directed mutagenesis.

The expression construct pDRC3 was used as a template to generate by means of site directed mutagenesis different enzyme variants of the recombinant prolyl oligopeptidase. The basis of the method leans on the DNA methylation tagging exerted by *E. coli* cells. An *in vitro* PCR amplification of the whole pDRC3 construct produced the desired mutated DNA molecules but lacking the original methylation pattern present otherwise in the parental DNA. The use of DpnI endonuclease allowed us to discriminate between parental DNA, methylated, and the newly mutated DNA, as only the former was digested. The adequate design of oligoprimers (see appendix table 41) permitted the insertion of the aimed DNA mutations. Following this strategy the pursued enzyme variants R643K, R643A, W595A, W595Y, W595F, F173A, M235A, M235I and C255A were generated.

2.3 Expression of the recombinant human prolyl oligopeptidase.

Once the prolyl oligopeptidase DNA coding sequence was successfully cloned as described in section 2.1, the expression of the protein was faced. The pET-28a(+) is a bacterial expression vector. The establishment of an expression protocol was carried out at the beginning with two different *E. coli* strains, BL21(DE3) (Invitrogen) and Rossetta(DE3) (Novagen) cells, which phenotypes show impoverished endogenous proteosoms and that carry genes encoding rare tRNAs. It was found, from the initial expression tests, that the expression of the heterologous protein was significantly better achievable with the BL21(DE3) than with the Rossetta(DE3) strain. A clone designed as pDRC3-1B1 was selected as expression candidate. The established protocol initiated expressions inoculating a pre-culture of 300 ml LB medium saturated with 100 mg/l kanamycin antibiotic. The inoculum of this pre-culture was always the glycerol stock of the clone of pDRC3-1B1. This pre-culture was grown overnight in an Infors shaker device (Infors) at 37°C in a shaking flask with 140 rpm orbital frequency. The following day a six liters total expression volume was usually carried out. In three-

liters flasks one liter LB medium saturated with 100 mg/l kanamycin antibiotic was used as unit of expression. 2 ml of the pre-culture was used to inoculate the expression cultures. The incubation at 37°C of these expression cultures, shaking at 140 rpm orbital frequency, usually lasted until an approximate OD₆₀₀ of 0.5 was reached. Then, parallelly, the incubation temperature was decreased down to 25°C [146] and a 2% (v/v) ethanol was added to the expression cultures [147]. After 45 minutes, the expression of the non-native protein was induced by adding to the cultures IPTG to a final 1 mM concentration. Usually the expression lasted for an interval of 4 hours. The cell biomass was then separated from the culture medium by pelleting the cells at 12'200 xg in a JLA8.1000 rotor (Beckman/Avanti J-20) for ten minutes. The cultures supernatant was discarded while the remaining cell biomass was resuspended in an appropriate volume of phosphate buffer, 50 mM NaH₂PO₄ pH 7. This solution was stored at -80°C until it was required.

2.4 Purification of the recombinant human prolyl oligopeptidase.

The biomass obtained with the above detailed expression protocol, section 2.3, needed to be pretreated before the purification was faced. After a gentle thawing of the samples at room temperature, the obtained cells were mechanically disrupted with a French Press device (Thermo IEC) [148]. Usually 1000 psi pressure rates were applied to the samples. A controlled sharp stepwise decrease of the pressure in the press chamber disrupted the cells, hence delivering their inner content. The thus generated cell debris were afterwards separated from the soluble content by pelleting them at 35'000 xg in a JLA16.250 rotor (Beckman /Avanti J-20) at 4°C for one hour. The pellet was discarded and the supernatant was diluted one-fold with pre-chilled phosphate buffer, 50 mM NaH₂PO₄ pH 7. This solution was then saturated up to 1 M NaCl and 20 mM Imidazol. Finally, the solution was filtrated with the help of a vacuum pump, first with Whatman microfiber filters and afterwards with Millipore nitrocellulose, 0.8 µm pore, filters. The resulting sample was used to initiate the chromatographic purification. For the purification of the overexpressed non-native protein standard chromatographic techniques were used. The chromatographic conditions were controlled with the help of an Äkta purifier[®] device (Amersham biosciences). The purification was carried out using always C10/10 columns (Amersham biosciences) at a temperature of 4°C. Three steps were necessary to accomplish the isolation of the recombinant protein.

The purification typically started with a chelating sepharose chromatography, IMAC. A hexahistidine tag, His_{x6}, was cloned in frame with the amino terminal sequence of the heterologous protein to allow during the purification the specific separation of the target protein. The specific interaction between the protein His_{x6} and an iminodiacetic acid

chelated transition metal, usually nickel, constitutes the main potential interaction between the chromatographic solid phase and the heterologous protein in an IMAC. This interaction allowed the separation of the non-native protein by affinity. The most relevant parameters associated to the chelating sepharose chromatography are listed in the table 8.

The elution of the adsorbed proteins appeared as a broad single peak as result of an increase of absorbance measured at 220 nm (see appendix table 40). This peak was always associated to the expected PEP-like activity.

Chelating sepharose	
Stationary phase: Cross-linked agarose, 6%, coupled to iminodiacetic acid groups	
Stationary phase volume	6 ml
Mobile phase	
Equilibration buffer	20 mM Imidazol/ 50 mM NaH ₂ PO ₄ / 1 M NaCl; pH 7
Elution buffer	500 mM Imidazol/ 50 mM NaH ₂ PO ₄ / 1 M NaCl; pH 7
Flow rate	2 ml/min
Fractions volume	2 ml
Gradient	96 ml linear between 0% and 100% elution buffer

Table 8 Summary of the basic parameters established for the performance of the IMAC chromatography.

The thus characterized eluent was pooled and afterwards it was dialyzed overnight against 4 liters of 50 mM NaH₂PO₄/ 1 mM DTT; pH 7 buffer.

The following chromatographic step in the purification involved a Q sepharose column. The expected pI value of the human prolyl oligopeptidase is mildly acid, 4.8 [35]. This ensures that the heterologous protein in the equilibration buffer conditions of the table 9 to be negatively charged. Hence, electrostatic interactions might allow the interaction between the heterologous protein and the cationically derivated solid phase of the Q sepharose column. The heterologous protein usually eluted early as the main peak of the chromatogram (see table 40 in appendix).

In the last purification step a phenyl sepharose column was applied. The selected active fractions from the previous step were pooled. The obtained sample was then saturated up to 30% (w/v) with (NH₄)₂SO₄. This step was carried out at 4°C, adding little by little the (NH₄)₂SO₄ powder to the stirring solution.

Q sepharose chromatography	
Stationary phase: 6% Cross-linked agaros coupled to quaternary ammonium groups	
Stationary phase volume	6 ml
Mobile phase	
Equilibration buffer	1 mM DTT/ 50 mM NaH ₂ PO ₄ ; pH 7
Elution buffer	1 mM DTT/ 50 mM NaH ₂ PO ₄ / 1 M NaCl; pH 7
Flow rate	2 ml/min
Fractions volume	1 ml
Gradient	94 ml linear between 0% and 50% elution buffer

Table 9 Summary of the basic parameters established for the performance of the Q sepharose chromatography.

The thus prepared sample was then loaded into the phenyl sepharose column pre-equilibrated with the equilibration buffer outlined in table 10. This salting-in has a global chaotropic protein surface dehydrating effect that leads to a slight increase of the surface protein hydrophobicity. Here then, favoured non-polar contacts allowed the adsorption of the heterologous protein to the phenyl column stationary phase. A controlled salting-out elution allowed the final separation of prolyl oligopeptidase as a pure protein, appendix table 40 and figure 6.

Phenyl sepharose chromatography	
Stationary phase: Cross-linked agarose, 6%, coupled to phenyl groups	
Stationary phase volume	6 ml
Mobile phase	
Equilibration buffer	1 mM DTT/ 50 mM NaH ₂ PO ₄ / 30% (w/v) (NH ₄) ₂ SO ₄ ; pH7
Elution buffer	1 mM DTT/ 50 mM NaH ₂ PO ₄ ; pH7
Flow rate	2 ml/min
Fraction volume	1 ml
Gradient	65 ml linear between 100% and 0% equilibration buffer

Table 10 Summary of the basic parameters established for the performance of the phenyl sepharose chromatography.

2.5 Dialysis and ultrafiltrations.

Dialysis is a technique used for the replacement of buffer components or for salt removal driven by a salt gradient mechanism [148]. Dialysis were conducted in cellulose based membranes with a molecular weight cut-off of 14 kDa (Roth).

Ultrafiltration is an useful technique for the concentration of biological samples that works on the basis of the differential flow rates of the different solutes of a solution through an ultrafiltration membrane [148]. Ultrafiltrations were conducted with a commercial kit (Vivasciences), following the suppliers recommendations, on cellulose based membranes with a 30 kDa molecular weight cut-off.

2.6 Protein content determination.

Two different methods were used for the determination of the protein content. One was the Bradford assay and the other was the measurement of absorbance at 280 nm. Both methods are based on spectrophotometric determinations that follow the Lambert-Beer law, equation 1 [149], where ϵ stands for extinction coefficient, c for the sample concentration and l for light pathlength.

$$A = \text{Log}(I_0/I) = \epsilon cl \quad \text{equation 1}$$

In the Bradford assay a dye, brilliant blue G250, forms in solution a stoichiometric complex with proteins. The protein–dye complex causes an absorption shift, from 465 to 595 nm, in the absorption maximum of the dye. Therefore, the amount of absorption at 595 nm is proportional to the amount of protein. In our case, a standard Bradford assay entailed the mixture of 25 μl of protein solution with 750 μl of Bradford reagent (Sigma). It followed a 5 minutes incubation at room temperature in darkness. Finally, the measurement of the absorbance at 595 nm allowed us to obtain the protein content by extrapolation from a standard curve.

The measurement of protein content might be done also by measuring directly the absorbance at a given wavelength, i.e. 280 nm. Therefore, in this case it is only possible to measure solutions of purified protein as the extinction coefficient, ϵ in equation 1, is a defined constant of each molecule. ϵ is a given value that can be inferred from the protein primary sequence, absorbance (A) is the measurable parameter and l is the path length of the light absorbing sample, which is usually known. Therefore, the calculation of the protein content of a solution of prolyl oligopeptidase was a direct and simple step for purified protein.

2.7 Enzymatic activity measurement.

The enzymatic activity measurements using spectrophotometric techniques, when possible, are of the most manageable and straightforward methods. Fluorescence is the physicochemical phenomenon in which a molecule can be electromagnetically excited. The excitation of a fluorophore entails that a permitted energetic transition of one of its electrons reverse to the energetic ground state by the emission of a photon

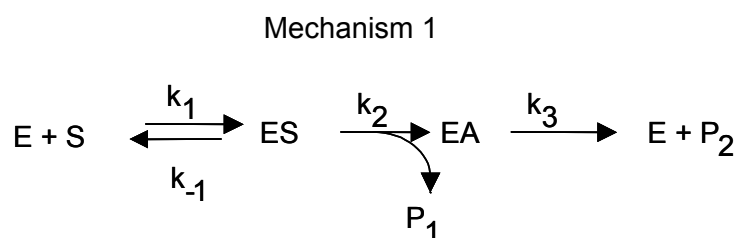
[148]. Here, specially useful are the 7-amido-4-methylcoumarin, AMC, peptidic derivatives. The free AMC group, but not the derivatized peptide, is a good fluorogenic molecule that might be excited at 380 nm and that emits at 460 nm. The peptide AMC derivatives contain a pseudo-peptide bond that links the AMC moiety to its peptidic counterpart. Therefore, can be unequivocally be related the increase of measurable fluorescence at 460 nm with the enzymatic liberation of free AMC.

An additional useful type of fluorogenic peptidase substrates are the defined as fluorescence resonance energy transfer, FRET, based substrates. This kind of substrates, as well known as internally quenched substrates, provide an overlap between the fluorescence spectrum of a donor moiety and the absorption spectrum of an acceptor moiety. In this case the energy might be transferred from the donor to the acceptor fluorophore. The efficiency of this energetic transfer is related to the spatial separation between both interacting moieties [148]. These principles are followed by peptides labelled with the Dabcyl/Edans moieties [150]. The digestion of the leading peptide nullfills the FRET effect of the Dabcyl/Edans pair, deriving in increments of fluorescence at 490 nm of the Edans group, after excitation at 340 nm.

Actually, the fluorescence measurements are recorded in relative units of fluorescence, RFU, that have no biological significance. This problem can be easily overcome by plotting the linear stoichiometric correlation between the RFU and the concentrations of the free fluorophore.

2.7.1 Kinetic measurements.

The use of the above described fluorogenic substrates represents a valuable tool to investigate the kinetic parameters associated with their hydrolysis. The kinetic mechanism followed by a peptidase like prolyl oligopeptidase is described by mechanism 1 shown in scheme 1 [79].



Scheme 1 Schematic depiction of the catalytic mechanism followed by prolyl oligopeptidase. E stands for enzyme, S for substrate, ES enzyme-substrate complex, EA acyl-enzyme complex, P₁ amino terminal leaving peptide, P₂ carboxy terminal leaving moiety. k_n denotes the respective rate constants that control the conversion between two different reaction steps.

An unireactant enzymatic reaction mechanism, scheme 1, can be characterized on the basis of the classical enzyme kinetic theory. In that sense, the most important assumption is that the enzyme-substrate complex, ES, should achieve the steady-state during the measurement interval. This basically means that $d[ES]/dt=0$. The steady-state requisite allows to correlate the different single rate constants noted in the mechanism 1 to a further more elaborated macroscopic complex constants that can be directly inferred from measurement of the initial velocities rates, see scheme 1. That means, the measurement of $-d[S]/dt$ or $d[P]/dt$. These constants are defined as Michaelis-Menten, K_m , and the turnover constants, k_{cat} . The plot of the measured initial velocities of hydrolysis, namely $-d[S]/dt$ or $d[P]/dt$, against their relative substrate concentration fits to a quadratic hyperbolic curve, equation 2, of which the steady-state K_m constant can be inferred [151].

$$V = V_{max}[S]/(K_m + [S]) \quad \text{equation 2}$$

2.7.2 Michaelis-Menten constant, K_m .

Experimentally a K_m constant could be measured in a 96-well microplate fluorescence reader. For a given substrate concentration 200 μ l PEP buffer (see appendix), 50 μ l substrate solution and 20 μ l enzyme solution were mixed. Typically the substrate concentrations used were in the range of 1/10- to 4-fold of the K_m constant. Each substrate concentration was measured with three replicas. The buffer and enzyme were usually mixed and pre-incubated at 37°C. The reaction was initiated by adding the substrate solutions in an inverse concentration order, starting with the lowest and finishing with the highest concentration. The record of increments of RFU was taken care to have a linear shape in order to meet the steady-state requirement. The thus obtained raw data were fitted to the equation 2 by means of the software Grafit.

2.7.3 Turnover constant, k_{cat} .

The value of the turnover constant, k_{cat} , is inferred from the obtained velocities when the kinetic reaction rate constant becomes zero at high substrate concentration. This situation is found in the asymptotic range of the hyperbolic Michaelis-Menten curve. On this range the enzyme achieves the maximal kinetic capacity which is expressed as the maximal measurable initial velocity, V_{max} , at the given steady-state. The turnover constant can be then calculated as follows, equation 3 [151].

$$V_{max} = k_{cat} [E] \quad \text{equation 3}$$

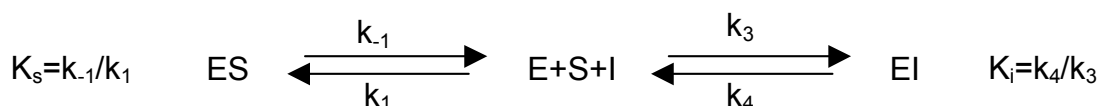
2.7.4 Specificity constant, k_{cat}/K_m .

The k_{cat}/K_m constant could be computed by direct calculation of the data obtained as described above in the sections 2.7.2 and 2.7.3.

2.7.5 Inhibition constant, K_i .

The measurement of an inhibitor K_i constant is an estimation of the affinity of the inhibitory molecule, I, for the enzyme. Depending on the mechanism of interaction of the molecule with the enzyme, inhibitors can be basically classified as competitive, non-competitive or uncompetitive [151]. The measurement of such constant can be related in any case to the steady-state and therefore it might be derived from the measurement of initial velocities.

Mechanism 2



Scheme 2 Representation of the binding mechanism of a competitive inhibitor, I, to an enzyme, E, in presence of the substrate, S. The related affinity constants of the substrate-enzyme complex, K_s , and the inhibitor-enzyme complex, K_i are described.

The molecules used in this work followed the mechanism depicted in scheme 2, that is a competitive inhibitory mechanism. The main feature of this mechanism is that inhibitor and substrate bind to the same enzyme locus, the active site. That is, the binding of either substrate or inhibitor is reciprocally exclusive. The presence of the inhibitor affects the steady-state and this influence can be described in terms of a modified Michaelis-Menten as described in equation 4 [151].

$$V = V_{max} [S] / (K_m (1+[I]/K_i) + [S]) \quad \text{equation 4}$$

It can be noticed from the analysis of the equation 4 that a competitive inhibitor influences the K_m by increasing its value in a inhibitor dependent manner by a factor of $(1+[I]/K_i)$. In practice, the determination of the K_i value is performed by measuring the different K_m constants, basically as noted above in section 2.7.2, but in the presence of different concentrations of inhibitor. The re-plot of the inverse of the initial rates against inhibitor concentrations follows a linear correlation with positive slopes known as Dixon plot. Different substrate concentrations should give Dixon plots that converge in the negative range of the abscissa axis precisely at the negative value of the sought K_i constant for the characterized molecule [151].

2.7.6 IC₅₀ constant.

The measurement of the IC₅₀ constant outstands because of its simplicity. The meaning of this constant is yet very limited. IC₅₀ is a pharmacologically useful parameter that reveals 50% of inhibition found at a given substrate concentration. The IC₅₀ is actually a particular case of a K_i constant measurement, it could be approximated to K_i by using the relationship of equation 5 [152].

$$K_i = IC_{50}/(1 + [S]/K_m) \quad \text{equation 5}$$

2.7.7 Slow-tight binding Inhibition.

Slow-tight binding inhibition is a special case of competitive inhibition. Normally, a classical competitive inhibition is characterized by large diffusion rate constants, namely k_3 and k_4 on mechanism of scheme 2. That means that although the inhibitor might have a strong tendency to occupy the enzyme active center, it would not have the capacity to prolong its residence and it would rapidly diffuse out again. The slow-tight binding inhibitors differ from the classical competitive inhibitors on the fact that the molecule-protein interaction is of high affinity and the equilibria between the enzyme, inhibitor and enzyme-inhibitor complex take place on a steady-state time scale of seconds to minutes [153].

Two different mechanisms have been proposed for the slow-tight binding inhibition. One, mechanism A, consider that the inhibitor rate constants of diffusion into and from the enzyme active center, k_3 and k_4 , are relatively small but driving to the formation of a very stable EI* complex. The other possible mechanism, mechanism B, consider that after a rapid enzyme-inhibitor complex formation, EI, an isomerization-like process occurs leading to a new enzyme-inhibitor complex, EI*, with an increased affinity. This EI* complex would be attained through a new equilibrium between EI and EI* controlled with the rate constants k_5 and k_6 [153].

In practice, the characterization of a slow-tight binding inhibition requires the characterization of the inhibitors in function of time. Actually, the basic definition of slow-tight binding mechanism is that of an inhibitor that exerts its function in a time depending manner. Therefore, in a slow-tight binding inhibition the variation of initial velocities between the starting and the final steady-state velocity as a function of time can be fitted to the integrated equation 6 [153].

$$P = V_s t + (V_0 - V_s)(1 - e^{-k_{obs} t})/k_{obs} \quad \text{equation 6}$$

Experimentally, the concentration of enzyme has to be rather low in order to avoid the interference of a substrate depletion effect with the progress curve. The progress curve of the substrate hydrolysis is measured within a wide range of inhibitor concentrations

for a given substrate concentration. The reaction without inhibitor serves as a control that no substrate depletion interferes. The reproduction of the same reaction profile but with different substrate concentrations allows to complete the experiment. The fitting of the resultant progress curves to the equation 6 allows to obtain the k_{obs} . This k_{obs} accounts for the rate of formation of the EI* complex. Afterwards, the correlation of the inferred k_{obs} with their respective inhibitor concentration for a given substrate concentration allows to differentiate between the above described mechanisms A or B. In case that the molecule follows the mechanism A, the inhibitor concentration and the calculated k_{obs} maintain a linear correlation driven by the equation 7 [132;154], in opposite case the mechanism B shows a hyperbolic correlation.

$$k_{obs} = k_4 + k_3 [I]/(1+[S]/K_m) \quad \text{equation 7}$$

Moreover, we treated the data as described elsewhere [132] where k_{obs} were fitted to equation 8.

$$K_{obs} = k_{off} + k'_{on}[I] \quad \text{equation 8}$$

k'_{on} was corrected for substrate competition applying equation 9 [132].

$$k_{on} = k'_{on}(1+[S]/K_m) \quad \text{equation 9}$$

To provide an accurate estimation of k_{off} the values were calculated using equation 10 [132]

$$k_{off} = k_{on}K_i \quad \text{equation 10}$$

The measurement of slow-tight binding inhibitors entails the handling of rather large amount of raw data that were computed with the software Prism.

2.7.8 Rate constants temperature dependence. Arrhenius and Eyring plots.

The temperature dependence of a chemical reaction is described to be influenced by temperature. The equilibrium constant that describes a chemical reaction follows a linear correlation with the inverse of the temperature. This relation is known as the van't Hoff reaction isochore and entails a measurement in a constant reaction volume [155]. The same principle can be applied if the catalysis is enzymatic. The van't Hoff isochore is the basis where the Arrhenius treatment is derived off. Arrhenius approach describes that rate constants of enzymatic reactions are sensitive to the temperature as follows in equation 11 [155].

$$K = P \exp[-E_a/(RT)] \quad \text{equation 11}$$

Arrhenius is actually an approach with empirical character. E_a stands for the minimal energy that reactants must have to form products and the pre-exponential factor, P , is a measure of the rate of collisions that occur irrespective of their energy [156]. Arrhenius might be seen as an approximation of the Eyring transition state theory. The

main assumption of the Eyring theory is that reactants end in products through an intermediate energetic activated state, known as transition state. In principle the theory allows relating the equilibrium constant for the formation of the transition state with the rate constant of the reaction by the expression of equation 12, known as Eyring equation [155].

$$k = \kappa (k_B T/h) K^\ddagger \quad \text{equation 12}$$

On the other hand, an enzymatic equilibrium constant can be expressed as described by the Gibbs-Helmholtz equation, equation 13 [155].

$$K^\ddagger = \exp (-\Delta G^{\ddagger 0}/RT) \quad \text{equation 13}$$

of equations 12 and 13 can be inferred equation 14 [155].

$$\ln(k/T) = [\ln \kappa + \ln (k_B/h) + \Delta S^{\ddagger 0}/R] - \Delta H^{\ddagger 0}/(RT) \quad \text{equation 14}$$

Therefore, with the Eyring approach they might be obtained directly the values of the thermodynamic parameters $\Delta H^{\ddagger 0}$ and $\Delta S^{\ddagger 0}$ that are associated to the studied transition state of the characterized rate constant. Experimentally, the measurement of rate constants dependence on temperature were performed by measuring the Michaelis-Menten and turnover constants as described above in sections 2.7.2 and 2.7.3 for the different temperatures ranging from 25°C up to 45°C. The data were computed as described elsewhere [157;158] using the software Excel.

2.8 Mass spectrometry.

Mass spectrometry is a direct and rapid method in order to characterize enzymatic activity. For that stands the matrix assisted laser desorption-ionization time of flight mass spectrometry, MALDI-TOF-MS, as a very useful technique for the characterization of peptidase activity. MALDI-TOF-MS takes profit of the interaction between the ultraviolet laser irradiation and some organic molecules. The principle establishes that the sample to analyze is mixed with a so-called matrix solution, that usually is formed by small organic molecules. In vacuum conditions, with an appropriate ultraviolet laser source, the matrix is excited. Theoretically, the electronic excitation of the π -electron aromatic system of the matrix molecules results in a thermal imbalance. This brings the matrix molecules to a phase transition by liberating molecules to the gas phase. In that context, proximal sample molecules reach synergistically the gas phase [148]. It has been experimentally demonstrated how during that process the matrix plays a central role in the ionization of the sample molecules. The ions that reach the gas phase find an electric field whose potential accelerates them. Then, the ionized molecules leave the source of ionization and flight through a concrete distance free of electric field until a mass spectrometer detector is

reached. Hence, at a given electric potential, molecules will spend different intervals to cross the distance between the source and the detector plates, always as a function of their mass. The measurement of such time enables to compute the ratio between the masses and the number of charges of the ionized molecules, m/z , following the equation 15 [148].

$$m/z = 2eUt^2/L^2 \quad \text{equation 15}$$

In frame of the MALDI-TOF mass spectrometry it is possible to characterize the peptidase activity of an enzyme as the hydrolysis of a putative substrate will result in peptides with recognizable different masses. A standard MALDI-TOF-MS experiment for the measurement of prolyl oligopeptidase activity was performed at 37°C. The peptide substrates were solved in water, as long their solubility allowed. In case that a peptide could have solubility problems it usually was solved in DMSO as stock-solution and consequently it was diluted in water. One volume of peptide solution was mixed with one volume of PEP buffer (see appendix). The peptide concentrations usually ranged between 0.5 and 1 mg/ml and a maximal 5% (v/v) DMSO concentration, if it proceeded, was accepted. This solution was then mixed with the enzyme in appropriate volumes in order to reach typical enzyme concentrations of 50 nM. The mixture was then incubated throughout time. At given time-points 10 µl samples were collected and mixed with 10 µl of 0.1% (v/v) TFA solution. This stopped any enzymatic reaction by acidic denaturation of the proteins. These samples needed then to be treated in order to mix them with the matrix solution. For that a commercial ZipTip_{C18} kit (Millipore) was used following the supplier recommendations. ZipTip_{C18} is a microscale reverse phase chromatographic based technology that allows the isolation, desalting and finally matrix mixture, prior to a MALDI-TOF-MS measurement of peptides up to 50 kDa molecular weight. The MALDI-TOF-MS measurements were recorded in a Voyager-DE™ PRO device (Applied biosystems).

2.9 SDS-PAGE.

Electrophoresis is a technique that was born on hands of the Swedish scientist Arne Tiselius [148]. If there is a common technique for protein characterization used in molecular biology laboratories this is the sodium dodecyl sulfate polyacrylamide gel electrophoresis, SDS-PAGE, a method introduced by Laemmli. In principle, a solid porous gel of polyacrylamide is mounted in an appropriate system. The system makes possible to apply an electric field through the gel, that during the process remains soaked in a Tris-HCl/Glycine buffer. This electrophoresis variant is indicated to run proteins in a denatured form. The heating denaturation of the samples, the SDS and DTT additives ensure it. SDS is an anionic detergent that associates with protein in a

constant ratio, 1.4 g SDS/ 1 g protein [148], that gives a constant negative charge per unit of protein mass. Therefore, the electric field can drag the SDS-protein ions through the polyacrylamide gel. Under these conditions exists a linear correlation between the logarithm of the molecular weight of the proteins and the relative mobility of the ion molecules. Therefore, proteins migrate in a SDS-PAGE only as a function of their molecular mass [148].

2.10 pH dependence of rate constants.

Classical serine peptidases are enzymes which catalytic mechanism is controlled by the action of a histidine residue that facilitates the formation and decomposition of the intermediate acyl-enzyme, see section 1.14. This histidine residue exhibits a pKa value of 7 [82]. The ionization of this catalytic histidine governs the pH dependence of the catalysis and fits to the theoretical simple dissociation curve described by equation 16 [87].

$$k_{\text{cat}}/K_m = k_{\text{cat}}/K_m [1/(1+10^{\text{pK}1-\text{pH}}+10^{\text{pH}-\text{pK}2})] \quad \text{equation 16}$$

The theoretical curve for the bell-shaped pH rate profiles, equation 16, can be modified when additional ionizing groups are influencing the enzyme catalysis. Thus, the equation 17 can be applied when an additional group modifies the curve on the acidic limb [104]

$$k_{\text{cat}}/K_m = k_{\text{cat}}/K_m [1/(1+10^{\text{pK}1-\text{pH}}+10^{\text{pK}1+\text{pK}2-2\text{pH}}+10^{\text{pH}-\text{pK}3})] \quad \text{equation 17}$$

When the additional ionizing residue modifies the bell shape of the pH rates profiles to a doubly bell-shaped profile the theoretical curve that can be applied is the described by equation 18 [104].

$$k_{\text{cat}}/K_m = k_{\text{cat}}/K_m 1[1/(1+10^{\text{pK}1-\text{pH}}+10^{\text{pH}-\text{pK}2})] + k_{\text{cat}}/K_m 2[1/(1+10^{\text{pK}2-\text{pH}}+10^{\text{pH}-\text{pK}3})] \quad \text{equation 18}$$

The pH dependencies of the prolyl oligopeptidase catalyzed substrates were investigated as described elsewhere [159]. Measurements were carried at 37 °C in a buffer system consisting of 0.05 M acetic acid, 0.05 M MES and 0.1 M N-Ethylmorpholine. This buffer system ensures a constant ionic strength over the entire used pH [160]. All enzyme activity determinations were performed under first-order rate law, i.e. at substrate concentrations below the $\frac{1}{4}K_m$. Therefore equation 2 could be approximated to $V/[S][E] \approx k_{\text{cat}}/K_m$. This allowed us to draw the pH-dependence of the specificity constant k_{cat}/K_m .

3.0 Results.

The aim of this work was to answer some questions about the enzymatic functionality of prolyl oligopeptidase. For that reason, different and successive steps needed to be fulfilled. First, the cloning of the coding sequence, and second, the establishment of readily reproducible expression and purification protocols of the post-proline cleaving enzyme. The enzyme kinetics have been extensively studied, but mainly focusing on the characterization of the residues belonging to the catalytic triad. Therefore, always trying to draw some conclusions from its category as a serine peptidase. Herein the focus was placed on the characterization of active site related residues that might have relevance either on the catalytic performance of the enzyme or on the binding properties of substrates and inhibitors.

3.1.0 Prolyl oligopeptidase. cloning, expression and purification.

3.1.1 Prolyl oligopeptidase cloning.

In order to clone the coding sequence of the prolyl oligopeptidase total RNA was isolated from the U343 glioma cell line. Thymine oligonucleotides were used in order to generate by RT-PCR a more stable cDNA pool. This cDNA pool was used as a template to specifically amplify with gene specific primers, hPEPEcoRI3' and hPEPNdeI5', the prolyl oligopeptidase coding sequence. An open reading frame of 2.1 kilobases was obtained. This DNA fragment was successfully sub-cloned into the pPCR-Script™ Cam SK(+) vector. This construct was named pDRC1. Afterwards, this first construct was used as a stable template to clone the coding sequence of the prolyl oligopeptidase into a commercial bacterial expression vector, pET-28a(+). A direct cloning strategy was assayed. The digestion of both, the pDRC1 construct and the commercial vector, pET-28a(+), with the EcoR I and Nde I endonucleases generated DNA fragments with overhanging complementary ends. The ligation of these fragments with the T4 ligase allowed us to obtain the pursued construct, pDRC3. This construct was denominated as the wild type recombinant human prolyl oligopeptidase.

On the basis of the cloned wild type construct, pDRC3, a wide range of enzyme variants were generated by means of site directed mutagenesis technology. Thus the generated variants, listed in a single code letter nomenclature, were R643A, R643K, W595A, W595F, W595Y, M235A, M235I, F173A and C255A.

3.1.2 Prolyl oligopeptidase expression.

Once the gene of prolyl oligopeptidase was cloned, the expression of the heterologous protein was established. The BL21(DE3) *Escherichia coli* strain expression system was

used. IPTG, a lactose analogue, allowed the controlled upregulation of the expression of the heterologous gene based on the T7 promotor. In standard conditions of cell growth, namely 37°C in LB medium, the yield of heterologous protein was rather low.

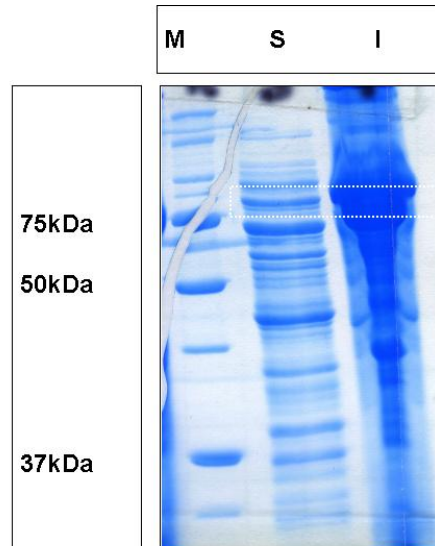


Figure 5 SDS-PAGE gel of the soluble fraction of a prolyl oligopeptidase expression. Lanes were labeled as M for marker, S for soluble protein and I for insoluble protein. Highlighted in a white dotted box the expression of the heterologous protein. On the left box are signed the molecular weight of the thickest bands of the protein ladder.

The figure 5 shows the result of a prolyl oligopeptidase test expression. The expression test cell debris were discarded and the soluble fraction of the expression was further analyzed by ultracentrifugation at 100'000 xg. High-speed centrifugation is usually used in order to separate cell protein aggregates, known as inclusion bodies, from the soluble active proteins [161]. The figure 5 shows the two different samples obtained upon this separation. In lane S the cellular proteins that remained in a soluble form are displayed, while in the lane I the heaviest cytoplasmatic particles, such as the big host protein complexes, and the heterologous protein stored as inclusion body aggregates are displayed. Basically, inclusion bodies are highly dense aggregates of inactive heterologous proteins that can account for up to a 30% of the total cellular protein [161]. To minimize, at least partially, the storage of the heterologous protein in inclusion bodies two strategies were pursued. First, the temperature of the expression was lowered down to 25°C, in opposition to the 37°C of optimal cell growth initially used [146]. Second, previous to the induction of the heterologous protein, the *Escherichia coli* endogenous chaperon system was upregulated by stressing the cells with the addition of a 2% (v/v) ethanol to the expression medium [162]. These two parameters

allowed us to increase significantly the expression of the soluble form of the non-native protein.

3.1.3 Prolyl oligopeptidase purification.

The strategy used to purify and isolate the expressed heterologous protein was strongly based on the specific interaction between the protein amino terminal hexahistidine tag, His_{x6}, and the nickel of the chelating chromatography. The whole purification process was optimized to only invest three chromatographic steps. The purification was carried out at 4°C in order to minimize unspecific proteolytic inactivation of the non-native protein. Previous to the chromatographic separation the resulting expression biomass was treated with a French Press to perform a mechanical disruption of cells [148]. The generated cell debris were separated from its soluble content by high-speed centrifugation at 35'000 xg for one hour. In order to minimize unspecific hydrophobic protein-protein interactions, that could interfere within the chromatographic separation, the resulting supernatant was diluted one-fold with an equal volume of 50 mM NaH₂PO₄; pH 7 buffer. The sample was then applied to the chromatographic separation. The established purification protocol is described in detail in the materials and methods section, point 2.4. Briefly, the purification was driven through three chromatographic steps. First, an affinity metal chelating resin allowed to specifically separate polyhistidine-epitope containing proteins from the crude extract. It was followed by a chromatography with an anion exchange Q sepharose resin that accomplished the protein separation by means of electrostatic interactions between the resin and the proteins. Finally, a hydrophobic interaction chromatography allowed us to isolate the target protein as a single visible band in SDS-PAGE gels, figure 6. This purification protocol was quantitatively and qualitatively characterized.

Table 11 shows the purification table of the recombinant prolyl oligopeptidase, revealing a rather low yield, in spite of the improvement achieved in the expression protocol. Therefore, only 0.6 mg pure protein per liter of expression culture was obtained. Furthermore, the purification table also illustrates how the percentage of recovery, seen in terms of amount of protein, yielded a rather limited production of the heterologous enzyme in a soluble form. Parallely, a qualitative characterization of the recombinant prolyl oligopeptidase isolation was depicted in figure 6. This SDS-PAGE gel demonstrates the purification progress of the established protocol and it clearly shows how the expression of the soluble form of the heterologous protein was indeed increased. This becomes obvious upon comparing both gels of figures 5 and 6, lanes S and CE, respectively.

However, note should be made on how the established protocol succeeded in isolating the non-native protein from the rest of endogenous *Escherichia coli* proteins. Thus, it became a reliable protocol in order to be applied for the isolation of all future prolyl oligopeptidase variants.

Purification Step	Volume (ml)	Protein (mg)	Recovery (%)	Activity Units (mU)	Specific Activity (U/mg) $\times 10^{-6}$	Purification factor
Initial sample	250	853.2	100	1.02	1.2	1
IMAC	40	19.1	2.23	1.31	68.3	56
Q sepharose	20	11.1	1.30	2.49	224	187
Phenyl sepharose	24	3.7	0.43	1.60	428	356

Table 11 Purification table of the isolation of the recombinant human prolyl oligopeptidase expressed in *Escherichia coli*. The initial sample is the result of a six liters expression volume. One unit of activity (U) accounts for the yield of 1 μmol AMC/ min.

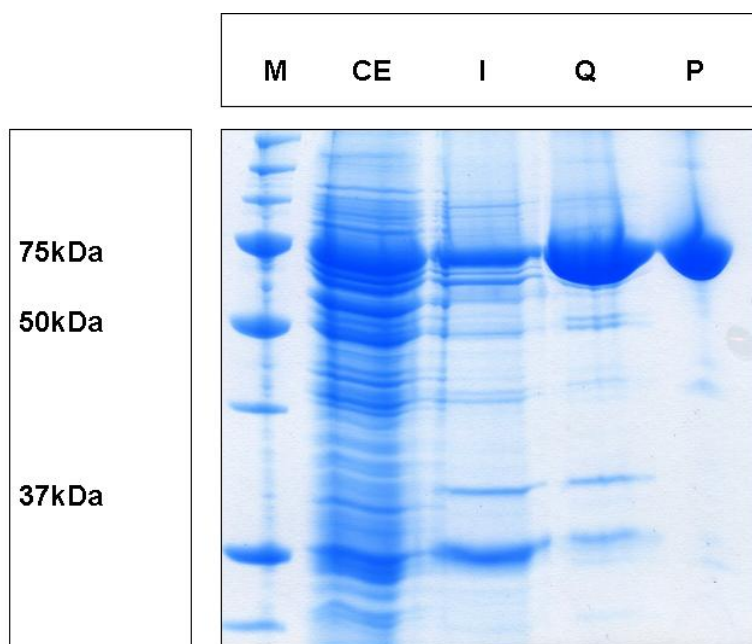


Figure 6 SDS-PAGE gel after performing the purification of the recombinant human prolyl oligopeptidase according to the established protocol outlined in table 11. Each lane shows a representative sample of each step of the chromatographic purification. Lanes were labeled as M for marker, CE for crude extract sample prior to the purification, I for IMAC chromatography, Q for Q sepharose chromatography and P for Phenyl sepharose chromatography. The molecular weight of the thickest bands of the protein ladder (M) are designated on the left box.

3.2 Recombinant human prolyl oligopeptidase kinetic characterization.

The purified recombinant human prolyl oligopeptidase was used in order to characterize the standard kinetic parameters, K_m and k_{cat} . Two different kind of synthetic substrates were used, 7-Amido-4-methylcoumarin (AMC) peptide derivatives and Fluorescence Resonance Energy Transfer (FRET) derivatives. The recombinant technology allowed us to generate specific enzyme variants. Thus, the exchange of selected residues helped us to discern their relevance in the enzyme catalytic mechanism and in the substrate binding pattern.

3.2.1 Wild type recombinant prolyl oligopeptidase catalyzed hydrolysis of AMC derivatives.

The data compiled in table 12 show the kinetic parameters of the wild type enzyme measured with AMC derivatives. Analysing the data one can see how the Michaelis-Menten constants, K_m , show lower values for all those substrates holding a proline as a main specificity. Nevertheless, two orders of magnitude difference were measured between the different proline containing substrates. Regarding the turnover constants, k_{cat} , the variability is less drastic and only one order of magnitude between the largest and smallest values being characterized.

Substrate	K_m (μM)	k_{cat} (s^{-1})	k_{cat}/K_m ($\text{mM}^{-1}\text{s}^{-1}$)
Z-GlyPro-AMC	87.9 (± 5.2)	46.30 (± 1.90)	526.7 (± 40)
Z-AlaPro-AMC	6.1 (± 0.5)	4.75 (± 0.15)	778.0 (± 70)
AlaAlaPro-AMC	29.3 (± 2.8)	6.14 (± 0.17)	210.0 (± 20)
AlaAlaAla-AMC	1563.0 (± 220)	10.90 (± 0.31)	6.9 (± 1)
AlaAlaCys-AMC	455.4 (± 55.1)	3.26 (± 0.24)	7.1 (± 1)
AlaAlaSer-AMC	74.3 (± 39.1)	0.03 (± 0.003)	0.4 (± 0.2)
GlyProPro-AMC	371.9 (± 29.2)	36.30 (± 1.63)	97.6 (± 8.8)

Table 12 Kinetic parameters of the recombinant human prolyl oligopeptidase determined with the AMC derivatives. K_m , Michaelis-Menten constant. k_{cat} , turnover constant. k_{cat}/K_m , specificity constant. The Measurement were performed as described in materials and methods, sections 2.7.2. and 2.7.3. The mean value (\pm SEM) of three measurements are given.

The substitution of the proline for alanine, cysteine or serine showed rather evident increments on the measured K_m values. Only serine was able to hold a similar Michaelis-Menten constant value in comparison to the ones of the proline containing substrates. Moreover, the non-proline containing substrates have comparable turnover

constants to the ones shown by the proline containing substrates. Significantly, the serine AMC derivative is showing the smallest k_{cat} value. The characterized second order constants, k_{cat}/K_m , displayed no dramatic variation between the comparable proline containing substrates, dipeptides and tripeptides AMC derivatives, respectively. Meanwhile, the rest of substrates displayed always at least a two order of magnitude impairment of the second order constant in comparison to the threshold shown by the proline AMC derivatives.

3.2.2 Wild type recombinant prolyl oligopeptidase catalyzed hydrolysis of FRET derivatives.

The table 13 shows the measured kinetic parameters of the wild type recombinant prolyl oligopeptidase obtained with Angiotensin FRET based substrates. No major differences were found between Angiotensin I and Angiotensin II. Thus, the Michaelis-Menten constants remained, in both cases, in the same range. The same happened with the measured turnover constants and the specificity constants. Otherwise, Angiotensin I and Angiotensin II, which only differ in one residue, shown a substrate inhibition pattern with measured K_i values on the low micromolar range. The exchange of the original proline residue in the Angiotensin II FRET peptide for an alanine, P5A-Angiotensin II, resulted in one order of magnitude increased Michaelis-Menten constant, but its measured turnover constant remained comparable, and in the same range, to the one shown by the original peptide. The exchange introducing a cysteine in place of the original proline residue, P5C-Angiotensin II, produced a still hydrolyzable substrate. In this case, the measured Michaelis-Menten constant resulted in one order of magnitude increase in comparison to the threshold achieved with the Angiotensin II substrate. Also, the turnover constant of this cysteine substrate variant led to an impairment of two orders of magnitude compared with the one of the original Angioten-

Substrate	K_m (μM)	k_{cat} (s^{-1})	k_{cat}/K_m ($\text{mM}^{-1}\text{s}^{-1}$)	K_i (μM)
Angiotensin I	2.14 (± 0.69)	1.85 (± 0.29)	864.5 (± 310)	26.16 (± 7.34)
Angiotensin II	1.42 (± 0.33)	1.19 (± 0.12)	838.0 (± 210)	30.32 (± 7.07)
P5A-Angiotensin II	38.00 (± 9)	1.07 (± 0.19)	28.2 (± 7)	N.D.
P5C-Angiotensin II	42.00 (± 14)	0.07 (± 0.017)	1.6 (± 0.07)	N.D.
P5S-Angiotensin II	N.D.	N.D.	N.D.	N.D.

Table 13 Kinetic parameters of the wild type recombinant human prolyl oligopeptidase determined with internally quenched substrates. Angiotensin I, Dabcyl-KVYIHPFE-Edans. Angiotensin II, Dabcyl-KVYIHPFE-Edans. P5A-Angiotensin II, Dabcyl-KVYIHAFE-Edans. P5C-Angiotensin II, Dabcyl-KVYIHCFE-Edans. P5S-Angiotensin II, Dabcyl-KVYIHSFE-Edans. N.D. not detected. The Measurements were performed as described in materials and methods, sections 2.7.2. and 2.7.2. The mean value (\pm SEM) of three measurements are given.

-sin II FRET derivative. Both Angiotensin II variants, P5A-Angiotensin II and P5C-Angiotensin II, showed a decrement of the calculated second order constant, one and two orders of magnitude, respectively. Furthermore, any substrate inhibition pattern was detected with these two variants of the Angiotensin II FRET derivative substrate. Finally, table 13 shows no data for the serine variant of the Angiotensin II, P5S-Angiotensin II, indicating that no enzymatic activity was detected with this substrate. It is noteworthy to outline that the specificities of prolyl oligopeptidase, either towards short derivatives, table 12, or long derivatives, tables 13 and 14, are very similar. That contrast with what is quoted in the literature where impairments of the specificities, by one to two orders of magnitude decrease, were reported between short derivatives and their elongated counterparts [163].

Additionally, in table 14 are summarized the kinetic parameters of the hydrolysis of a different lead peptide, NAP, that was derivatized as FRET. NAP is an eight amino acid long neuropeptide with two potential proline cleavage sites. In principle, the values obtained with this NAP substrate are comparable to the data collected in the table 13. Interestingly, the substrate inhibition pattern reappeared with the use of these substrates.

Substrate	K_m (μM)	k_{cat} (s^{-1})	k_{cat}/K_m ($\text{mM}^{-1}\text{s}^{-1}$)	K_i (μM)
NAP	1.16 (± 0.17)	0.45 (± 0.02)	387.9 (± 0.15)	95.42 (± 21.84)
P3A-NAP	1.72 (± 0.35)	0.52 (± 0.03)	302.3 (± 0.14)	N.D.
P7A-NAP	7.75 (± 2.90)	0.24 (± 0.03)	30.9 (± 0.02)	N.D.

Table 14 Kinetic parameters of the recombinant wild type human prolyl oligopeptidase determined with internally quenched NAP based substrates. FRET peptides NAP: Dabcyl-KNAPVSIPQE-Edans, P3A-NAP: Dabcyl-KNAAVSIPQE-Edans, P7A-NAP: Dabcyl-KNAPVSIAQE-Edans. N.D.: not detected. The measurement were performed as described in materials and methods, sections 2.7.2. and 2.7.3 The mean value (\pm SEM) of three measurements are given.

A pattern that disappeared when either of the proline residues was exchanged for alanine, P3A-NAP and P7A-NAP. Moreover, it is noteworthy to mention that different specificities were obtained by the two proline cleavage sites.

3.2.3 Temperature and pH dependencies of prolyl oligopeptidase catalyzed substrate hydrolysis.

The temperature dependence of the prolyl oligopeptidase hydrolysis of different substrates was studied. The data obtained from the correlation of the temperature with the kinetic constants are summarized in the figure 7 and tables 15-A and 15-B. The

measurements were performed in a range of temperatures, from 25°C to 45°C, that was sufficient to render differences and similarities. As a result of the obtained Eyring plots it was possible to infer the related thermodynamic parameters, table 15-A. In this case the data of all different characterized substrates fitted properly to linear curves. The Arrhenius plots allowed us to infer the empiric parameters summarized in table 15-B for the same studied substrates. In this case not all of the curves fit a linear regression. Particularly in two cases, namely Z-AlaPro-AMC and Angiotensin II DabcyI-KVYIHPFE-Edans, did not show proper linear correlations. However, both approaches, Eyring and Arrhenius plots, were approached as described elsewhere [157;158]

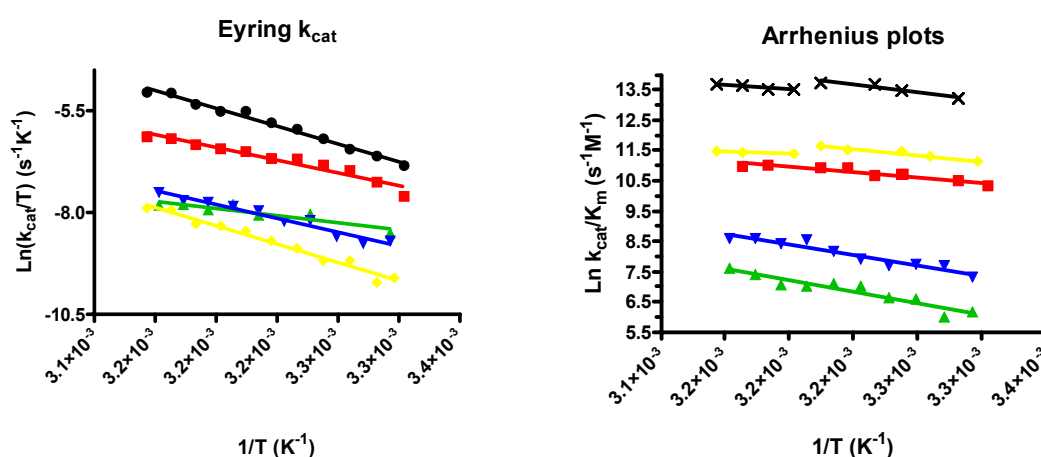


Figure 7 Eyring and Arrhenius plots of the PEP catalyzed substrate hydrolysis. On the left hand graph are displayed the Eyring plots of the temperature dependence of the k_{cat} constants of the different measured substrates. On the right hand graph are displayed the obtained Arrhenius plots of the temperature dependence of the k_{cat}/K_m constant of different substrates. Both graphs show in red (●) Z-GlyPro-AMC, in yellow (●) Z-AlaPro-AMC, in green (●) GlyProPro-AMC, in blue (●) AlaAlaPro-AMC and in black (●) Angiotensin II, DabcyI-KVYIHPFE-Edans. The Measurements were performed as described in materials and methods, sections 2.7.2. and 2.7.3.

Substrate	$\Delta H^{\ddagger 0}$ (kJ·mol ⁻¹)	$\Delta S^{\ddagger 0}$ (J·mol ⁻¹ ·K ⁻¹)	$\Delta G^{\ddagger 0}$ (kJ·mol ⁻¹)
Z-GlyPro-AMC	52.1	-84	77.1
Z-AlaPro-AMC	74.9	-27	82.9
AlaAlaPro-AMC	56.6	-81	80.8
GlyProPro-AMC	25.9	-180	79.7
Angiotensin II	72.8	-10	75.7

Table 15-A Summary table of the thermodynamic parameters obtained from the Eyring plots shown in figure 7. Enthalpy, $\Delta H^{\ddagger 0}$, entropy, $\Delta S^{\ddagger 0}$ and Free Gibbs energy $\Delta G^{\ddagger 0}$. Angiotensin II: DabcyI-KVYIHPFE-Edans. The parameters were calculated as described elsewhere [157;158].

Substrate	Ea (kJ·mol ⁻¹)	k ₁ (M ⁻¹ s ⁻¹)	k ₂ /k ₋₁
Z-GlyPro-AMC	28.3	3.1·10 ⁰⁹	9.9·10 ⁻⁰⁶
Z-AlaPro-AMC	35.2	1.0·10 ¹¹	6.8·10 ⁻⁰⁷
AlaAlaPro-AMC	57.2	1.6·10 ¹³	8.9·10 ⁻¹¹
GlyProPro-AMC	63.6	5.8·10 ¹³	7.5·10 ⁻¹²
Angiotensin II	42.1	1.2·10 ¹³	5.8·10 ⁻⁰⁸

Table 15-B Summary table of the parameters inferred from the Arrhenius plots shown in figure 7. Ea, activation energy, k₁ and k₂/k₋₁ kinetic rate constants of the kinetic mechanism shown in scheme 1, Angiotensin II: DabcyI-KVYIHPFE-Edans. The parameters were calculated as described elsewhere [157;158].

The table 16 gathers the inferred pKa values of enzymatically relevant residues and the specificity constants of the prolyl oligopeptidase turnover pH-dependencies measured with different proline containing substrates. The obtained data show how they were found notable shifts, particularly, on the inferred pKa values on the acidic limb of the

Substrate	pKa ₁	pKa ₂	pKa ₃	k _{cat} /K _m (μM ⁻¹ s ⁻¹)	k _{cat} /K _m (μM ⁻¹ s ⁻¹)	Eq.
AlaAlaPro-AMC	6.64 (±0.05)	7.98 (±0.04)	N.D.	0.52 (±0.02)	N.D.	16
Z-GlyPro-AMC	5.43 (±0.35)	5.86 (±0.48)	7.75 (±0.07)	0.52 (±0.03)	N.D.	17
Z-AlaPro-AMC	4.77 (±0.88)	6.31 (±0.99)	8.09 (±0.06)	0.93 (±0.03)	N.D.	17
GlyProPro-AMC	5.92 (±0.15)	6.22 (±0.22)	7.95 (±0.04)	0.086 (±0.003)	N.D.	17
Angiotensin I	6.14 (±0.10)	8.31 (±0.31)	7.67 (±0.41)	0.17 (±0.02)	0.98 (±0.57)	18

Table 16 Summary table of the parameters obtained from the measured pH-dependencies of the catalyzed turnover of the indicated substrates. The data were fitted to the theoretical curves of equations (Eq.) 16, 17 and 18, see section 2.10. pKa₁ pKa₂ and pKa₃ stand for the pKa values of catalytically relevant residues and k_{cat}/K_m for the pH independent specificity constant. Angiotensin I, DabcyI-KVYIHPFE-Edans. The experiments were performed as described elsewhere [164].

curves, with pKa₁ values ranging between 4.77 and 6.64, while the calculated pKa values on the basic limb did not vary to such a degree with pKa's ranging between 7.67 and 8.09. Particularly relevant is the doubly bell-shaped pH dependence measured with the FRET derivative, Angiotensin I. This outlines the presence of two differentiated active forms of the enzyme, as already stated before for the porcine enzyme [98].

3.3.0 Recombinant human prolyl oligopeptidase arginine 643 variants.

The relevance of the prolyl oligopeptidase residue Arg⁶⁴³ has been highlighted in literature. Arg⁶⁴³ is the only responsible residue to build the S₂ pocket in the enzyme's active site [67]. The crystal structures of the porcine prolyl oligopeptidase show how on

the guanidinium moiety of the arginine side-chain is pivoting a complex hydrogen bond network. The arginine's guanidinium moiety is anchored, from one side, by the carboxy moiety of the Asp¹⁴⁹ side-chain, and from the other side, interacts with the substrate main chain carbonyls on the P₂ and P₄ positions (PDBid 1E8N). Additionally, the main chain Arg⁶⁴³ amide group is coordinating the catalytic Asp⁶⁴¹, figure 8.

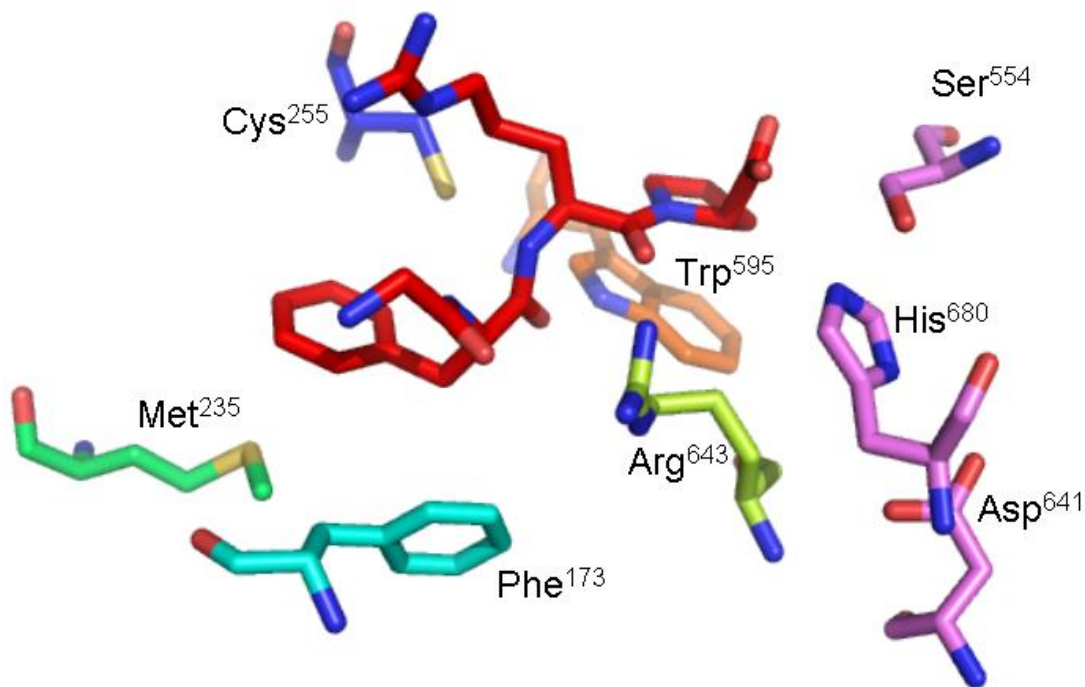


Figure 8 Porcine prolyl oligopeptidase active site related residues on stick representation from the published crystal structure with PDB id 1uoo. In pink are identified the residues of the catalytic triad, in red the ProArgPheGly co-crystallized tetrapeptide, in orange Trp⁵⁹⁵, in yellow Arg⁶⁴³, in blue Cys²⁵⁵, in green Met²³⁵ and in magenta Phe¹⁷³.

3.3.1 Recombinant human prolyl oligopeptidase alanine 643 variant.

The data compiled in the table 17 show the kinetic parameters obtained with the R643A prolyl oligopeptidase variant. The measurement with short derivatives did not succeed when substrates did not contain proline in their sequences. Thus, the AlaAlaAla-AMC, AlaAlaCys-AMC and AlaAlaSer-AMC were not suitable substrates to be used in order to obtain proper curves. The remaining proline containing substrates were the only one being processed by this enzyme variant. Generally, the observed Michaelis-Menten constants vary extremely. Thus, the dipeptide derivatives showed values on the proximity of the micromolar range, whereas the tripeptide derivatives

gave values beyond the millimolar range, therefore, two-fold increased values. Regarding the turnover constants, it is easily noticeable that no major differences are observed between them. Finally, the calculated second order constants particularly vary within this variant. Up to three orders of magnitude of difference between the most specifically recognized substrate, the dipeptide Z-AlaPro-AMC derivative, and the one that is not thus acknowledged, GlyProPro-AMC.

Substrate	K_m (μM)	k_{cat} (s^{-1})	k_{cat}/K_m ($\text{mM}^{-1}\text{s}^{-1}$)
Z-GlyPro-AMC	140.9 (± 25.9)	1.10 (± 0.1)	7.7 (± 1.5)
Z-AlaPro-AMC	15.4 (± 2.7)	1.79 (± 0.2)	116.0 (± 22)
AlaAlaPro-AMC	1031.0 (± 40)	3.58 (± 0.1)	3.47 (± 0.16)
AlaAlaAla-AMC	N.D.	N.D.	N.D.
AlaAlaCys-AMC	N.D.	N.D.	N.D.
AlaAlaSer-AMC	N.D.	N.D.	N.D.
GlyProPro-AMC	2337.0 (± 167)	0.97 (± 0.06)	0.42 (± 0.04)

Table 17 Kinetic parameters of the recombinant human R643A prolyl oligopeptidase variant determined with AMC derivatives. N.D.: not detected. The measurements were performed as described in materials and methods, sections 2.7.2. and 2.7.3. The mean value (\pm SEM) of three measurements are given.

3.3.2 Recombinant human prolyl oligopeptidase lysine 643 variant.

The table 18 summarizes the kinetic data obtained with the R643K prolyl oligopeptidase variant. The values gathered in table 18 made evident some parallelisms with the data shown in the table 17. Also, this variant is not able to process substrates lacking proline in their sequences. The K_m constants vary dramatically, ranging from the low micromolar to the millimolar range. Furthermore, the dipeptide derivatives are displaying the lowest values whereas the tripeptides the highest. The results obtained from both variants, summarized in tables 17 and 18, are indeed very

Substrate	K_m (μM)	k_{cat} (s^{-1})	k_{cat}/K_m ($\text{mM}^{-1}\text{s}^{-1}$)
Z-GlyPro-AMC	141.34 (± 17.8)	3.23 (± 0.19)	22.8 (± 0.0032)
Z-AlaPro-AMC	19.52 (± 2.7)	6.19 (± 0.29)	317.1 (± 0.047)
AlaAlaPro-AMC	405.60 (± 19.9)	2.84 (± 0.09)	7.0 (± 0.4)
AlaAlaAla-AMC	N.D.	N.D.	N.D.
AlaAlaCys-AMC	N.D.	N.D.	N.D.
AlaAlaSer-AMC	N.D.	N.D.	N.D.
GlyProPro-AMC	1802.00 (± 118)	5.06 (± 0.24)	2.8 (± 0.2)

Table 18 Kinetic parameters of the recombinant human R643K prolyl oligopeptidase variant measured with AMC derivatives. N.D.: not detected. The Measurements were performed as described in materials and methods, sections 2.7.2. and 2.7.3. The mean value (\pm SEM) of three measurements are given.

similar. On the other hand, the characterized k_{cat} values for the analyzed lysine variant stay in a rather narrow range. This again stands out a parallelism between the R643A and the R643K variants. In this case, the R643K variant is displaying for most of the substrates evidently higher turnover constants. Up to 5-fold increase in the most advantageous case. The second order rate constants calculated with the R643K variant demonstrated its preferential specificity for the proline containing dipeptides in front of the tripeptide ones. The R643A and R643K variants maintain the same relation between the specificity constants of the different substrates, although the last showed improved values in comparison to the former.

3.4.0 Recombinant human prolyl oligopeptidase tryptophan 595 variants.

If there is a residue that might play a main role in the prolyl oligopeptidase specificity it might be argued that it is the Trp⁵⁹⁵ [67]. The x-ray structure of the porcine prolyl oligopeptidase is defining a S₁ pocket with a pronounced hydrophobic character, figure 8. The side-chain of Trp⁵⁹⁵, Phe⁴⁷⁶, Val⁶⁴⁴, Val⁵⁸⁰ and Tyr⁵⁹⁹ are building the S₁ pocket. In this set of residues, the indole ring of the Trp⁵⁹⁵ side-chain has been indicated to enhance the enzyme specificity by recognition of the pyrrolidine ring of the proline substrate [67].

3.4.1 Recombinant human prolyl oligopeptidase alanine 595 variant.

The kinetic parameters measured with the W595A variant using AMC surrogates were collected in the table 19. Once again, the enzyme variant W595A is only showing turnover with those substrates containing proline in their primary sequences. Alanine, cysteine or serine are residues not processed by this chimeric peptidase. The successfully characterized substrates displayed Michaelis-Menten constants ranging

Substrate	K_m (μM)	k_{cat} (s^{-1})	k_{cat}/K_m ($\text{mM}^{-1}\text{s}^{-1}$)
Z-GlyPro-AMC	116.52 (± 34.91)	0.44 (± 0.05)	3.77 (± 1.20)
Z-AlaPro-AMC	162.23 (± 22.66)	1.39 (± 0.12)	8.56 (± 1.40)
AlaAlaPro-AMC	3200.00 (± 800)	1.15 (± 0.26)	0.36 (± 0.12)
AlaAlaAla-AMC	N.D.	N.D.	N.D.
AlaAlaCys-AMC	N.D.	N.D.	N.D.
AlaAlaSer-AMC	N.D.	N.D.	N.D.
GlyProPro-AMC	2800.00 (± 666)	0.22 (± 0.03)	0.08 (± 0.02)

Table 19 Kinetic parameters of the recombinant human W595A prolyl oligopeptidase variant determined with AMC derivatives. N.D.: not detected. The measurements were performed as described in materials and methods, sections 2.7.2. and 2.7.3. The mean value (\pm SEM) of three measurements are given.

from the micromolar to the high millimolar. Particularly they were measured with the dipeptide derivatives the smallest K_m constants, whereas with the proline containing tripeptides the largest K_m were obtained. As well, the turnover constants are distributed over a rather narrow range of values. No dramatic differences might be appreciated, although between the highest and the lowest k_{cat} one order of magnitude difference was characterized. The resulting second order constants, as a consequence of the inverse increased of K_m in front of the decrease of k_{cat} , were in comparison to the values obtained with the wild type enzyme rather low.

3.4.2 Recombinant human prolyl oligopeptidase phenylalanine 595 variant.

In the table 20 were collected the kinetic parameters measured with the W595F prolyl oligopeptidase variant using AMC surrogate substrates. Interestingly, the generation of this prolyl oligopeptidase variant brought back the original enzymatic capacity of hydrolysis of the non-proline containing substrates. Thus, this enzyme, in comparison for example with its counterpart W595A variant, is able again to process substrates with an alanine or a cysteine in their sequences, AlaAlaAla-AMC and AlaAlaCys-AMC, but not serine, AlaAlaSer-AMC. The Michaelis-Menten constants for the different measured substrates vary within this variant in extreme, ranging from the low micromo-

Substrate	K_m (μM)	k_{cat} (s^{-1})	k_{cat}/K_m ($\text{mM}^{-1}\text{s}^{-1}$)
Z-GlyPro-AMC	154.0 (± 22)	16.06 (± 1.42)	104.28 (± 20)
Z-AlaPro-AMC	48.2 (± 8.3)	3.64 (± 0.27)	75.50 (± 14)
AlaAlaProAMC	943.8 (± 233.5)	5.69 (± 0.79)	6.03 (± 2)
AlaAlaAla-AMC	11712.0 (± 2718)	1.72 (± 0.33)	0.15 (± 0.04)
AlaAlaCys-AMC	320.0 (± 90)	0.03 (± 0.003)	0.94 (± 0.02)
AlaAlaSer-AMC	N.D.	N.D.	N.D.
GlyProPro-AMC	2874.0 (± 266)	16.79 (± 1.35)	5.8 (± 0.7)

Table 20 Kinetic parameters of the recombinant human W595F prolyl oligopeptidase variant determined with AMC derivatives. N.D.: not detected. The measurements were performed as described in materials and methods, sections 2.7.2. and 2.7.3. The mean value (\pm SEM) of three measurements are given.

-lar to the high millimolar. It outstands the fact that within the tripeptides the lowest K_m constant was measured with AlaAlaCys-AMC, even in front of proline containing substrates like GlyProPro-AMC and AlaAlaPro-AMC. The measured turnover constants for the analyzed W595F variant resulted, as well, in very scattered values. AlaAlaCys-AMC is showing the lowest measured turnover constant, while GlyProPro-AMC shows a k_{cat} three orders of magnitude larger than the former. The magnitudes of the measured k_{cat} constants, in comparison to the previous W595A variant, increased significantly, in some cases up to three orders of magnitude. The resulting second

order constants vary, as well, between the highest and lowest values three orders of magnitude. This chimeric enzyme shows higher specificities towards the dipeptide derivatives than for the tripeptide derivatives.

3.4.3 Recombinant human prolyl oligopeptidase tyrosine 595 variant.

The kinetic parameters obtained from the enzymatic characterization of the W595Y prolyl oligopeptidase variant were compiled in the table 21. In comparison to the previous W595A and W595F variants, the W595Y variant is processing, in addition to the proline containing derivatives, only the alanine AMC derivative, AlaAlaAla-AMC. The K_m constants, following the tendency, show lower values for the dipeptide than for the tripeptide derivatives. The amino terminal blocked dipeptides show Michaelis-Menten constants in the low micromolar range whereas the free amino terminal tripeptides show Michaelis-Menten constants over the millimolar range. Regarding the turnover constants, the W595Y variant shows relatively scattered values. Comparing to the previous W595A and W595F variants, W595Y shows a bigger impairment of the k_{cat} constants for those substrates that better behaved with the W595F variant, thus Z-GlyPro-AMC and GlyProPro-AMC. The rest of proline containing substrates maintain, AlaAlaPro-AMC, or slightly improve, Z-AlaPro-AMC, their turnover constants when they are compared to the ones measured with the W595F variant.

Substrate	K_m (μM)	k_{cat} (s^{-1})	k_{cat}/K_m ($\text{mM}^{-1}\text{s}^{-1}$)
Z-GlyPro-AMC	62.8 (± 10.4)	2.89 (± 0.19)	46.02 (± 8)
Z-AlaPro-AMC	54.0 (± 9.8)	7.77 (± 0.35)	143.88 (± 26)
AlaAlaPro-AMC	2972.0 (± 605)	5.33 (± 0.82)	1.79 (± 0.5)
AlaAlaAla-AMC	3955.0 (± 1012)	0.27 (± 0.05)	0.07 (± 0.02)
AlaAlaCys-AMC	N.D.	N.D.	N.D.
AlaAlaSer-AMC	N.D.	N.D.	N.D.
GlyProPro-AMC	1227.0 (± 239)	1.32 (± 0.14)	1.07 (± 0.2)

Table 21 Kinetic parameters of the recombinant human W595Y prolyl oligopeptidase variant determined with AMC derivatives. N.D.: not detected. The measurements were performed as described in materials and methods, sections 2.7.2. and 2.7.3. The mean value (\pm SEM) of three measurements are given.

The alanine tripeptide surrogate shows with the W595Y variant one order of magnitude drop on its measured turnover constant in comparison to the one measured with the W595F variant. The calculated specificity constants show, globally, lower values in comparison to the ones found with the W595F variant. The proline containing dipeptide AMC derivative, Z-AlaPro-AMC, displays the highest specificity constant and the non-proline containing tripeptide, AlaAlaAla-AMC, displays the lowest specificity constant, with a four orders of magnitude lower k_{cat}/K_m in comparison to the former.

3.5.0 Recombinant human prolyl oligopeptidase phenylalanine 173 variant.

Phenylalanine 173 belongs to a set of residues that in prolyl oligopeptidase are the responsible of the building of the S₃ active site pocket [67], figure 8. The importance of this S₃ pocket is related to the endopeptidase activity of prolyl oligopeptidase as the endopeptidase character of the enzyme is enhanced by the non-polar environment achieved in the S₃ pocket, in which construction phenylalanine 173 is involved [67].

3.5.1 Recombinant human prolyl oligopeptidase alanine 173 variant.

The table 22 collects the kinetic parameters belonging to the measurements performed with the F173A prolyl oligopeptidase variant. This variant is not able to process such substrates holding in their sequences either cysteine, AlaAlaCys-AMC, or serine, AlaAlaSer-AMC. The Michaelis-Menten constants of the different measured substrates might be differentiated again. On the one hand, the group of dipeptide derivatives, that have low K_m values, and on the other hand, the group of tripeptide derivatives, with K_m values up to two orders of magnitude larger than the ones shown by the former. The characterized turnover constants are within this variant particularly high, but as well

Substrate	K _m (μM)	k _{cat} (s ⁻¹)	k _{cat} /K _m (mM ⁻¹ s ⁻¹)
Z-GlyPro-AMC	380.0 (±74)	43.96 (±7.14)	115.60 (±0.03)
Z-AlaPro-AMC	18.0 (±1.6)	4.03 (±0.14)	223.80 (±0.02)
AlaAlaPro-AMC	3328.0 (±62)	2.79 (±0.03)	0.84 (±0.02)
AlaAlaAla-AMC	3297.0 (±288)	0.21 (±0.01)	0.063 (±0.006)
AlaAlaCys-AMC	N.D.	N.D.	N.D.
AlaAlaSer-AMC	N.D.	N.D.	N.D.
GlyProPro-AMC	2482.0 (±159)	33.00 (±1)	13.29 (±1.00)

Table 22 Kinetic parameters of the recombinant human F173A prolyl oligopeptidase variant determined with AMC derivatives. N.D.: not detected. The measurements were performed as described in materials and methods, sections 2.7.2. and 2.7.3. The mean value (±SEM) of three measurements are given.

scattered. A difference of two orders of magnitude was found between the maximal k_{cat} of Z-GlyPro-AMC and the minimal k_{cat} of AlaAlaAla-AMC. In comparison to the wild type enzyme, the dipeptide substrates show comparable specificity constants, but always lower. The remaining substrates display rather low specificities with k_{cat}/K_m constants ranging between one and four orders of magnitude lower for GlyProPro-AMC and AlaAlaAla-AMC respectively, than their dipeptidic counterparts.

3.6.0 Recombinant human prolyl oligopeptidase methionine 235 variants.

The residue Met²³⁵ has been pointed to participate in the construction of the S₃ pocket in active site [67]. Like Phe¹⁷³ and Cys²⁵⁵, Met²³⁵ might contribute to form a non-polar

environment in the enzyme's active site which might be responsible for the endopeptidase characteristic activity of prolyl oligopeptidase, figure 8.

3.6.1 Recombinant human prolyl oligopeptidase alanine 235 variant.

The data shown in the table 23 are the kinetic parameters obtained with the M235A prolyl oligopeptidase variant. This variant, along with all here presented variants, does not cleave the serine containing substrate, namely AlaAlaSer-AMC. The analysis of the obtained Michaelis-Menten constants demonstrates how most of the substrates show with this enzyme variant a rather low K_m constants, staying on the proximity of the low micromolar range. Only two of the measured K_m values rose up to the millimolar range, the ones belonging to AlaAlaAla-AMC and GlyProPro-AMC. The calculated turnover constants were rather very similar. Although some differences might be found, they do not seem to be substantial. Finally, the calculated second order constants show how the M235A variant still displays always preference for the proline containing AMC derivatives.

Substrate	K_m (μM)	k_{cat} (s^{-1})	k_{cat}/K_m ($\text{mM}^{-1}\text{s}^{-1}$)
Z-GlyPro-AMC	87.83 (± 7.37)	3.57 (± 0.18)	40.6 (± 4.0)
Z-AlaPro-AMC	5.35 (± 0.86)	0.52 (± 0.02)	97.2 (± 16.0)
AlaAlaPro-AMC	78.15 (± 3.99)	0.96 (± 0.02)	12.3 (± 0.7)
AlaAlaAla-AMC	960.00 (± 51)	0.64 (± 0.01)	0.67 (± 0.04)
AlaAlaCys-AMC	142.50 (± 15.4)	0.87 (± 0.05)	6.1 (± 0.8)
AlaAlaSer-AMC	N.D.	N.D.	N.D.
GlyProPro-AMC	1118 (± 75)	3.00 (± 0.1)	2.7 (± 0.2)

Table 23 Kinetic parameters of the recombinant human M235A prolyl oligopeptidase variant determined with AMC derivatives. N.D.: not detected. The measurements were performed as described in materials and methods, sections 2.7.2. and 2.7.3. The mean value (\pm SEM) of three measurements are given.

The measured specificities decreased by two orders of magnitude between the maximal and minimal values obtained from the proline containing AMC derivatives. It significantly outstands how the cysteine AMC derivative, AlaAlaCys-AMC, shows not only a specificity constant one order of magnitude higher than its counterpart with alanine in the primary sequence, AlaAlaAla-AMC, but as well up to two fold higher than a substrate like GlyProPro-AMC.

3.6.2 Recombinant human prolyl oligopeptidase isoleucine 235 variant.

The results compiled in the table 24 display the kinetic parameters obtained with the M235I variant using AMC derivatives. The analysis of the K_m constants measured with this variant shows how the values are concentrated in the micromolar range, only

AlaAlaAla-AMC jumps up to the millimolar range. In that sense, the most significant change, in relation to the variant M235A, is that the substrate GlyProPro-AMC shows in this case a Michaelis-Menten constant one order of magnitude smaller. The turnover constants are clearly higher than the ones observed in the previous related variant, M235A. However, their k_{cat} vary the most only by one order of magnitude.

Substrate	K_m (μM)	k_{cat} (s^{-1})	k_{cat}/K_m ($\text{mM}^{-1}\text{s}^{-1}$)
Z-GlyPro-AMC	35.2 (± 4.2)	47.7 (± 2.2)	1355.0 (± 170)
Z-AlaPro-AMC	15.3 (± 3.3)	12.5 (± 0.9)	817.0 (± 190)
AlaAlaPro-AMC	85.1 (± 4.34)	14.8 (± 0.3)	174.0 (± 9)
AlaAlaAla-AMC	1129.0 (± 58)	8.85 (± 0.24)	7.8 (± 0.4)
AlaAlaCys-AMC	232.4 (± 15.2)	1.7 (± 0.1)	7.3 (± 0.6)
AlaAlaSer-AMC	N.D.	N.D.	N.D.
GlyProPro-AMC	330.0 (± 12)	34.7 (± 0.6)	105.2 (± 4)

Table 24 Kinetic parameters of the recombinant human M235I prolyl oligopeptidase variant determined with AMC derivatives. N.D.: not detected. The measurements were performed as described in materials and methods, sections 2.7.2. and 2.7.3. The mean value (\pm SEM) of three measurements are given.

The specificity constants demonstrate that this variant, in any case, still shows preference for the proline containing substrates. This variant emphasizes its importance regarding the non-containing proline substrates. Thus, AlaAlaAla-AMC and AlaAlaCys-AMC have very similar k_{cat}/K_m values. The former, as a result of a higher turnover, and the last, as a result of a lower K_m constant but in general all substrate parameters being very proximal to the wild type reference values.

3.7.0 Recombinant human prolyl oligopeptidase cysteine 255 variant.

The Cys²⁵⁵ is a residue that has been as well assigned to the S_3 pocket [67], figure 8. This residue has attracted a special attention because the use of thiol modifying reagents was deleterious for the enzyme's activity. The modified cysteine was demonstrated to be the Cys²⁵⁵ [104]. Actually the Cys²⁵⁵ in such position is able to sterically influence the substrate from the P_1 up to the P_3 positions.

3.7.1 Recombinant human alanine 255 prolyl oligopeptidase variant.

The kinetic data collected in the table 25 belong to the C255A prolyl oligopeptidase variant. All measured K_m constants stay in a rather narrow range. In particular the k_m value obtained from the GlyProPro-AMC derivative is the lowest compared to all the other generated enzyme variants. The measured turnover constants are rather high for the dipeptide derivatives. Particularly, it outstands the value measured for Z-AlaPro-

AMC which increases five-fold in comparison to the measured k_{cat} with wild type enzyme. Nevertheless, the turnover rates for the C255A variant are comparable to the ones measured with the wild type enzyme.

Substrate	K_m (μM)	k_{cat} (s^{-1})	k_{cat}/K_m ($\text{mM}^{-1}\text{s}^{-1}$)
Z-GlyPro-AMC	68.45 (± 3.83)	39.2 (± 1.4)	572.6 (± 40)
Z-AlaPro-AMC	16.10 (± 1.61)	23.4 (± 1.2)	1453.0 (± 160)
AlaAlaPro-AMC	76.3 (± 4.8)	5.19 (± 0.14)	68.0 (± 5)
AlaAlaAla-AMC	185.6 (± 6.7)	0.147 (± 0.002)	0.79 (± 0.03)
AlaAlaCys-AMC	447.0 (± 58)	1.49 (± 0.16)	3.3 (± 0.5)
AlaAlaSer-AMC	N.D.	N.D.	N.D.
GlyProPro-AMC	135.0 (± 10)	3.84 (± 0.19)	28.4 (± 3)

Table 25 Kinetic parameters of the recombinant human C255A prolyl oligopeptidase variant determined with AMC derivatives. N.D.: not detected. The measurements were performed as described in materials and methods, sections 2.7.2. and 2.7.3. The mean value (\pm SEM) of three measurements are given.

3.8.0 Characterization of prolyl oligopeptidase inhibitors.

3.8.1 Slow-tight binding ammonium methyl ketone inhibitor.

A competitive slow-tight binding inhibition is basically defined as the inhibition that shows a time dependent pattern [153].

rhPEP variant	K_m GlyProPro-AMC (μM)	K_i (nM)
wild type	136 (± 9)	7.6 (± 0.5)
R643A	5158 (± 886)	2007.0 (± 213)
R643K	2550 (± 418)	154.0 (± 14)
W595A	6785 (± 1860)	9577.0 (± 1557)
W595F	1254 (± 243)	372.0 (± 55)
W595Y	1085 (± 122)	207.0 (± 21)
F173A	2367 (± 1001)	65.6 (± 19.1)
M235A	200 (± 12)	6.9 (± 0.5)

Table 26 On the table's head the molecular structure of the ammonium methyl ketone inhibitor, AMK, is shown. They are highlighted, in red the benzyloxycarbonyl group, in blue the diketone structure, in orange the pyrrolidine ring, in green the reactive carbonyl function and in pink the ammonium methyl moiety. Michaelis-Menten constant, K_m , of the substrate GlyProPro-AMC and the affinity constant, K_i , of the AMK inhibitor, AH683 (see appendix table 42) determined with the different prolyl oligopeptidase, rhPEP, variants: wild type, R643A, R643K, W595A, W595F, W595Y, F173A and M235A are listed. The measurements were performed as described in materials and methods section 2.7.5. The mean value (\pm SEM) of three measurements are given.

The mechanism of action of such inhibitors involves either a rather slow diffusion of the inhibitor into and from the active site or a fast formation of an enzyme-inhibitor complex which undergoes afterwards a slow isomerization reaction [153]. Table 26 summarizes the kinetic data measured with the slow-tight binding ammonium methyl ketone Z-L-Pro-L-Pro-AMK inhibitor, also referred to as AMK or AH683, for the different prolyl oligopeptidase variants generated within this work.

3.8.2 Competitive irreversible heteroarylketone inhibitor.

Competitive irreversible inhibitors bind to the enzyme's active site, which undergoes a chemical modification that abolishes its enzymatic competence. Table 27 summarizes the kinetic data characterized with the irreversible heteroarylketone inhibitor Z-L-Ala-L-Pro-BT, also referred to as HAK or AJN118 molecule (see appendix table 43), for the different prolyl oligopeptidase variants produced within this work.

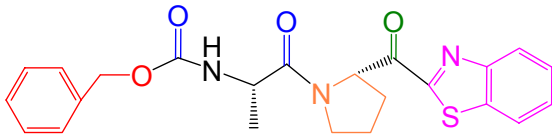
Structure of the Z-L-Ala-L-Pro-BT inhibitor		
		
rhPEP variant	K_m GlyProPro-AMC (μM)	K_i (nM)
wild type	144 (± 9)	0.57 (± 0.08)
R643A	11143 (± 8457)	58.6 (± 7.8)
R643K	8334 (± 3845)	1.98 (± 0.18)
W595A	11510 (± 8250)	191 (± 66)
W595F	2339 (± 485)	6.7 (± 0.8)
W595Y	1230 (± 159)	2.53 (± 0.27)
F173A	1486 (± 220)	2.01 (± 0.18)
M235A	227 (± 12)	0.068 (± 0.004)

Table 27 On table's head the molecular structure of the heteroarylketone inhibitor, HAK, is shown. They are highlighted, in red the benzyloxycarbonyl group, in blue the diketone structure, in orange the pyrrolidine ring, in green the reactive carbonyl function and in pink the benzothiazole aromatic system. Michaelis-Menten constant, K_m , of the substrate GlyProPro-AMC and the affinity constant, K_i , of the HAK inhibitor, AJN118 (see appendix table 43), determined with the different prolyl oligopeptidase, rhPEP, variants: wild type, R643A, R643K, W595A, W595F, W595Y, F173A and M235A are listed. The measurements were performed as described in materials and methods section 2.7.5. The mean value (\pm SEM) of three measurements are given.

3.8.3 Competitive diketone inhibitor.

A competitive inhibitor is characterized because it is increasing the apparent K_m for the substrate while the maximal initial rate, V_{max} , remains unchanged. Table 28 summarizes the kinetic data measured with the simple competitive diketone inhibitor,

as well known here as DK or AH769 molecule (see appendix table 44), for the different prolyl oligopeptidase variants being generated.

Structure of the diketone inhibitor		
rhPEP variant	K_m GlyProPro-AMC (μM)	K_i (nM)
wild type	353 (± 36)	19.9 (± 1.06)
R643A	7497 (± 2290)	318214.0 (± 46372)
R643K	3332 (± 1054)	510.0 (± 88)
W595A	2920 (± 661)	161800.0 (± 45515)
W595F	1974 (± 349)	379.0 (± 54)
W595Y	1155 (± 257)	3437.0 (± 631)
F173A	2382 (± 602)	1588.0 (± 212)
M235A	189 (± 10)	31.0 (± 2)

Table 28 On table's head the molecular structure of the diketone inhibitor, DK, is shown. They are highlighted, in blue the diketone structure, in red the p-methylphenylene ring and in orange the thiophene group. Michaelis-Menten constant, K_m , of the substrate GlyProPro-AMC and the affinity constant, K_i , of the DK inhibitor, AH769 (see appendix table 44), measured with the different prolyl oligopeptidase, rhPEP, variants: wild type, R643A, R643K, W595A, W595F, W595Y, F173A and M235A are listed. The measurements were performed as described in materials and methods section 2.7.5. The mean value (\pm SEM) of three measurements are given.

3.8.4 Inhibitors derivatization.

3.8.4.1 Ammonium methyl ketones inhibitor derivatization.

Table 29 summarizes the parameters of the derivatization of the Z-L-Pro-L-Pro-AMK scaffold (see appendix table 42 for the inhibitors molecular structure). This ammonium methyl ketone inhibitor was mainly modified on its ammonium methyl group, which was exchanged for different heterocycle molecules. Thus, in the AH684 molecule the ammonium methyl was exchanged for a pyrrolidine ring, in AH686 for a morpholine ring, in AH687 for a piperidine ring and in AH688 for a pyridine ring. In the AH673 two main changes, the ether function of the benzyloxycarbonyl group was exchanged for a double amine function and the ammonium methyl was replaced for a simple alcohol moiety. Finally, the derivatization of compounds AH690-4 and AH691 was achieved by substituting in an imidazol ring, in the AH690-4 molecule, and in a piperazine ring, in the AH691 inhibitor, two times the Z-L-Pro-L-Pro arm of the original scaffold, giving symmetric molecules around the pointed ring.

Ammonium methyl ketone scaffold derivatives	
Molecule	K _i (nM)
AH683	7.62 (±0.50)
AH684	119.1 (±20.9)
AH685	9.9 (± 0.45)
AH686	5.1 (±0.12)
AH687	24.9 (±0.48)
AH688	5.81 (±0.09)
AH673	0.39 (±0.01)
AH690-4	0.33 (±0.01)
AH691	2.03 (±0.05)

Table 29 Constants of the PEP-inhibition determined with different ammonium methyl ketone derivatives. See appendix table 42 for the inhibitors molecular structure. For each structure are given its code and its measured K_i constant. The measurements were performed as described in materials and methods, section 2.7.5., using the wild type prolyl oligopeptidase. The mean value (±SEM) of three measurements are given.

3.8.4.2 Heteroaryl ketones inhibitor derivatization.

Table 30 summarizes the inhibitory constants of the generated molecules as a result of a derivatization of the heteroaryl ketone Z-L-Ala-L-Pro-BT inhibitor scaffold. In this case, the derivatization was mainly carried out by exchange of the L-amino acid substituents of the original inhibitor for either more or less bulky residues or charged amino acids.

Heteroaryl ketone derivatization		
Molecule	K _i (nM)	IC ₅₀ (nM)
AJN 118	0.57 (±0.08)	0.12 (±0.03)
AH 807	N.A.	1360.00 (±536)
ZW 215	0.057 (±0.007)	N.A.
AH 810	N.A.	>10000.00
AH 817	4.92 (±0.52)	N.A.
AH 829	3.24 (±0.26)	N.A.
AH 831	12.2 (±4.5)	N.A.
AH 839	12.1 (±2.4)	N.A.
AH 851	19.7 (±8.7)	N.A.
AH 815	0.11 (±0.08)	N.A.

Table 30 Constants of the PEP-inhibition determined with different heteroaryl ketone derivatives. For each structure are given its code and either its measured K_i or IC₅₀ constants. See appendix table 43 for the inhibitors molecular structure. The measurements were performed as described in materials and methods, sections 2.7.5. and 2.7.6., using the wild type prolyl oligopeptidase. The mean value (±SEM) of three measurements are given.

Thus, the original scaffold Z-L-Ala-L-Pro-BT was modified as follows (See appendix table 43). In the molecule ZW215 a phenylalanine was introduced instead of the alanine residue. In AH807, the original L-Ala-L-Pro sequence was exchanged for L-

Phe-L-Ala. In AH810, the new sequence L-Phe-L-Gly was introduced. In AH817, a double proline ring was formed with a L-Pro-L-Pro sequence. In the AH829, a basic arginine was introduced resulting in the sequence L-Arg-L-Pro. In the molecule AH831, an aspartate residue was introduced instead of the alanine, giving a L-Asp-L-Pro sequence. In the molecule AH839 an extension of the chain was achieved by inserting a third residue, resulting in the sequence L-Gly-L-Phe-L-Pro, whereas in the molecule AH851 the opposite was followed and the elimination of the alanine residue gave a single amino acid molecule, Z-L-Pro-BT. Finally in the AH815 molecule the benzothiazole group, abbreviated BT, was exchanged for a smaller thiazole moiety.

3.8.4.3 Diketones inhibitor derivatization.

In the table 31 were collected the inhibitory parameters of the different diketone derivates (See appendix table 44 for the inhibitors molecular structure). It starts with the AH707 compound, which lacks the methyl substituent on the phenyl aromat. In the AH741 molecule the phenyl moiety is bonded with a propyl ether chain to the rest of the molecule.

Diketone derivatives		
Molecule	K _i (nM)	IC ₅₀ (nM)
AH769	19.9 (±1.06)	38.1 (±4.6)
AH707	25.9 (±2.35)	N.A.
AH741	199.0 (±48.6)	N.A.
AH708	N.A.	40500 (±3940)
AH751	N.A.	5960 (±498)
AH711	N.A.	97400 (±7260)
AH754	N.A.	1000000
AH713	N.A.	1620 (±364)
AH755	75.6 (±6.52)	N.A.
AH732	58.5 (±3.78)	N.A.
AH771	7.6 (±0.591)	N.A.
AH897	15600.0 (±887)	N.A.
AH738	113.0 (±37.4)	N.A.

Table 31 Constants of the PEP-inhibition determined with different diketone inhibitor derivatives. For each structure are given its code and either its measured K_i or IC₅₀ constants. Molecular structures are shown in the appendix table 44. The measurements were performed as described in materials and methods using the wild type recombinant prolyl oligopeptidase, sections 2.7.5. and 2.7.6. The mean value (±SEM) of three measurements are given.

In the AH708 analogue the ether function, that bonds the phenyl ring to the diketone group, is missing because it was exchanged for an alkyl chain. In the AH751 molecule the phenyl ring that belongs to the diketone function, was exchanged for an alkyl chain. In the AH711 analogue the ether function was exchanged for an amine function and

the thiophene group for a phenyl aromat. In the AH754 molecule the ether function was exchanged for a thioether function. In the AH713 molecule the thiophene was exchanged for a phenyl ring. In the AH755 analogue the thiophene ring was substituted for a furan ring. The phenyl ring, in the AH732 molecule, was exchanged for a dibenzocyclopentane ring. In the AH897 molecule the thiophene ring was substituted with a thiazole ring. In the AH738 molecule the phenyl ring was exchanged for a naphthalene ring. Finally, in the molecule AH771 the phenyl ring was exchanged for a thiophene ring.

3.8.4.4 Slow-tight binding inhibitors, k_{on} and k_{off} rate constants characterization.

Inhibitor	K_i (nM)	$k_{on} \times 10^5$ ($M^{-1}s^{-1}$)	$k_{off} \times 10^{-5}$ (s^{-1})
AH673	0.39 (± 0.007)	37.80 (± 12.6)	150.0 (± 50.3)
AH683	7.62 (± 0.5)	0.50 (± 0.25)	38.8 (± 21.0)
AH687	24.90 (± 0.4)	0.14 (± 0.02)	34.5 (± 4.34)
AH688	5.81 (± 0.09)	0.05 (± 0.018)	2.9 (± 1.08)
AH689	3.99 (± 0.06)	5.82 (± 1.83)	233.0 (± 75.8)
AH690-3	28.20 (± 0.55)	8.45 (± 1.07)	2380.0 (± 318)
AH690-4	0.33 (± 0.008)	410.00 (± 41.7)	1350.0 (± 15)
AH685	10.40 (± 0.194)	0.22 (± 0.12)	22.8 (± 12.5)
AH686	5.07 (± 0.122)	2.18 (± 0.98)	110.0 (± 48.0)
AH681	7.16 (± 0.155)	1.53 (± 0.23)	110.0 (± 18.0)
AH691	2.03 (± 0.05)	0.34 (± 0.06)	6.9 (± 1.2)

Table 32 Inhibition constants of the PEP-inhibition determined with different diketone slow-tight binding inhibitors. In the first column outlines the inhibitor codes. The second column shows the calculated inhibition constants, K_i . The third and fourth columns show the inhibitor diffusion rate constants k_{on} and k_{off} respectively. See appendix tables 42 and 43 for the molecular structure of the characterized inhibitors. The mean value (\pm SEM) of three measurements are given.

Table 32 summarizes the rate constants parameters that characterize the slow-tight binding inhibition of the ammonium methyl ketone, AMK, based inhibitors. The slow-tight binding behaviour was characterized as described elsewhere [132].

3.9.0 MALDI-TOF-MS characterization of the prolyl oligopeptidase activity.

The use of the MALDI-TOF mass spectrometry was a very useful technique in order to characterize the peptidase activity of real peptide substrates. Regarding the substrates hydrolysis there are two major advantages. First, the size of the substrates is not, in principle, a limiting factor. Therefore, it is possible to characterize the hydrolysis of real

natural peptides. Second, in comparison to the fluorogenic derivatives, there is absence of any restriction for the characterization of substrate P_n' positions.

The substrate size exclusion is one of the hallmarks that has defined, since early, prolyl oligopeptidase. That is the main reason why MALDI-TOF appeared to be an adequate technique to characterize the cleavage of peptide substrates, that because of their size, are not suited for any kind of derivatization. The prolyl oligopeptidase substrate length exclusion was assayed using the peptide Neuropeptide Y, an 36 amino acid long neuropeptide. Three different substrate length variants were generated, by shortening the original 36 amino acid long peptide from the carboxy terminus six residues each time, see table 33.

Peptide name	Sequence	Cleavage site						
		P ₅	P ₈	A ₁₂	P ₁₃	A ₁₄	A ₁₈	A ₂₃
NPY 1-36	YPSKP ₅ DNP ₈ GEDA ₁₂ P ₁₃ A ₁₄ EDMA ₁₈ R YYSA ₂₃ LRHYINLITRQRY	-	-	-	-	-	-	-
NPY 1-30	YPSKP ₅ DNP ₈ GEDA ₁₂ P ₁₃ A ₁₄ EDMA ₁₈ R YYSA ₂₃ LRHYINL	+	-	-	+	-	-	+
NPY 1-24	YPSKP ₅ DNP ₈ GEDA ₁₂ P ₁₃ A ₁₄ EDMA ₁₈ R YYSA ₂₃ L	+	-	-	+	-	-	+

Table 33 Summary table of the cleavage pattern of the Neuropeptide Y peptide variants by prolyl oligopeptidase. In the sequence column are shown the one letter code primary sequences of the tested peptides. The potential cleavage sites are indicated with the respective residue number, taking as first the residue on the amino terminal side. On the right boxes, for each potential cleavage site, (-) denotes a non-detected cleavage, (+) denotes a detected cleavage.

Additionally, the peptide Humanin was as well used as a lead peptide, to generate different variants. Humanin, HN, is a 24 amino acid long peptide with neuroprotective features. In principle, Humanin has two potential proline cleavage sites. Interestingly, this peptide allowed earlier to unveil the prolyl oligopeptidase post-cysteine specificity [165]. Table 34 summarizes the MALDI-TOF-MS characterization of the prolyl oligopeptidase hydrolysis of this peptide. The original Humanin peptide was modified exchanging the respective residues of the P₃ position regarding the Cys₈ and Pro₁₉ cleavage sites.

Interestingly out of the data shown in table 34 two facts triggered our interest. First, the post-cysteine cleavage is a singularity of this particular peptide? Second, what are the reasons for lack of hydrolysis of the Pro₁₉? Regarding the first question, one needed then to describe the same hydrolysis specificity in a different peptide. Therefore, it was

Peptide name	sequence	cleavage site		
		P ₃	C ₈	P ₁₉
HN	MAP ₃ RGFSC ₈ LLLLTSEIDL ₁₉ VKRRA	+	+	-
F6A-HN	MAP ₃ RGASC ₈ LLLLTSEIDL ₁₉ VKRRA	+	+	-
F6D-HN	MAP ₃ RGDSC ₈ LLLLTSEIDL ₁₉ VKRRA	+	-	-
D17A-HN	MAP ₃ RGFSC ₈ LLLLTSEIALP ₁₉ VKRRA	-	+	-
D17F-HN	MAP ₃ RGFSC ₈ LLLLTSEIFLP ₁₉ VKRRA	-	+	-

Table 34 Summary table of the cleavage pattern of the Humanin peptide variants, HN, by prolyl oligopeptidase. In the sequence column are shown the one letter code primary sequence of the tested peptides. The potential cleavage sites are indicated with the respective residue number, taking as first the residue on the amino terminal side. On the right boxes, for each potential cleavage site, (-) denotes a non-detected cleavage, (+) denotes a detected cleavage.

synthesized a peptide variant of one of the PEP well known *in vitro* substrates, Substance P. The original peptide was modified by exchanging a proline residue for a cysteine residue, P4C-SP, generating thus the peptide sequence shown in table 35.

Peptide	sequence	Peptide product		
		P ₂	C ₄	G ₉
P4C-SP	RP ₂ KC ₄ QQFFG ₉ LM	-	-	+

Table 35 Summary table of the cleavage pattern of the Substance P peptide variant, P4C-SP, by prolyl oligopeptidase. In the sequence column is shown the one letter code primary sequence of the tested peptide. The potential cleavage sites are indicated with the respective residue number, taking as first the residue on the amino terminal side. On the right boxes, for each potential cleavage site, (-) denotes a non-detected cleavage, (+) denotes a detected cleavage.

No post-cysteine cleavage was detected using the Substance P variant, P4C-SP. Therefore, the approach was slightly changed. Instead of testing chimeric peptides we looked for natural peptides with endogenous cysteine cleavage sites. This is actually not so straightforward as many of the peptides with cysteine residues are building disulfide bridges. Only a single example was found in the literature [105].

The search of new putative endogenous prolyl oligopeptidase substrates on porcine brain extracts unveiled a series of peptides as potential substrates of the enzyme [105]. Among the characterized peptides we could distinguish a fragment of the S100 calcium-binding protein, VTTACHEF. This peptide arose as potential substrate in order to validate the prolyl oligopeptidase post-cysteine specificity, figure 9.

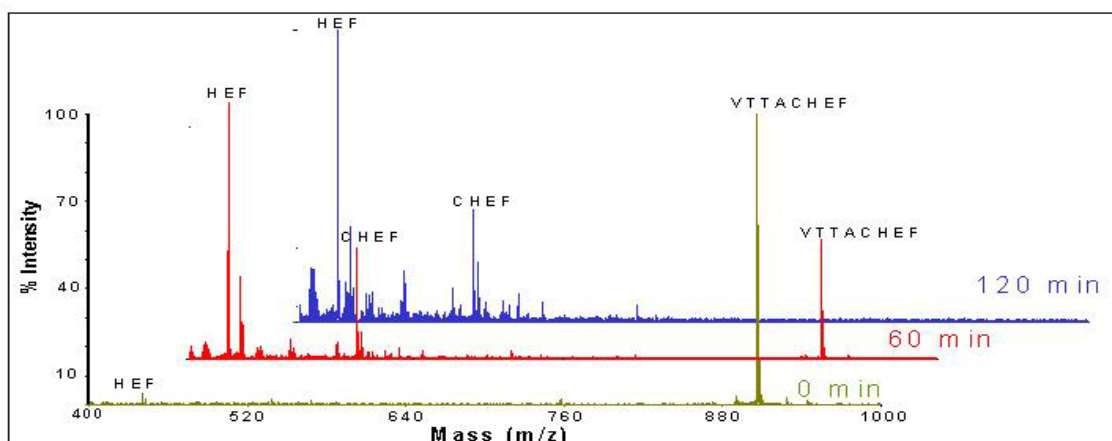


Figure 9 MALDI-TOF-MS spectra of the time depending hydrolysis of the peptide VTTACHEF with prolyl oligopeptidase. The green spectra shows the full length peptide at incubation time zero. The red spectra shows three peaks, first the uncleaved peptide, VTTACHEF, and two product peptides CHEF and HEF. The blue spectra shows the total conversion of the full length peptide into the product peptides CHEF and HEF.

In addition to the post-cysteine cleavage, the Humanin peptide made evident the singularity of the Pro₁₉ as it was not generally recognized as cleavage site. This triggered our curiosity because in principle the Pro₁₉ should be a suitable target for prolyl oligopeptidase. Our first approach looked for an explanation on the amino terminal side of the not cleaved proline. In that sense, three amino terminal shortened versions of the original 24-long amino acid substrate were produced. The sequences of the three different peptides, 13-24HN, 15-24HN and 17-24HN, are shown in table 36. Interestingly, the recombinant prolyl oligopeptidase did not show a special sensitivity towards the Humanin peptide variants 13-24HN, 15-24HN and 17-24HN. As well, on these shortened Humanin peptides the Pro₁₉ site remained uncleaved. Then, the reason for the hydrolytic resistance had to be found in the carboxy primary sequence of the proline cleavage site of the 17-24HN peptide, DLPVKRRA.

Peptide name	sequence	Cleavage site P ₁₉
13-24HN	TSEIDL ₁₉ VKRRA	-
15-24HN	EIDL ₁₉ VKRRA	-
17-24HN	DLP ₁₉ VKRRA	-

Table 36 Summary table of the hydrolysis pattern of the Humanin variants, 13-24HN, 15-24HN and 17-24HN, by prolyl oligopeptidase. In the sequence column are shown the one letter code primary sequences of the tested peptides. The potential cleavage site is indicated with a residue number, taking as first the residue on the amino terminal side of the original Humanin peptide. On the right boxes, for each potential cleavage site, (-) denotes a non detected cleavage.

Therefore, the octapeptide DLPVKRRA was used as lead peptide in order to generate different variants to unveil the influence of the substrate P_n' positions. Four different peptides were generated exchanging the respective amino acid for histidine. The tested peptides allowed then to characterize the substrate positions from the P_2' to the P_4' . The results obtained with this approach disclosed the relevance of the P_n' substrate residues in Humanin, figure 10. Like we did with the newly described post-cysteine cleavage, one needed to validate the likelihood of the strong influence of the P_n' substrate sites in order to discard the possibility of any exceptionality. The following approach was intended. Angiotensin is known to be a reliable good *in vitro* substrate of prolyl oligopeptidase and therefore we used the Angiotensin peptide as the lead peptide. To the original Angiotensin II primary sequence was added by the same motif that was found to be inhibitory in the 17-24HN peptide, the "KRR" motif. An alanine scanning of this "KRR" motif was performed. This resulted in six different angiotensin II variants which hydrolysis is summarized in table 37.

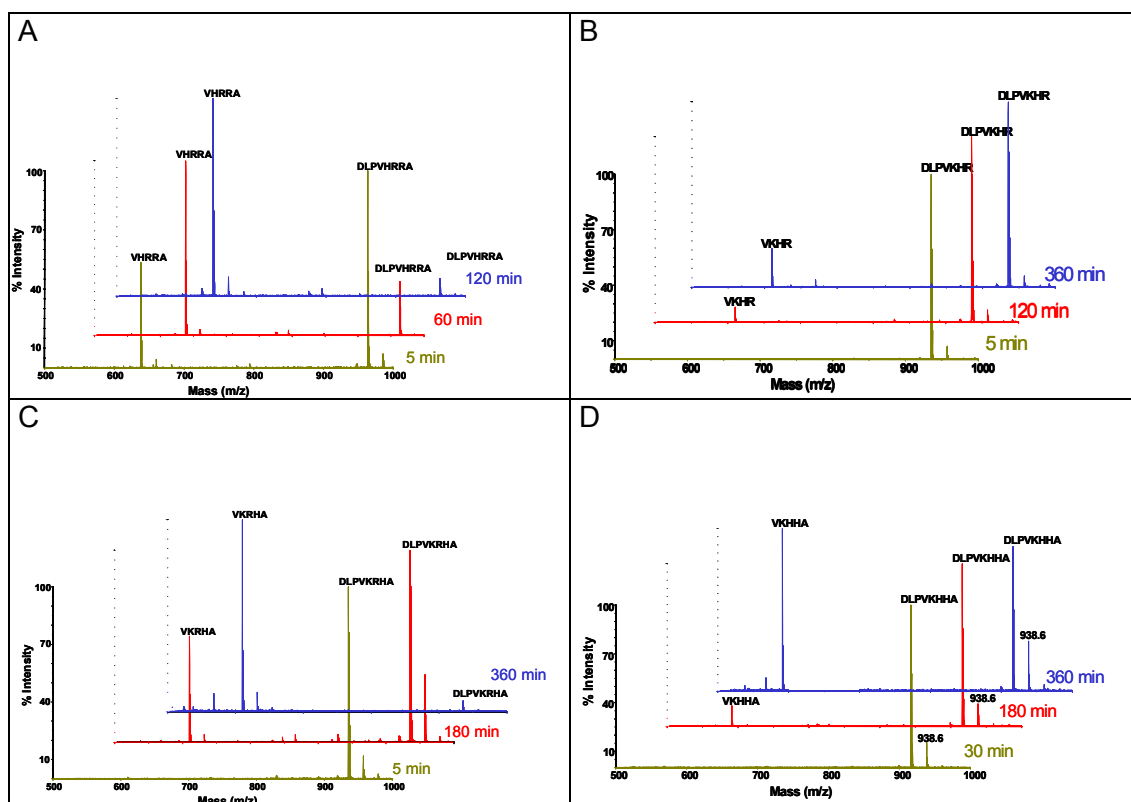


Figure 10 MALDI-TOF-MS spectra of the time depending hydrolysis of the variants of the lead peptide DLPVKRRA by prolyl oligopeptidase. All four diagrams show in green the earliest measured time point, in red an intermediate time point and in blue the latest measured time point. In the box A is shown the cleavage of the peptide DLPVHRRRA, in the box B the peptide DLPVKHRA, in the box C the peptide DLPVKRHA and in the box D the peptide DLPVKHHA.

The different Angiotensin substrates variants allowed us to review the influence of the P_n' substrate sites in a independent peptide.

Peptide	Sequence	Cleavage
SM1056	DRVYIHPFKRA	+
SM1057	DRVYIHPFARR	+++
SM1058	DRVYIHPFKAR	++
SM1059	DRVYIHPFKRA	+
SM1060	DRVYIHPFKRR	+
Angiotensin II	DRVYIHPF	++++

Table 37 Summary table of the hydrolysis pattern of the variants of the lead peptide Angiotensin II, DRVYIHPF. The first column shows the name of the peptide, the second column summarizes the primary sequence of the peptide and the last column summarizes the degree of hydrolysis of the post-proline cleavage of each tested peptide. A qualitative ranking denotes the rates of hydrolysis as lowest with (+) and the highest with (++++).

On the one hand a possible explanation for the catalytic importance of Arg⁶⁴³ was already pursued characterizing its related variants, described above in the sections 3.3.1 and 3.3.2., but on the other hand it resulted interesting to describe the influence of the coordination of the P₂ carbonyl function of the substrate by the guanidinium moiety of the Arg⁶⁴³ from the other side, the substrate side.

The generation of two different substrate variants of the Angiotensin peptide was intended. These two Angiotensin variants carried modifications concerning the main chain. In one case the peptide generated was lacking the carbonyl function of the residue in P₂ position in relation to the post-proline cleavage site, resulting in a reduced angiotensin. On another case, the peptide was methylated on the amine function of the main chain of the residue on P₁' position in relation to the post-proline cleavage site, thereby resulting in a methylated angiotensin. Figure 11 shows the representative spectra of the hydrolysis of the Angiotensin I peptide and its related variants, the reduced and methylated Angiotensin respectively.

One hour for the former and four hours incubation interval for the last Angiotensin variants are shown. In addition to these experiments, similar substrates were generated but this time derivatized as fluorogenic peptides. AlaAlaΨ[CH₂-NH]Pro-AMC, as reduced, and Dabcyl-KDRVYIHPΨ[CO-NMe]FHE-Edans, as methylated, amide bond variants. Prolyl oligopeptidase as well did not succeed in hydrolyzing them. Even though this spectrofluorometric approach did not reveal any turnover of these peptides, as poor substrates they appear to be useful to measure their affinity constant. AlaAlaΨ[CH₂-NH]Pro-AMC shown a K_i constant worth in 268±26 μM, while Dabcyl-KDRVYIHPΨ[CO-NMe]FHE-Edans gave a K_i constant of 0.33±0.01 μM.

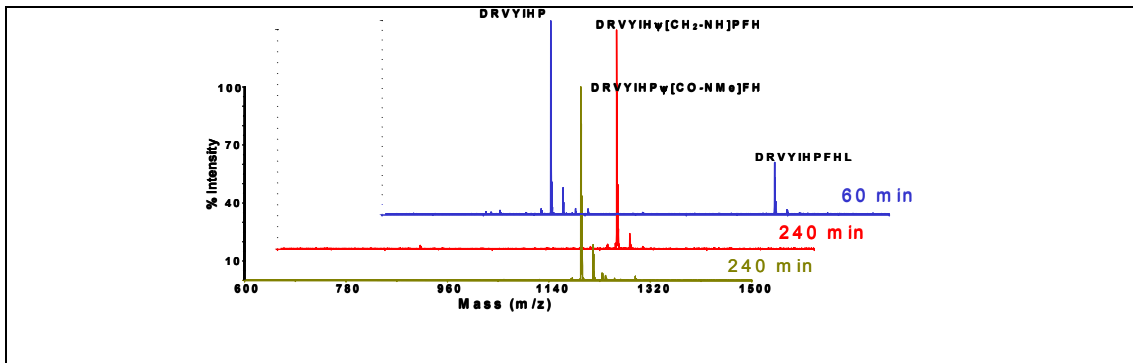


Figure 11 MALDI-TOF spectra of the time depending cleavage of the angiotensin peptide variants. In blue the spectra of the original Angiotensin I, DRVYIHPFHL, in green the spectra of the methylated Angiotensin, DRVYIHP[CO-NMe]FH, and in red the spectra of the reduced Angiotensin, DRVYIHP[CH₂-NH]PFH.

4.0 Discussion.

4.1 Expression and purification of the recombinant human prolyl oligopeptidase variants.

The established protocols for the expression and purification of the wild type prolyl oligopeptidase enzyme allowed us to face with confidence the isolation of the different enzyme variants. Regardless of this, the simple substitution of the native residues arose with significantly altered rates of expression, usually lowered, figure 12. Specially with the variants R643A and W595A they were found notable decays on the yields of expression. Thus, in comparison to the expression levels of the wild type enzyme, the expression of the R643A and W595A variants did generate, in terms of final purified protein, a tenth of the original expected protein amount. This is suggesting that during the expression of the heterologous protein the substituted residues could play a relevant role in the folding mechanism. It might be possible that the loss of these residues to have as consequence increased rates of aggregation due to slight changes in structure during the expression process [166]

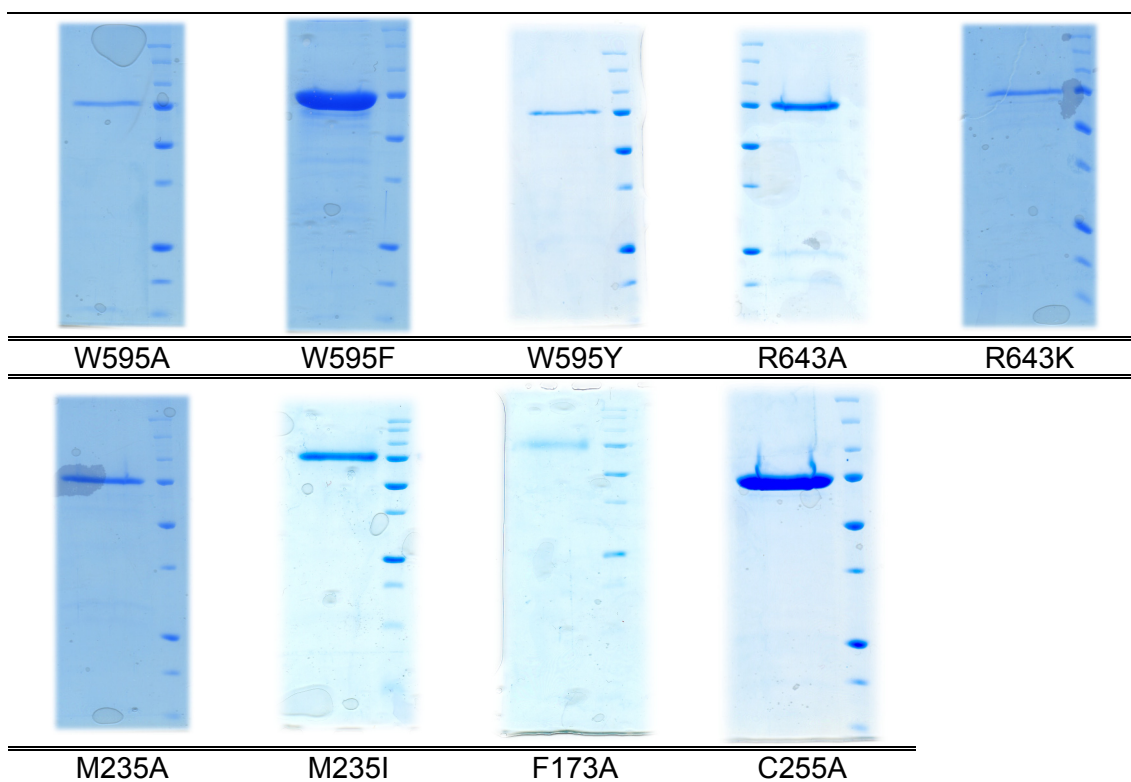


Figure 12 SDS-PAGEs of the different prolyl oligopeptidase variants purified within this work.

4.2 Recombinant wild type prolyl oligopeptidase.

Although prolyl oligopeptidase has been extensively kinetically characterized, the amount of available kinetic data concerning the 7-amino-4-methylcoumarin (AMC) derivatives is actually not abundant. However, more information is available regarding the kinetic characterization of the prolyl oligopeptidase hydrolysis of paranitroaniline, (pNA) surrogate substrates. Thus, it is easier to find in the literature the more diverse contributions that have been made regarding the kinetic characterization of the prototypic prolyl oligopeptidase substrate, Z-Gly-Pro-pNA, see table 38.

Source	K_m (μM)	k_{cat} (s^{-1})	k_{cat}/K_m ($\mu\text{M}^{-1}\text{s}^{-1}$)	reference
rpPEP	14.7 \pm 1.5	95.6 \pm 5.7	6.5	[91]
rpPEP	5.9 \pm 0.5	32.5 \pm 1.2	5.5	[87]
pPEP	1.7	2.1	1.2	[167]
rfPEP	160.0 \pm 9.5	16.9 \pm 1.5	0.105 \pm 0.009	[77]
rfPEP	53.0	N.A.	N.A.	[49]
TdPEP	830.0	112.7	0.13	[168]
rhPEP	33.1 \pm 0.07	3.9 \pm 0.04	0.11 \pm 0.005	present work

Table 38 Kinetic parameters obtained with the prolyl oligopeptidase hydrolysis of the chromogenic substrate Z-GlyPro-pNA. Recombinant porcine prolyl oligopeptidase (rpPEP), muscle purified porcine prolyl oligopeptidase (pPEP), recombinant *Pyrococcus furiosus* prolyl oligopeptidase (rfPEP), purified *Treponema denticola* prolyl oligopeptidase (TdPEP), recombinant human prolyl oligopeptidase (rhPEP), not available (N.A.).

The data presented as an example in the table 38 demonstrate that the aim to define an exact value for these kinetic parameters is rather unlikely. The enzyme source diversity and the different measurement conditions explain to a great extent the reason why such dispersed kinetic parameters were obtained. There is, even, a larger shortage of data regarding the available kinetic parameters of AMC derivatives. Table 12 summarizes the steady-state kinetic constants of the hydrolysis of different AMC surrogates with recombinant human prolyl oligopeptidase. The hydrolysis of the standard prolyl oligopeptidase substrate, Z-GlyPro-AMC, allowed us to characterize a K_m of 87.9 \pm 5.2 μM , a k_{cat} of 46.3 \pm 1.9 s^{-1} and a k_{cat}/K_m of 0.53 \pm 0.04 $\mu\text{M}^{-1}\text{s}^{-1}$. Those values are comparable to the ones found in the literature, like for example, a K_m of 20 \pm 3 μM and k_{cat} of 19 \pm 1 s^{-1} [134] or the K_m of 3.4 \pm 0.4 μM and k_{cat}/K_m of 1.9 \pm 0.07 $\mu\text{M}^{-1}\text{s}^{-1}$ [79]. The table 12 shows in addition the steady-state kinetic constants of other different tripeptide AMC derivatives. Thus, AlaAlaPro-AMC was characterized with a K_m of 29.3 \pm 2.8 μM and a k_{cat} of 6.14 \pm 0.17 s^{-1} . Those values are comparable to the kinetic constants reported for the substrate Succinyl-GlyPro-AMC, that although negatively charged it has as well an amino terminal charged moiety, with a K_m of 460 \pm 230 μM

and a k_{cat} of $48 \pm 19 \text{ s}^{-1}$ [134]. Therefore, one can conclude that the parameters reported here can be compared to the findings previously reported in literature.

A further analysis of the data collected in table 12 allowed us to notice how an inverse correlation of their kinetic parameters between the two dipeptide derivatives, namely Z-GlyPro-AMC and Z-AlaPro-AMC, exists. The Z-GlyPro-AMC substrate has a 14-fold higher Michaelis-Menten constant, and as well, a 10-fold higher turnover rate constant than the Z-AlaPro-AMC substrate. A similar relationship was as well found characterising pNA derivatives hydrolyzed by the *Pyrococcus furiosus* prolyl oligopeptidase which ratio $K_m(\text{Z-GlyPro-pNA})/K_m(\text{Z-AlaPro-pNA})$ was shown to be approximately 4, although their turnover rates remained comparable [77]. It appears to be relevant to discern the reason why between so close structurally related substrates such evident differences could be characterized. The prolyl oligopeptidase x-ray crystal structures co-crystallized with ligands have demonstrated that the ligands P_2 side-chain is orientated towards the empty inner cavity of the β -propeller domain [157]. This orientation does not provide any direct interaction between the P_2 ligand side-chain and the protein. Therefore, the lower K_m constant of Z-AlaPro-AMC can only be achieved through the remaining interactions existing between the substrate backbone at the P_2 position and the enzyme, namely the interaction with the Arg⁶⁴³. Basically, these kinetic parameters reveal that the methyl side-chain group of the alanine residue in the Z-AlaPro-AMC substrate influences to such an extent the physicochemical properties of the substrate main chain that it results in a completely different hydrolytic pattern. Therefore, one can conclude that the interaction between the substrate P_2 main chain carbonyl group and the enzyme is indeed relevant regarding the hydrolysis of AMC surrogates, as one could expect arising from such a highly conserved interaction [169]

$K_m = K_s k_3 / (k_2 + k_3)$	Michaelis-Menten constant
$k_{\text{cat}} = k_2 k_3 / (k_2 + k_3)$	Turnover constant
$k_{\text{cat}}/K_m = k_2/K_s$	Specificity constant

Scheme 3 Formulation of the Michaelis-Menten steady-state constants as function of the single rate limiting constants of the reaction described in scheme 1 [170].

It should be taken into account that K_m and k_{cat} steady-state constants are complex constants, see scheme 3 [170], defined on the basis of the kinetic reaction described by the mechanism 1, scheme 1. One can argue that the second order rate constant is usually depending on the nature of the substrate leaving group [79]. In our case both substrates, Z-GlyPro-AMC and Z-AlaPro-AMC, hold the same leaving moiety, AMC,

and therefore, in both cases the AMC moiety should have the same influence over the catalysis. On the other hand in the case of serine proteases, with peptide and amide substrates the K_m values were shown to approach K_s , scheme 3, [87]. In that sense, the analyzed substrates share a high structural homology, therefore, it is not expected that changes in K_s might appear in order to balance the Michaelis-Menten constant. On the other hand, both substrates show very similar specificity constants, and therefore, it is expected that the acylation k_2 rate constant do not vary extremely between both substrates. Consequently, the k_3 first order rate constant, scheme 3, might be the mostly affected step during the entire reaction mechanism. It seems reasonable to think that the enzyme deacylation is the most affected step, as the structural differences on the compared substrates are on the moieties that precisely remain bound to the enzyme. It might be possible that for Z-AlaPro-AMC the deacylation step to be slow enough to make k_3 smaller than k_2 , and then, approaching k_{cat} to k_3 , and in contrast, for Z-GlyPro-AMC it might be a fast enough process that makes k_3 much bigger than k_2 , and therefore, k_{cat} might rather approach k_2 . In that context, the ratio k_3/k_2 would change with the used substrate. The K_m of Z-GlyPro-AMC might approach to K_s , while in the case of Z-AlaPro-AMC it might approach to $K_s k_3/k_2$. It is important then to conclude that the side-chains of the substrates are able to exercise strong influences over their mainchain backbones. Those influences might be relevant enough to differentially modulate the catalysis of prolyl oligopeptidase when short AMC derivatives are characterized.

Furthermore, it appears to be relevant to point out how the extension of the amino terminal blocked Z-AlaPro-AMC to the AlaAlaPro-AMC entails, likewise, an increase of the Michaelis-Menten constant. Actually, there is a substantial structural difference between the amino terminal blocked dipeptide and the free amino terminal tripeptide. This is, the amino terminal positively charged moiety might interfere with the non-polar S_3 pocket of the active site [67]. This might easily explain the increase on K_m between the discussed dipeptide and the tripeptide. Otherwise, the comparison between these two substrates, Z-AlaPro-AMC and AlaAlaPro-AMC, does not reveal a significant difference between their measured turnover constants. In accordance, it could also be shown how the use of the succinyl-GlyPro-pNA substrate entailed an increase of the measured K_m in comparison to the one measured with Z-GlyPro-pNA, whereas the k_{cat} remained for both substrates in the same order of magnitude [91]. As well in our case both substrates display very similar turnover constants and therefore it might be argued that the increased K_m constant is likely a direct consequence of an increase of the affinity constant, K_s , and not because the variation of any other rate constant. This agrees with the idea that the binding of the tripeptide substrate worsened because of

the presence of the positive amino terminal charge interfering with the non-polar active site S_3 pocket. This is indicating the importance of the interaction requirements that need to be satisfied within the S_3 subsite to achieve a proper substrate accommodation and it additionally allowed us to conclude that the non-polar nature of the interactions in the S_3 pocket, in contrast to the S_2 subsite, are basically different involving substrate side chain rather than main chain interactions.

Additionally, the hydrolysis of the substrate GlyProPro-AMC was characterized. The data of the table 12 show how this substrate, in comparison to AlaAlaPro-AMC, displays a one order of magnitude increase of its Michaelis-Menten constant, but as well, it shows one order of magnitude improvement of its turnover constant. The increase in k_{cat} is not strong enough to balance the increased K_m , and therefore, the resulting specificity constant is one order of magnitude lower than the one calculated for AlaAlaPro-AMC. The inhibitor Z-pro-prolinal is structurally similar to the GlyProPro-AMC substrate as both contain a double pyrrolidine based structure. The co-crystallization of the inhibitor with the porcine prolyl oligopeptidase [67] has shown how the double pyrrolidine ring adopts a conformational configuration that place the amino terminal blocking group, Z, in front of the S_3 subsite. The free amino terminal group of the substrate might be forced to interact with such non-polar environment because of the restricted conformation of the double proline. Thus, it has been shown how the binding of substrates to their peptidases usually follow a highly conserved pattern of interactions [169] and this could explain how these two substrates find different solutions to fulfill the same binding requirements. The amino terminal charged moiety in AlaAlaPro-AMC might have, in contrast to GlyProPro-AMC, more freedom to shield itself from the S_3 subsite hydrophobicity. The turnover constant could be seen as the constant of the acyl-enzyme complex breakdown. Hence, the higher turnover measured with the GlyProPro-AMC is indicating that the regeneration of the free enzyme might be easily achieved with the GlyProPro-AMC substrate than with the AlaAlaPro-AMC.

Further analysis of the table 12 showed how prolyl oligopeptidase is able to recognize specifically non-containing proline AMC derivatives. Alanine has been already shown to be a residue processed by prolyl oligopeptidase [171]. The hydrolysis of the AlaAlaAla-AMC substrate allowed us to characterize a K_m constant two orders of magnitude higher than the one shown by AlaAlaPro-AMC. The non-proline containing substrate, in comparison to AlaAlaPro-AMC, displayed non significant differences on the measured k_{cat} . This resulted in a decreased specificity constant which kept the value by two orders of magnitude under the threshold set by AlaAlaPro-AMC. It seems that with AlaAlaAla-AMC the loss of the pyrrolidine ring, and additionally, the presence of the

amino terminal positive charge impaired dramatically the binding features of this substrate, whereas its rate of hydrolysis was actually not affected. Therefore, it might be expected that the variation on K_m is mainly due to the negative contributions of an increased K_s constant, see in scheme 1.

Serine has been additionally shown to be hydrolyzed by prolyl oligopeptidase, although only as a poor substrate [172]. Among the data gathered in table 12 it appears the fact that with the serine containing substrate could be measured a Michaelis-Menten constant of the same range of that for AlaAlaPro-AMC. In contrast, the calculated turnover constant of the AlaAlaSer-AMC substrate was dramatically affected. The k_{cat} value dropped two orders of magnitude in comparison to the one measured for the proline containing tripeptide derivative. Thus the specificity constant of the serine containing substrate decreased up to three orders of magnitude in comparison to the value shown by its counterpart, the proline containing tripeptide substrate. It has, hence, the lowest specificity among the analyzed substrates in table 12, a result that agrees with the data found in literature [172].

Finally, the most interesting data of the table 12 are the ones belonging to the cysteine containing substrate, AlaAlaCys-AMC. It should be pointed out that these data confirm and quantify the rare post-cysteine cleavage performed by a mammalian enzyme for the first time. Before, this cleavage could only be described analytically [165]. Hence, with these data we are able to support the feasibility of this new prolyl oligopeptidase specificity. The hydrolysis of the cysteine containing substrate was characterized with a K_m constant one order of magnitude higher than the one measured with AlaAlaPro-AMC, but on the other hand, the turnover constant of its hydrolysis remained in the same range than the one of the proline containing tripeptide surrogate. The resulting specificity constant for the cysteine containing substrate is two orders of magnitude lower than the one observed with AlaAlaPro-AMC, but it is notably comparable to the specificity constant characterized for the AlaAlaAla-AMC substrate. We are then able to extend the prolyl oligopeptidase specificity with the support of concrete kinetic data. Now cysteine, together with proline, alanine and, in a lesser extent, serine are residues clearly susceptible to prolyl oligopeptidase hydrolysis. Regarding the merops data base [81], two hundred hits were given in answer to a search of post-cysteinylyl peptidase activity. Most of them were metallopeptidases, and therefore prolyl oligopeptidase is the first mammalian serine peptidase described with a proved and quantified *in vitro* post-cysteinylyl activity.

Table 13 summarizes the kinetic parameters obtained with the hydrolysis of FRET derivatives of the peptide Angiotensin. With the first analysis of the obtained data one can denote how among the different characterized FRET peptides one was not

enzymatically hydrolyzed, the serine variant, P5S-Angiotensin II. The measured steady-state kinetic parameters of the Angiotensin I and Angiotensin II FRET derivatives are very similar, almost copies. Angiotensin I has slightly higher K_m and k_{cat} constants, but actually, they are not significantly different compared to the ones obtained with the Angiotensin II. This fact might be interpreted as a lack of restrictive specificity on the S_2' - S_3' enzymes subsites, as these are the differentially affected subsites within the catalysis of these two substrates. The obtained K_m values approached significantly to the characterized affinity K_s constants for other pentapeptides [157]. It is therefore expected that the here characterized K_m constants might represent, as well, a true value of the peptide's affinity. Furthermore, the exchange of the original proline for alanine in the P_1 position, P5A-Angiotensin II substrate, arose with one order of magnitude increase in measured K_m . The same substrate displayed a measured turnover constant comparable to the one obtained with Angiotensin II. This suggests that probably the increase in Michaelis-Menten constant was due to an increase of the affinity constant, K_s . On the other hand, when in the Angiotensin II FRET derivative the proline residue was exchanged for a cysteine residue, P5C-Angiotensin II, the measured Michaelis-Menten constant increased one order of magnitude, and in parallel, the turnover constant decreased two orders of magnitude. Nevertheless, comparing the K_m constants of the P5C-Angiotensin II and P5A-Angiotensin II it is noticeable their resemblance and therefore, it might be argued that as well the cysteine FRET substrate variant suffers the impairment on K_m as a result of an impaired binding. In addition, it could be suggested that both substrate variants might have a similar binding mode.

Very interestingly, the measurement with the Angiotensin I & II FRET derivatives did show a substrate inhibition pattern actually absent with the alanine, P5A-Angiotensin II, and cysteine, P5C-Angiotensin II, substrate variants, figure 13. This additional parameter, K_i , might indicate the presence of a certain flexibility on the binding mode of these substrates which is allowing a non-productive substrate binding arising with an inhibitory profile [134].

Table 14 shows the data concerning an additional characterized FRET derivative based on the NAP peptide [173] as lead peptide. The parameters show a high likeness with the ones found in table 13. Interestingly, it outstands the substrate inhibition pattern that, like it was suggested above, it might be the result of a possible non-productive substrate binding. This is suggesting the existence of additional relevant interactions present in the hydrolysis of the FRET derivatives but maybe not in the hydrolysis of AMC surrogates. As well, it outstands the difference on specificities between both proline cleavage sites. This underlines the importance of the primary

sequence surrounding proline as factor that is influencing importantly the enzyme's specificity.

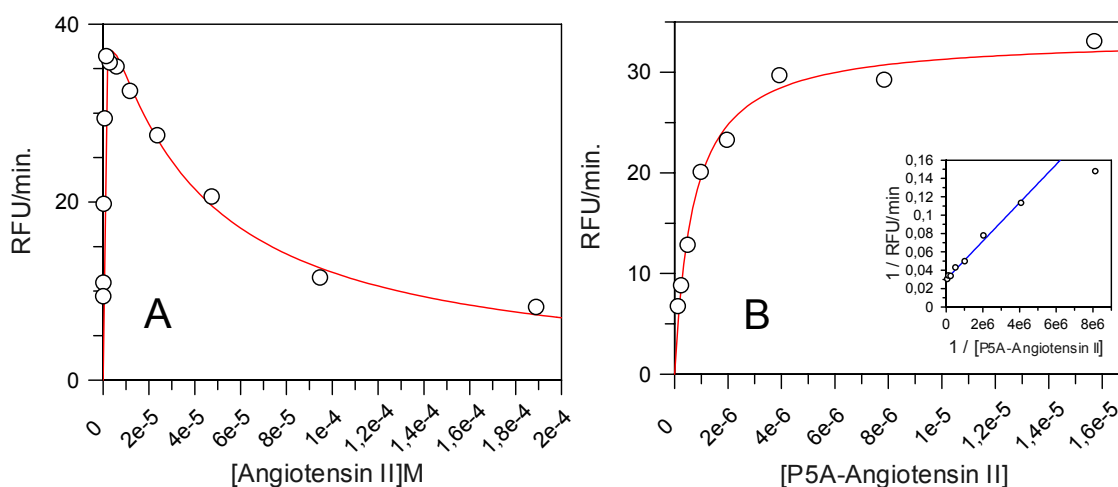


Figure 13 Plots of the prolyl oligopeptidase hydrolysis initial rates against substrate concentration of the FRET derivatives Angiotensin II, DabcyI-KVYIHPFE-Edans, A, and the substrate variant P5A-Angiotensin II, DabcyI -KVYIHAFE-Edans, B. See table 13 for kinetic parameters.

In order to get a deeper comprehension of prolyl oligopeptidase kinetic attributes the temperature dependences of the specificity constant, k_{cat}/K_m , and turnover constant, k_{cat} , for different proline containing substrates were characterized, see figure 7. This approach allowed us to compare different proline specificities in a range of temperatures arising from 25 °C to 45 °C. At first it outstanced the fact that it was possible to draw temperature plots over a range of temperatures that is rather high, up to 45 °C. This might be taken as a sign of the protein stability that actually contradicts what it was stated before in the literature [157]. The analysis of the curves obtained with the Arrhenius plots, in figure 7, shows how two tendencies were followed among the characterized substrates. On the one hand, the set of substrates Z-GlyPro-AMC, AlaAlaPro-AMC and GlyProPro-AMC, that showed proper linearities in the range of measured temperatures, whereas the two substrates Z-AlaPro-AMC and Angiotensin II, deviated from linearity on the Arrhenius plot. The loss of linearity of the Arrhenius plots might be indicative of changes in the rate-limiting steps of the enzymatic reaction [157], and therefore this is supporting that the different proline containing substrates could have different rate limiting steps during their hydrolysis. In this context, it might account as an additional influential effect the changes on the *cis-trans* isomerization rates of the proline containing substrates that as well might occur along the temperature increment [99]. The Arrhenius plots displayed on figure 7 allowed us to compute for the different substrates three parameters, as outlined in table 15-B. These

parameters are the activation energy, E_a , the second order rate constant k_1 and the quotient of the first order rate constants, k_2/k_{-1} , defined as a measure of the substrate stickiness [157]. It is clear to see that Z-GlyPro-AMC, Z-AlaPro-AMC and Angiotensin II share similar high values of k_2/k_{-1} , while the tripeptide substrates, AlaAlaPro-AMC and GlyProPro-AMC, show much lower coefficients than the ones displayed by the former. This paradoxically suggests that the amino terminal blocked dipeptide derivatives might tend to stay shorter in the active site than the tripeptides do, maybe because of the differential amino terminal positive charge. The comparison of the activation energies, table 15-B, shows how the lowest value was found for Z-GlyPro-AMC, while the highest was found with GlyProPro-AMC. This, actually, does not correlate with their turnover rate constants, since both substrates have the highest measured turnover rates, table 12. In this sense, it could be argued that while Z-GlyPro-AMC reach easily the transition state, namely lower E_a , GlyProPro-AMC might comparatively find on its higher substrate stickiness, k_2/k_{-1} , a substantial compensatory effect. Finally, the determined second order rate constants, k_1 in table 15-B, indicate how for the analyzed substrates the rates of access to the active site are lower for the smaller than for the larger substrates. That might suggest that maybe the larger substrates find better chances of secondary interactions on the pathway of access to the active site than the smaller ones. Then, it could be expected a common pathway of substrate access that would restrict more, but not hinder, the largest substrates. In contrast, this access pattern would represent a wider open field for the smallest substrates, offering more freedom, and therefore postponing comparatively their productive access to the active site.

The Eyring plots of the turnover rate constants gave in all cases, in contrast to the Arrhenius plots, good linear correlations. The transition state accounts for a higher ordered state in comparison to the ground state [174] and this leads to negative entropy values. Therefore, in our case the entropy values indicate that GlyProPro-AMC, and to a lesser extend Z-GlyPro-AMC and AlaAlaPro-AMC, reach much higher ordered transition states than the rest of substrates. In this case, the higher entropy might account for one of the forces that is contributing to achieve with GlyProPro-AMC higher rates of hydrolysis, table 12. The rest of substrates, although with lower values, as well display negative entropic values. In any case the values of entropy are rather low, like it has been already shown elsewhere [157;158], thus indicating this that maybe for all substrates no drastic reorganization of the water shield surrounding reactants might take place. In addition, table 15-A compiles the enthalpies determined for the hydrolysis of different proline containing substrates. Noteworthy, the calculated enthalpy for the GlyProPro-AMC derivative is the lowest found, while the rest of tested

peptide derivatives have two to three-fold higher calculated enthalpies. In an enzymatic reaction the enthalpy accounts for the energetic requirements for the breaking of the hydrogen bonds of the water shell and, as well, the breaking of the covalent peptide bond [158]. Therefore, the enthalpy numbers indicate that for GlyProPro-AMC, in comparison to the rest of substrates, the breakdown of the peptide bond is the most easily achieved. This correlates with the fact that the GlyProPro-AMC turnover rate constant was significantly one of the highest here characterized, table 12. Furthermore, in agreement the substrates with comparatively lower hydrolysis rate constants, Z-AlaPro-AMC, table 12, and Angiotensin II, table 13, have as well the highest calculated enthalpies.

Prolyl oligopeptidase was further characterized by characterizing the pH-dependencies of its catalysis, see table 16. In contrast to classical serine peptidases, prolyl oligopeptidase deviates from the classical bell-shaped pH-rate profiles. In this sense, the data compiled in the table 16 demonstrate that the measured pseudo-first order rate constants usually do not fit to a classical simple bell-shaped pH-dependency, see equation 16. This strongly corroborates what is extensively stated in the present literature, for example, for the porcine [87;98;104;157] and the archeon [77] prolyl oligopeptidase enzymes. Within this work they were measured the activity pH-dependencies of different proline containing substrates, see table 16. Thus, while AlaAlaPro-AMC hydrolysis was properly fitting to a simple bell-shaped profile, equation 16, the rest of AMC derivatives showed better fits with a modified simple bell-shaped on the acidic limb of the equation, equation 17. Finally, the Angiotensin I FRET derivative showed the most dramatic deformation of the bell-shaped curve, displaying a doubly bell-shaped curve pH-dependence, equation 18, suggesting the existence of either at mild acidic and alkaline pH of two different active enzyme forms [175]. These differences of the enzyme behaviour can be better appreciated on the figure 14. One can conclude that the variation of the activity pH-dependencies is a strongly substrate influenced effect. In this sense, it was already shown how different amino acid exchanges in a model lead peptide substrate were as well able of modifying the pH-rate profiles of the porcine prolyl oligopeptidase catalysis between bell-shaped and doubly bell-shaped pH-rate profiles [157]. The existence for prolyl oligopeptidase of such a complex pH-rate profiles has been explained on terms of a putative additional acidic group, either glutamate or aspartate, that might perturbate the pKa of the catalytic imidazole [98]. Nevertheless, it has not been yet suggested the identity of a particular residue that might be implicated in these issues, as the kinetic determination of pKa values represent an apparent constant and their interpretation is not always straightforward [176]. Regarding the available crystal structure PDB1uoo the residues

Asp¹⁴⁹, Glu²⁰¹, Asp⁶³⁹, Asp⁶⁴² and Glu⁶⁹² are located within a 6Å radius distance away from the His⁶⁸¹ and they might be taken as possible candidates to influence the catalytic histidine. Finally, it is important to conclude how labile the electrostatic environment of the enzyme's active site is, thus being malleable and susceptible upon substrate hydrolysis [157].

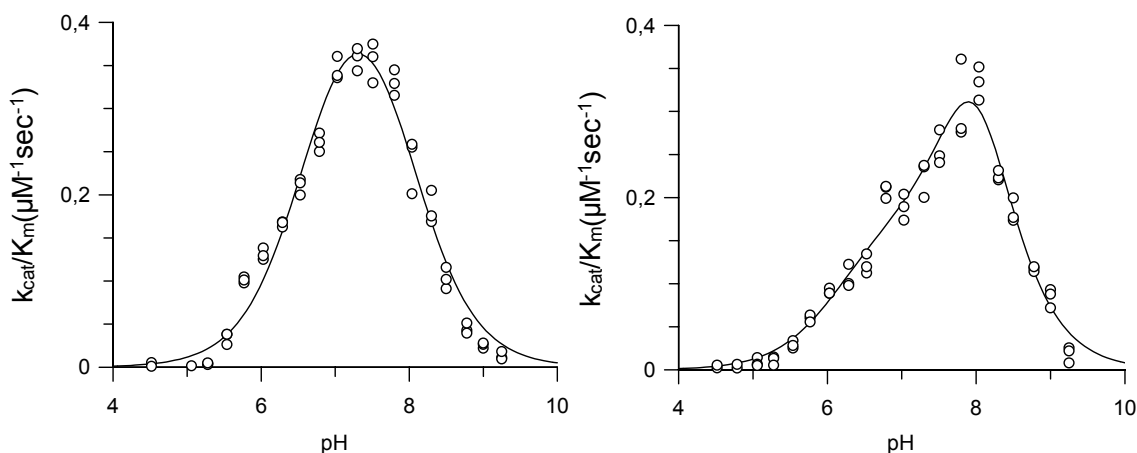


Figure 14 pH-rate profiles of the prolyl oligopeptidase hydrolysis of AlaAlaPro-AMC (left panel) and Angiotensin I (right panel). The data were fitted to the theoretical equation 16 for the substrate AlaAlaPro-AMC and equation 18 for the substrate Angiotensin I.

4.3 Recombinant human prolyl oligopeptidase Arg⁶⁴³ variants.

In the tables 17 and 18 the kinetic parameters of the enzyme variants related to the Arg⁶⁴³ residue were collected. As described above, Arg⁶⁴³ was suggested to play a central role in the binding pattern of the substrates to the enzyme [67]. Significantly, Arg⁶⁴³ is one of the residues conserved with a 100% of identity rate among twenty-eight different sequences of prolyl oligopeptidase [29]. It is also, interesting to see how the structural features of Arg⁶⁴³ noted above are conserved within other related enzymes of the S9 family, like in dipeptidyl peptidase 4 with the residue Arg¹²⁵ [67]. As already mentioned, the non-containing proline AMC surrogates were not hydrolyzed with the variants R643A and R643K. The K_m constants of the amino terminal blocked dipeptide derivatives of both variants highly resemble. In that sense the R643K variant is not able to compensate the lack of the arginine. Nevertheless, the dipeptide derivatives did not suffer a dramatic variation of their K_m values in comparison to the wild type values. This is a surprising finding, as it was expected from the available literature this residue to play a strong role in the substrate binding. This is suggesting that for such dipeptides the contributions of the Arg⁶⁴³ to the binding of the substrates might be not so relevant as it was expected. Regarding the tripeptides derivatives, AlaAlaPro-AMC and GlyProPro-AMC, the consequences appeared to be different.

On the one hand, with these substrates the measured K_m of the R643A and R643K visibly dropped in comparison to the wild type values. On the other hand, with the R643K variant only a rather weak recovery of the K_m constants were noticeable. It is convenient to keep in mind that in these cases the positive amino terminal charge of the tripeptides will easier hinder the substrate binding in the defective active site as already suggested above for the wild type enzyme. All that might indicate that in principle Arg⁶⁴³ contributions to the substrate binding weight less than expected. The analysis of the turnover constants of the recombinant prolyl oligopeptidase R643A and R643K variants allowed to evidence that globally the k_{cat} constants were impaired in comparison to the *a priori* measured k_{cat} constants of the wild type enzyme. The decrease is not homogeneous. Interestingly, the substrates with higher turnovers in the wild type enzyme, Z-GlyPro-AMC and GlyProPro-AMC, were impaired in a larger extent than the ones with originally lower k_{cat} constants, such as Z-AlaPro-AMC and AlaAlaPro-AMC. On the other hand, the measured k_{cat} constants of the R643K variant were, in general, higher than the ones obtained with the R643A variant, which represents a notable catalytic recovery in most of the cases. To our understanding, these data are supporting the suggested as substrate assisted catalysis (SAC) mechanism in which the Arg⁶⁴³ might play a role [89]. The background behind the SAC mechanism suggests that the substrate itself might be able to enhance the enzyme catalysis [177]. In the case of prolyl oligopeptidase an extensive network of hydrogen bonds is indeed pivoting on the guanidinium moiety of the Arg⁶⁴³ side-chain. In this network the amide P₁' substrate leaving group interacts with the carbonyl moiety of the substrate P₂ which is anchored by the Arg⁶⁴³ side-chain. This substrate conformation might facilitate the general acid catalysis, by enhancing the transfer of the proton from the imidazolium group to the leaving moiety [89]. It is convenient to add that the peptide bond on the amino terminus of proline residues are defective in resonance stabilization [1], therefore their carbonyl functions are electronically enriched [10]. Hence, it appears to be relevant there is a need of a specific stabilization of such carbonyl groups, a stabilization that might have relevance regarding the prolyl oligopeptidase catalysis. As Arg⁶⁴³ interacts specifically with the carbonyl function of the P₂ position it is expected that during the enzyme catalysis Arg⁶⁴³ might fill the electronic sink of that carbonyl function. As already mentioned, the substrates with originally higher turnover rates were more affected than the rest upon the Arg⁶⁴³ variants. That is as well corroborating that the Arg⁶⁴³ influence depend on the nature of the analyzed substrate.

4.4 Recombinant human prolyl oligopeptidase Trp⁵⁹⁵ variants.

In the tables 19, 20 and 21 the kinetic parameters of the different generated variants that are related to the Trp⁵⁹⁵ residue are compiled. This residue has been pointed to carry out such specific interactions with the substrate pyrrolidine side-chain that is able to define alone the entire enzyme specificity [67;157]. In this respect, the W595A variant, in comparison to the wild type parameters, showed K_m values for Z-GlyPro-AMC and GlyProPro-AMC that vary in a lesser extent, one order of magnitude variation as maximum, than the respective constants of the Z-AlaPro-AMC and AlaAlaPro-AMC substrates, which constants drop two orders of magnitude. These differences might reflect a possible distinctive binding mode of those substrates as the main specificity factor, namely Trp⁵⁹⁵, is herein affected. One could conclude that the void of the Trp⁵⁹⁵ entailed a general increase of the characterized K_m . The loss of the Trp⁵⁹⁵ might impulse within the W595A variant a new hydrophobic equilibrium that might result in a distorted S_1 subsite arising with an increase of the measured K_m as a result of a worsened substrate affinity.

The primary specificity of prolyl oligopeptidase is enhanced by the action of the Trp⁵⁹⁵ indole functional group, but the S_1 pocket is, in addition, aligned by the residues Phe⁴⁷⁶, Val⁶⁴⁴, Val⁵⁸⁰ and Tyr⁵⁹⁹ [67]. Thus, it has been suggested that the interplanar geometry between side-chains of protein residues have in the polar interactions an important determinant [178]. Therefore, the conformation of the tryptophan side-chain could be expected to be strongly influenced by the interactions of its imino moiety. The available crystal structures of the enzyme have shown how the proline pyrrolidine and the tryptophan indole groups are in a parallel stacking fashion while the indole's imino moiety is coordinated by the main chain carbonyl group of the substrate P₃ position. Hence the substrate attackable conformation might be also conditioned by these polar interactions of the side chain indole imino moiety. Actually, a restrictive interpretation of the hydrophobic character of the S_1 pocket [67] might have overwhelmed the possible influence of polar interactions within the bosom of the S_1 pocket. The relevance of polar forces on the configuration of the S_1 was investigated with different variants. The substitution of the Trp⁵⁹⁵ for phenylalanine, table 20, represented an inherent increase of hydrophobicity in the S_1 subsite. The Kyte-Doolittle hydrophobicity scale categorizes phenylalanine as the strongest non-polar residue with a constant of 2.8, whereas tryptophane with -0.9 and tyrosine with -1.3 have clearly a hydrophilic character [179]. The substitution for phenylalanine had a positive influence as the different substrates either maintained, such as with Z-GlyPro-AMC and GlyProPro-AMC, or as in most of the cases, recovered their K_m constants in relation to the W595A variant. This indicates how the aromatic ring might have efficiently reorganized the S_1 pocket architecture in

order to accommodate the different characterized substrates. Nevertheless, it has to be outlined that these K_m values still hardly approach to the wild type values. The last is supporting the idea that the polar interactions of the Trp⁵⁹⁵ side-chain are still necessary but, somewhat, dispensable. The exchange of Trp⁵⁹⁵ for tyrosine, table 21, aimed to balance the hydrophilic aspect of the original indole moiety. This means, that although tyrosine will probably not adopt the exact proper conformation, the anchor of the hydroxyl moiety is expected to enhance a more stable conformation and maybe it could provide a fruitful polar interaction with the substrate. Actually, with the W595Y variant, in comparison to the W595F and W595A variants, a relatively large recovery of the determined K_m constants were obtained. Indeed, attraction patterns of proline were found to be higher with tryptophan, histidine and tyrosine [179]. Already here one can conclude that indeed the contributions of Trp⁵⁹⁵ to prolyl oligopeptidase catalysis play a main role on the definition of the proper and catalytically functional accommodation of the substrates.

The determined turnover constants of the three Trp⁵⁹⁵ related variants showed how important is the planar interaction, known as π - π interaction [180], held between the pyrrolidine substrate side-chain and the tryptophan indole side-chain to achieve an efficient catalysis. The loss of such interaction in the W595A variant entailed an impairment worth in two orders of magnitude for the hydrolysis of the substrates Z-GlyPro-AMC and GlyProPro-AMC, see table 19. Nevertheless, although there is as well a detriment, it is much less severe for Z-AlaPro-AMC and AlaAlaPro-AMC. The replacement of the indole ring for the aromatic phenyl ring in the W595F variant showed an overall improvement of the measured turnover constants, table 20. Hence, prolyl oligopeptidase catalysis depends to a large extent on the planarity of the Trp⁵⁹⁵ which might allow achieving a proper conformation that makes feasible the nucleophilic attack. There are three proposed π - π interaction conformations possible: face to face, edge-to-face and offset stacket [180]. The first is unfavourable, it is actually not observed, the second and third are permitted and favourable [180]. In our case the second orientation, edge-to-face, something like a "T-orientation", seems unlikely, because it would change the handiness of the hydrolyzable peptide bond. The last orientation, offset stacked, seems to be the most reasonable, so far it is the one found in the crystal structures of the enzyme. This interaction would place the imino group of the pyrrolidine side-chain centered on the slightly polarized phenyl moiety [178].

The exchange of the Trp⁵⁹⁵ for tyrosine, table 21, affected very interestingly the measured turnovers. With this variant Z-AlaPro-AMC and AlaAlaPro-AMC were shown to have turnovers comparable to the wild type original levels. Otherwise, although Z-GlyPro-AMC and GlyProPro-AMC improved notably one order of magnitude their

turnovers, in comparison to the W595A variant values, they did not reach the wild type turnover rate levels. These data are confirming in our opinion the above suggested differential hydrolytic pattern of both set of substrates. To our understanding, the data all together support the relevance of the polar interactions within the bottom of the S₁ pocket. First, just hydrophobic interactions between the proline side-chain and the S₁ site would entail large attractive van der Waals' energies [180] whose disruption would be energetically too expensive for an efficient catalysis, and second, imposed polar interactions between the proline side-chain and the S₁ site should be, comparatively to the hydrophobic ones weaker and moreover, strongly orientation dependent [180]. Therefore we can conclude that possibly Trp⁵⁹⁵ does not just stacks the pyrrolidine proline moiety, but also enables a feasible nucleophilic attack to occur by using polar contacts to bring the substrates into the proper conformation.

4.5 Recombinant human prolyl oligopeptidase Phe¹⁷³ variant.

The table 22 compiles the kinetic parameters of the F173A variant. The Phe¹⁷³ in the wild type enzyme is suggested to be aligned in a non-polar environment of the active site which would account as the S₃ pocket [67]. The different determined K_m constants for the F173A are, in comparison to the wild type values, one to two orders of magnitude larger. Only AlaAlaAla-AMC escapes to this tendency, maybe because its original K_m was already in the millimolar range. The neutral dipeptide derivatives are expected to maintain π - π interactions [180] between their benzyloxycarbonyl moiety and the Phe¹⁷³ aromatic side-chain. As a result of the lowered S₃ pocket hydrophobic environment achieved with the F173A variant, the π - π stabilizing interactions lose importance and therefore the binding of these substrates might weaken, thereby increasing their K_m constants. In contrast, it would be expected with this variant that the exchange of phenylalanine for alanine to be followed by an improvement of the conditions for the settlement of the amino terminal charge of the tripeptide derivatives, but actually it was not thus. It is extreme the case of the AlaAlaPro-AMC substrate, which measured K_m dropped two orders of magnitude in comparison to the wild type. Regarding their K_m constants, even the rest of tripeptides were, likewise, very negatively influenced indicating this that the S₃ subsite is attaining its apolarity not only with Phe¹⁷³ contributions. Actually, the interaction between a phenyl ring and a positive charge of a free amino terminus might not be necessarily unstable. It is known as a cation-aromatic effect the favourable interaction between a positive charge and a phenyl ring [179]. In the cation-aromatic effect there is a slight polarization of the electron density of the aromatic ring where the negative clouds are slightly concentrated on the center of the ring favouring the interaction with cationic charges

[178]. This phenomenon, cation-aromatic interaction, is not singular so far it has been extensively described in different proteins [178]. The cation-aromatic effect might be seen as a plausible explanation for a relative favourable accommodation of a charged amino terminal moiety in such a non-polar S_3 subsite. Therefore, the loss of the phenylalanine side-chain might account, as we could see with our kinetic parameters, for an increment of the K_m constant as a result of an impaired substrate binding of the tripeptide derivatives.

The examination of the turnover constants of the F173A variant reveals that for most of the characterized substrates, in comparison to wild type values, no significant variation were characterized. Only the turnover of the AlaAlaAla-AMC decreases by one order of magnitude. The only lowered hydrolysis rates of the alanine derivative might disclose how the amino terminal stabilizing interactions have a determinant compensatory and promoting effect on the hydrolysis on this substrate, as the first specificity, alanine at P_1 , does not fulfill by itself all requirements for an appropriate hydrolysis. One can conclude that although more active site residues might be implicated Phe¹⁷³ indeed plays a clear predominant role restricted to form the non-polar environment of the S_3 pocket, which is mainly defining the enzyme endopeptidase specificity.

4.6 Recombinant human prolyl oligopeptidase Met²³⁵ variants.

In the tables 23 and 24 are gathered the kinetic data measured with the Met²³⁵ related variants. This methionine has been postulated to simply contribute, like Phe¹⁷³, to the formation of the non-polar S_3 prolyl oligopeptidase pocket [67]. The presence of this residue in the mammalian enzyme active sites is covered with a rather low sequence homology, just a 30% identity was described [29]. The loss of the slightly polar sulfur containing side-chain in the M235A variant entailed, compared to wild type enzyme, no virtual change on the determined K_m constants. Only the K_m of GlyProPro-AMC dropped by one order of magnitude in comparison to the K_m of the wild type enzyme. Otherwise, it was very interesting to observe the effect of this variant on the characterized turnover rate constants. All values of the measured turnover constants dropped homogeneously by one order of magnitude in comparison to the k_{cat} s determined with the wild type enzyme. These results entail two important consequences, first, unlike we demonstrated above for Phe¹⁷³, unexpectedly Met²³⁵ does not appear to play the same role in the architecture of the S_3 pocket to form a non-polar subsite which would define the endopeptidase specificity and second, Met²³⁵ very interestingly gives evidence to have rather a strong relevance upon substrate catalysis. Then the question arises of how can this residue, remotely located from the catalytic triad, influences so drastically the enzyme turnover? One possible answer is

that while Met²³⁵ has little implication in the initial accommodation of the substrate it could be otherwise involved in posterior events occurred during the catalysis, like for instance as a result of substrate conformational changes during the formation of the tetrahedral intermediate. To our understanding, this explanation is additionally supported by the data obtained with the M235I variant, table 24. The K_m constants of the M235I variant remained, as well, not disturbed but its turnover constants, in comparison to the M235A variant, were again restituted, approaching the threshold shown by the constants measured with the wild type enzyme. Isoleucine and methionine are indeed close isosters, their side-chains are expected to protrude similarly into the active site, thus indicating that the involved interactions have a pure sterical nature. Actually, catalytic helping motions have been already suggested to explain the catalytic influence of active site distal residues [181-184]. For example, a molecular dynamic approach has been successfully applied to explain how in horse liver alcohol dehydrogenase (EC 1.1.1.1), HLADH, non-catalytic residues use pushing motions in order to colocalize in the active site the alcohol substrate and the oxydized nicotinamide adenine dinucleotide cofactor, NAD⁺, in an reactive ground state conformation [185]. In the case of Met²³⁵ it is sterically related to the non-ordered loop involving the residues 192-205, 3.98Å distance between Met²³⁵ and Gln²⁰⁸ in the structure with PDB id 1QFS. Molecular Dynamics simulations have interestingly indicated that possibly the flexibility of this loop could contribute to the mechanism of substrate selectivity [186] and therefore one could speculate that Met²³⁵ also might be affected by the motions accompanying to the loop 192-205 flexibility. One could conclude that very interestingly Met²³⁵ would rather play a main role upon substrate catalysis instead of simply participating in the definition of the enzyme's substrate affinity.

4.7 Recombinant human prolyl oligopeptidase Cys²⁵⁵ variant.

Analysing the data obtained with the C255A variant, table 25, one can recognize how, in contrast to the values of the wild type enzyme, the different measured K_m did not vary extremely. Only the AlaAlaAla-AMC substrate shows a relevant decrease in the measured K_m constant. On the other hand, the exchange of Cys²⁵⁵ for alanine did not influence the turnover of Z-GlyPro-AMC, but unexpectedly it did change the k_{cat} constant of Z-AlaPro-AMC. A five-fold increased turnover, in comparison to the wild type values, was measured when the Z-AlaPro-AMC was hydrolyzed with the C255A variant. That is not an unusual result, as well a related variant of the same prolyl oligopeptidase, the C255T, was found to improve the turnover of an internally quenched peptide substrate in almost one-fold [104] or for example a nicked variant of prolyl oligopeptidase was shown to improve its specificity nearly six fold in comparison

to the wild type enzyme [186]. In addition, in the literature they were shown cases of enzyme improved catalysis as a result of engineered protein [187] and are as well common techniques, such as the DNA shuffling, which allow the *in vitro* improvement of enzyme turnovers [188]. Compared to the wild type enzyme, the tripeptide derivatives AlaAlaPro-AMC and AlaAlaCys-AMC showed with the C255A variant that the k_{cat} constants were slightly affected, while AlaAlaAla-AMC and GlyProPro-AMC turnovers dropped two and one order of magnitude respectively. The localization of Cys²⁵⁵ in the crystal structure of porcine prolyl oligopeptidase is indeed curious. Although the Cys²⁵⁵ has been only ascribed to the S₃ pocket [67], it is also true that it extends its potential contacts from the S₁ pocket to the P₂-P₃ substrate peptide bond. Cys²⁵⁵ sulfur atom in the PDB1H2Y crystal structure is actually relatively equidistant to the side-chains of Trp⁵⁹⁵, 3.83Å to the carbon δ 1, of Phe⁴⁷⁶, 4.22Å to the carbon ϵ 1, of the carbonyl moiety of the P₂-P₃ substrate peptide bond, 4.47Å to the carbon of the P₃ carbonyl function and 4.14 Å to the benzyloxycarbonyl moiety of the substrate. A study of the interaction partners of sulphhydryl groups in proteins found that 70% of cases the free cysteine residues contacted with carbonyl groups [189], like it does Cys²⁵⁵ with the substrate P₃ carbonyl. On the other hand, the pK_a of the Cys²⁵⁵ has been titrated to a value of 9.77 [104], that would mean that a thiolate anionic form of the Cys²⁵⁵ would not be achieved in the measured conditions. In opposition, it has been also suggested that the delocalization of the negative charge of the sulfur atom to a carbonyl group, by meaning of a S \cdots C=O interaction, might propitiate a decrease of the pK_a of a cysteine [189]. The polarization of the Cys²⁵⁵ sulphhydryl, because of an interaction with the carbonyl carbon of the substrate P₃, seems unlikely as the distance between both atoms is 4.47Å. A much larger distance than the maximal 3.5Å usually used to consider seriously a possible hydrogen bonding. Therefore, an acute reduction of the Cys²⁵⁵ pK_a, that could lead to the formation of the thiolate anion, is not expected under our measurement conditions. Therefore, the privileged position of the Cys²⁵⁵ in the prolyl oligopeptidase active site might make it sensitive to the bulkiness of the substrate and consequently, it might be possible that the Cys²⁵⁵ residue could have a similar role like the one suggested above for Met²³⁵ although in this case showing a specific nature for each of the different substrates [181]. Thus, Cys²⁵⁵ could as well participate in enzyme motions that are, in this case, enhancing the catalysis of Z-AlaPro-AMC, while they hinder the catalysis of AlaAlaAla-AMC and GlyProPro-AMC. One can conclude that as already suggested for Met²³⁵, Cys²⁵⁵ could as well have a more defined participation in posterior steps of the catalysis but in this case modelling differently the hydrolysis due to different protein-substrate contacts. Finally, the C255A variant allowed us to still measure hydrolysis of the AlaAlaCys-AMC substrate. The parameters are comparable

to the ones obtained with the wild type enzyme. This actually ruled out any direct implication of the Cys²⁵⁵ on the catalytic mechanism of the cysteine containing substrates, discarding the possibility of two enzymatic activities in one active site.

4.7 Inhibitors binding pattern.

Regarding the mechanism described in scheme 2, the K_i constant characterizes the binding of a competitive inhibitor. The data collected in tables 26, 27 and 28 show the affinity constants, K_i , for three different sort of inhibitors. In table 26 were collected the determined inhibitory constants of the ammonium methyl ketone molecule, AMK, in table 27 the inhibitory constants of the heteroarylketone compound, HAK, and in table 28 were compiled the inhibitory constants of the diketone molecule, DK. The hydrolysis of the substrate GlyProPro-AMC, which showed a high turnover, see table 12, and in addition has no solubility problems, was inhibited using the different prolyl oligopeptidase active site variants. The variation of the K_i constant in function of the variants allowed us to unveil the interactions that are ruling the binding of these inhibitors to the enzyme and their relative relevance. One can conclude that the three different characterized molecules showed a very similar binding pattern. This can be summarized as, first, all three compounds were characterized with the major affinity impairments when they were measured with the variants R643A and W595A, second, in all cases the K_i constants recovered extensively their wild type levels when they were characterized with the variants R643K, W595F and W595Y, and third, a relatively insignificant variation of the determined K_i constants were observed with the variants F173A and M235A.

The three inhibitors presented above showed that the strength of their affinities lies on the interactions they establish with the residues Arg⁶⁴³ and the Trp⁵⁹⁵. The co-crystallization of prolyl oligopeptidase with Z-prolyl-prolinal [67] showed how this molecule is establishing two polar interactions with the enzyme, one with the guanidinium group of the Arg⁶⁴³ and the other with the imino moiety of the indole Trp⁵⁹⁵ side-chain. These interactions are established through a diketone construct, two carbonyl moieties separated by four carbon atoms, that is actually also present in the structure of the herein studied inhibitors. In addition to the confirmed role of the polar interactions, the most interesting effect is that the drop of the K_i constants was comparable for both R643A and W595A variants. This is strongly suggesting that the action of the diketone function might work in a concerted manner with the pyrrolidine/indole stacking interaction in the S₁ pocket. Nevertheless, the increase of K_i was with the AMK and the HAK inhibitors three-fold higher for the W595A than for the R643A variant. This is indicating that the tryptophan indole side-chain planarity is

making more relevant contributions than the single polar interaction of the Arg⁶⁴³ is doing. The DK inhibitor, otherwise, showed an opposite balance. The polar interaction with the Arg⁶⁴³ is more relevant than the planar-polar contributions of the Trp⁵⁹⁵, as it is indicated by the one-fold lower measured K_i constant of the W595A variant, see table 28. The variants R643K, W595F and W595Y showed, in comparison to their counterpart variants R643A and W595A, good correlations with the recovery of the inhibitors affinity. These variants confirmed the relevance of the polar interaction between the carbonyl function and the Arg⁶⁴³ side-chain. The interaction between the Trp⁵⁹⁵ side-chain and the pyrrolidine moiety, for the AMK and HAK molecules, or the thiophene moiety, for the DK molecule, is expected to be a dominantly planar π - π interaction [180]. The W595F and W595Y variants confirmed the relevance of this π - π interaction. The lack of a proper polar interaction between the indole imino group and the diketone moiety revealed herein as well its importance. Still one order of magnitude difference between the K_i constants of the W595F or W595Y variants and the ones of the wild type enzyme were characterized. More marked differences between these three inhibitors appeared on the interaction of their benzyloxycarbonyl moiety in the AMK and HAK molecules, and the phenyl ring in the DK inhibitor with the S_3 subsite. The binding of the DK inhibitor is comparatively the one more affected by the loss of the Phe¹⁷³ residue, two orders of magnitude increase of the K_i , whereas the remaining inhibitors showed only one order of magnitude difference. This emphasizes the difference between a simple competitive inhibitor, which aim is only to bind to the enzyme active site, therefore all contributions favoring the binding are relevant, and a slow-tight binding or irreversible inhibitors, whose binding might undertake an ulterior process to closer interact with the enzyme. This close interaction is promoted in the AMK and HAK molecules with a carbonyl function which is susceptible to be attacked by the nucleophile Ser⁵⁵⁴. This carbonyl function lacks on the thiophene group of the DK molecule. In the AMK and HAK molecules, the reactive carbonyl carbon is achieved with adjacent electronegative atoms that subtract electron density from this reactive atom. This groups are the ammonium methyl for the AMK molecule, and benzothiazole for HAK molecule, respectively. The benzothiazole is expected to act like a good leaving group, after putative acylation occurs, whereas the ammonium methyl group is expected to attract the nucleophilicity of the active Ser⁵⁵⁴, but not enhancing an acylation. The characterization of benzoxazole ketone derivatives for the human neutrophil elastase supported the idea that the amine moiety of its heterocycle might act as a proton acceptor, stabilizing the imidazolium group in the tetrahedral intermediate [190], a scenario that could be easily reproduced as well with the HAK inhibitor in the prolyl oligopeptidase active site. Finally, to notice the innocuous effect of

the M235A variant over the binding properties of the DK and AMK inhibitors as the measured K_i constants for these molecules did not vary compared to the K_i values of the wild type enzyme. This still supports the catalytic role of the Met²³⁵ suggested above. In contrast, it outstands the interesting binding enhancement found with the same variant when the HAK inhibitor was characterized. One order of magnitude decreased K_i that revealed a better accommodation of its benzyloxycarbonyl moiety. The reason why this improvement is detected with the HAK molecule, and not with the AMK surrogate, might be found in their different bulkiness. The HAK is a rather larger than the AMK molecule and the loss of the Met²³⁵ might contribute to better accommodate to the whole molecule in the active site like it was previously shown in the characterization of *N*-Acyl-pro-pyrrolidine derivatives [191]. One could conclude that the major determinants differentiating the binding of small molecules are related rather to the S_3 subsite than to the S_1 - S_2 subsites which are configuring otherwise a canonical binding pattern that all binding molecules need to fulfill [191].

4.8 Inhibitors derivatization.

AMK scaffold. Once the precise binding pattern of the inhibitor molecules was computed a more detailed characterization of their binding features was pursued following a derivatization strategy. With the derivatization of the AMK scaffold, table 29 and appendix table 42, the role of the ammonium methyl moiety was investigated. This group is expected to withdraw electron density from its neighbor atoms intending to generate a reactive carbonyl function. Such carbonyl function is becoming a potential candidate to interact with the nucleophile Ser⁵⁵⁴. The exchange of the ammonium methyl moiety for a morpholine, AH686, or a pyridine, AH688, rings did not influence the measured K_i , in contrast its substitution for a piperidine ring, AH687, or a pyrrolidine ring, AH684, entailed respectively an increase of one and two orders of magnitude of the characterized K_i constants. It was before determined the electron withdrawing capacity, σ_I value, of a serie of heterocycles [192], but actually the correlation with the molecules K_i affinity constants did not fully succeed [190]. Hereafter, it seems reasonable to think that the inhibitor strength might be rather better related to steric and electrostatic effects, more than to any other parameter. When the original charged methyl ammonium moiety was replaced with a dimethyl amine group, AH685, no variation of the affinity constant was characterized indicating that no electrostatic but rather a polar interaction is taking place. Furthermore, the accomodation of the ammonium methyl group within the S_1' pocket was better reproduced with the morpholino, AH686, and pyridinium, AH688, rings than with the pyrrolidine, AH684, or piperidine, AH687, rings. This is indicating that steric interactions enabling the

enhancement of the inhibitors affinities are on the enzyme S' subsites still possible. Nevertheless, the relevance of such S' interactions are contradicted when the exchange of the amine moiety for a hydroxy moiety, AH673, improved the measured K_i by one order of magnitude, probably as a result of an increased induction effect of the hydroxy group in front of the original amine. The molecules AH690-4 and AH691 are symmetrically built around the heterocycle, imidazolium, in the AH690-4 analogue, and piperazine, in the AH691 surrogate, offering therefore two reactive carbonyl moieties per molecule which might increase the affinity by improving probabilities of interaction with the active Ser⁵⁵⁴.

HAK scaffold. The derivatization of the HAK compound, table 30 and appendix table 43, showed that the loss of the pyrrolidine ring in the AH807 analogue, alanine replacing proline, and the AH810 analogue, proline exchanged by glycine, was characterized with IC_{50} values that dropped respectively by four and six orders of magnitude in comparison to the IC_{50} constant of the original molecule. This gives evidence that the enzyme pyrrolidine specificity rules the binding features of this family of molecules over any other circumstance. Very interesting were the results obtained with the exchanges on the P₂ inhibitor positions. Thus exchange of the alanine in AJN118 for a bulky phenylalanine, ZW215 molecule, improved the measured K_i constant one order of magnitude while the replacement for proline, AH817, arginine, AH829, or aspartate, AH831, was followed by one and two orders of magnitude increased K_i constants. One can conclude that in contrast to what the crystallographic data [157] are indicating, no main interactions of the enzyme with substrates and inhibitors in P₂ position, the inhibitors affinity characterization strongly suggested the relevance of this position. Given the evident lack of substrate side-chain-protein interaction it might be speculated that solvation at the P₂ position could as well play an important role [193;194]. Moreover, the length of the HAK molecule was characterized with the analogue AH839, which holds an additional glycine, and with the AH851 analogue, which is lacking the original alanine residue, in both cases leading to an increase of the characterized K_i by two orders of magnitude. This clearly indicates that the inhibitor benzyloxycarbonyl moiety has a rather narrow area of interaction within the active center of prolyl oligopeptidase. The benzyloxycarbonyl moiety of the AH839 analogue could interfere with the arginines Arg²⁵² and Arg¹²⁸, builders of a putative S₄ pocket [157], while the shorter form of the inhibitor, the AH851 analogue, the benzyloxycarbonyl moiety might interfere with Arg⁶⁴³.

Finally, the substitution of the benzothiazole moiety, AJN118, for a smaller thiazole, in the AH815 analogue, did not affect the molecule affinity as the measured K_i only varied very slightly. This is in accordance with the similar electron density withdrawing

capacities of both molecules, 0.37 σ_1 for benzothiazole and 0.34 σ_1 for thiazole [190]. However, the comparison of the AH815 analogue with the ZW215 molecule reveals one order of magnitude difference on K_i constant, indicating again the probable presence of steric interactions on the S' subsites of the enzyme that regarding the crystal structure 1e8n are implicating the involvement of the residues Tyr⁴⁷³, Phe⁴⁷⁶ and Ile⁴⁷⁸. Nevertheless it could be as well speculated that the inhibition is enhanced by stabilization of the imidazolium group in the tetrahedral intermediate by the inhibitor heterocyclic amine in β position in relation to the reactive carbonyl [190]. In that sense, it agrees that on the derivatization of peptidyl α keto heterocycles inhibitors of prolyl oligopeptidase correlating properly the position of the amine within the heterocycle and the potency of the different analogues, being necessary a sp^2 nitrogen atom at a β position in relation to the reactive carbonyl [195].

DK scaffold. The characterization of the prolyl oligopeptidase S_3 subsite was also approached with a derivatization of the DK derivatives, table 31 and appendix table 44. The replacement of the amino terminal phenyl ring for either a biphenylcyclopentane, in the AH732 analogue, or for a naphthalene ring, in the AH738 molecule, was translated in comparison to AH769 in a relevant impairment of affinities with three- and six-fold larger K_i . This is indicating that prolyl oligopeptidase S_3 subsite, where these moieties might interact, is indeed defined to confine only certain bulky groups. In that context the exchange of the phenyl ring for a thiophene moiety, in the AH771 analogue, brought along an affinity improvement that could be justified in terms of the easier accommodation of the smaller thiophene ring in the S_3 pocket. On the other hand, the distance separating the diketone group and the phenyl moiety was investigated. The analogue AH741 with a stretched aliphatic chain of six atoms, and the AH708 molecule with a trimmed aliphatic chain of four carbons were characterized with increased K_i and IC_{50} constants, one and three orders of magnitude respectively. This clearly indicates that only a defined distance exists between the S_1 and S_3 subsites allowing the most productive interactions. This contrasts otherwise to the reported behaviour of α -keto heterocycle inhibitors of prolyl oligopeptidase for which longer phenylbutanoyl analogues were more potent than the corresponding benzyloxycarbonyl derivatives [195].

Additionally, the exchange of the ether function, placed between the phenyl ring and the diketone group of original molecule AH769, for an amine, in the AH711 analogue, or a thioether, in the AH754 molecule, entailed a significant drop in the characterized IC_{50} constants by three and four orders of magnitude, respectively. This is a very

interesting finding as the crystallographic information available [67] is not indicating a any clear role of this moiety while the kinetic data are highlighting as very relevant.

The loss in the AH751 analogue of the phenyl ring associated to the diketone function, was characterized with an increased IC_{50} by two orders of magnitude. One can argue that the aliphatic link between both carbonyls are allowing *cis-trans* isomerizations of the diketone moiety that are hindering the necessary formation of the polar contacts with Arg⁶⁴³ and Trp⁵⁹⁵ side-chains.

Finally, the chemical substitution of the thiophene moiety in the original molecule AH769 for a phenyl ring in the AH713 analogue or a thiazole ring in the AH897 molecule, entailed dramatic drops of the characterized IC_{50} constants, while the substitution for a furan group in the AH755 molecule, had comparatively less influence. This is indicating that the S_1 pocket is sterically restricted, accepts better five than six membered rings moieties and needs to fulfill the appropriate polar interactions to accommodate specifically a ligand. Similarly, the substitution of a pyrrolidine for a thiazole ring represented a two orders of magnitude improvement of the affinity of a inhibitor [131]. The thiophene moiety had a lower K_i than the furan derivative, AH755. and surprisingly three orders of magnitude lower than the thiazole derivative, AH897. This suggests the relevance of the polar interactions in the bossom of the S_1 pocket as it demonstrates that the accommodation of the thiazole, in contrast to the thiophene isoster, hinders the binding of its analogue. Thiophene and thiazole are expected to stack against the Trp⁵⁹⁵ side-chain in the S_1 pocket, but the amine moiety of the thiazole might, otherwise, hinder this interaction, as it is shown by its measured K_i constant. One could argue as well that at this position an interaction with the oxyanion builder Tyr⁴⁷³ might play a role.

4.9 Slow-tight binding inhibitors characterization.

The slow-tight binding mechanism exerted by the AMK inhibitor, AH683, and its related derivatives, table 32 and appendix table 42, was characterized. As described above, the interaction between a reactive carbonyl group and the enzyme active Ser⁵⁵⁴ plays a main role in the inhibitory pattern of this family of molecules. Thus, this interaction is expected to be enhanced by the electron withdrawing capacity of the methyl ammonium group on the family of AMK molecules. Table 32 shows a list of molecules that mainly differentiate on the different electron withdrawing moieties with what they have been derivatized [137].

The analysis of the data compiled in the table 32 makes evident that the here characterized constants are comparable to the data elsewhere quoted for other molecules [130;132], and in addition, demonstrates that the inhibitory mechanism

followed by the different molecules are different even though they have in many cases similar affinity constants.

Thus, molecules with very similar K_i constants, AH673 and AH690-4, have comparatively different behaviour as shown by the determined k_{on} and k_{off} constants. AH690-4 is finding a faster access to the active site, one order larger k_{on} , while AH673 is able to establish a longer association with the enzyme, one order of magnitude smaller k_{off} . Their electron withdrawing moieties are radically different, a hydroxy group for AH673 and an imidazolium moiety for AH690-4. Therefore, it seems reasonable to think that given the higher electronegativity of an oxygen atom, it could be expected the hydroxy group more efficiently to polarize the carbonyl function and therefore achieve a tighter interaction with the active serine while the imidazolium derivative could take profit of its symmetry, that is two reactive carbonyl groups per molecule, to increase its probabilities of interactions and thus achieve a more readily binding. Additionally, in this case the marked difference bulkiness of the molecule is indicating that, first, in principle steric hindrance are not jeopardizing the action of the inhibitors, and second, even the interactions with the S' subsites could be in this case meaningful [89].

Furthermore, it is interesting to compare between the molecules AH690-3 and AH690-4, which has a symmetric structure around the imidazolium group whereas the former does not. The K_i of the simple inhibitor, AH690-3, dropped comparatively two orders of magnitude as a result of a drop on K_{on} by two orders of magnitude, indicating that the duplication of reactive carbonyls and as well the possible presence of S' interactions, are indeed favouring the interaction with the active site .

In that sense it is interesting to see how other molecules that showed even lower diffusion k_{on} rate constants are in contrast much better inhibitors, as they have lower K_i constants. The AH689 molecule actually showed a very similar k_{on} constant in comparison to AH690-3, but in contrast it displays an by one order of magnitude lower diffusion k_{off} constant. Structurally, AH689 has as an electron withdrawing moiety a six membered heterocycle ring, a derived morpholine moiety, whereas the AH690-3 has a five membered ring imidazol. Steric interactions on the S' subsites could compensate the mechanism of action of these molecules, but actually given their similar bulkiness rather a differential inductive effect might play here a more relevant role. The molecules AH689 and AH686 have in common most of their molecular structure. In both cases the characterized values of k_{on} and k_{off} were very similar. This is indicating that the presence of the charged moiety, morpholinium in the AH689, is in principle not representing an obvious advantage contributing to further enhance the molecule's affinity. A similar analysis might be applied to the pair of molecules, AH683 and AH681. Both molecules share most of their structural features, AH681 has an ammonium ethyl

moiety instead of the ammonium methyl that the AH683 molecule has. The compared molecules have very similar K_i constants, but in contrast, the k_{on} rate constant is one order of magnitude better for AH681 while its k_{off} constant is one order of magnitude higher than the one of AH683. According to previous results it does not seem likely to find here differential induction effects and maybe the steric interactions on the S' subsite are more likely to define the affinity.

It was surprising to notice how the loss of the cationic charge of the methyl ammonium group, in the AH685, entailed a drop of one order of magnitude on characterized K_i that regarding the diffusion constants might be explained as the result of an impairment of the induction capacity of the involved amine as the k_{on} dropped two-fold in comparison to the molecule AH683. This is indicating that the cationic forms could indeed enhance the inductive phenomenon. Accordingly, a molecule like AH688, with a pyridinium as electron withdrawing moiety, showed a nano molar range K_i constant. Exceptionally is its k_{on} constant, that is the lowest within the compared molecules, although its k_{off} is, in opposition, very low. This is suggesting that the cationic charge, together maybe with extended non-polar interactions, is positively enhancing in this case the reactivity of its neighboring atoms. Interestingly the inductive effect is here opposite as the k_{off} is being more affected. This statement would be further corroborated with the molecule AH687 that with a piperidine moiety, a six membered ring heterocycle like it is in the pyridine, has in spite of a one order of magnitude higher K_i indicating again the relevance of the cationic form of the electron withdrawing moiety. Nevertheless, the structural flexibility of the electron withdrawing moiety might be as well relevant. They seem to be favoured the planar moieties, like the one of the aromatic pyridinium, in front of the more flexible moieties, like the one of piperidine group that could show either a "boat" or a "chair" conformations. The molecule AH691 has a symmetric shape build around a piperazine heterocycle. In contrast to AH690-4, also symmetric, the diffusion k_{off} constant is the dominating factor dragging its K_i to the nano molar range. Identically it might be argued that the multiplicity of reactive carbonyls increased the chances of interaction within this molecule. Finally, one can conclude from the heterogeneous behaviour of the different AMK molecules that a clear structure-activity correlation does not exist, although basically it was confirmed by the relevance of the electron withdrawing capacity of the AMK moieties as the driving force defining the slow-tight binding mechanism of these molecules.

4.10 MALDI-TOF-MS characterization of prolyl oligopeptidase hydrolysis pattern.

The characterization of the hydrolysis of the peptide Neuropeptide Y, table 33, rendered us the possibility to profile two of the main features that distinguishes prolyl

oligopeptidase. The use of shortened variants of the Neuropeptide Y allowed us to confirm the well known oligopeptidase character of the enzyme. The original Neuropeptide Y is a 36 amino acid long peptide, NPY 1-36 in table 33, that is not processed by prolyl oligopeptidase and only when the peptide size was shortened by six residues on its carboxy terminus, NPY 1-30 in table 33, it could be detected its hydrolysis. The same was found using an even shorter version of the Neuropeptide Y, NP Y 1-24 in table 33. This is corroborating the oligopeptidase specificity of the post-proline cleaving enzyme. Otherwise, more relevant to us herein was to realize how behind the selection of substrates there might lay a subtle mechanism. It has been supported that the β -propeller acts as a gating filter for the selection of the substrates [67]. In that sense, first, it could be generated chimeric disulfide bridges on the β -propeller that increased its rigidity and abolished the enzyme catalysis [75] and second, it could be achieved the heterologous expression of the β -propeller, independently of the α/β -hydrolase domain, as a folded and stable single domain [70]. All that together suggested that in the substrate selection mechanism the β -propeller oscillates between two conformations, open/inactive and close/active. The close conformation might entail the closure of the whole peptide substrate in the inner cavity of the β -propeller. On the other hand, it is interesting to notice a particularity that have not been underlined before for prolyl oligopeptidase. Analysing the data collected in table 33 one can glimpse how the hydrolysis of the NPY 1-30 or NPY 1-24, see figure 15, seems to follow a sequence of priorities. It was qualitatively noticeable how the peptides are processed by cleaving first the Pro₅ and afterwards the Pro₁₃. That seems to indicate a sequential process of recognition of the possible proline cleavage sites. In principle, it might be expected that prolyl oligopeptidase, as oligopeptidase, is not discriminating among the different possible cleavage sites on the basis of their localization within the peptide. The measurement of the hydrolysis of the peptides NPY1-30 and NPY 1-24 with MALDI-TOF actually suggested the opposite. It seems that the enzyme is able to hierarchize among the different proline cleavage sites of these peptides on the basis of their relative localization to the amino terminal end. The first peak always corresponds to the cleavage of the Pro₅, then sequentially it follows the peak corresponding to the cleavage of Pro₁₃ and after appears the peak corresponding to the hydrolysis of the Ala₂₃, figure 15. The same is evident for the other members of the S9 family that display an aminopeptidase activity. This would suggest the existence of secondary binding sites that might lead to this subtle control of substrate hydrolysis. Dipeptidyl peptidase 4, DP4, is as well a post-proline cleaving enzyme, although with aminopeptidase activity.

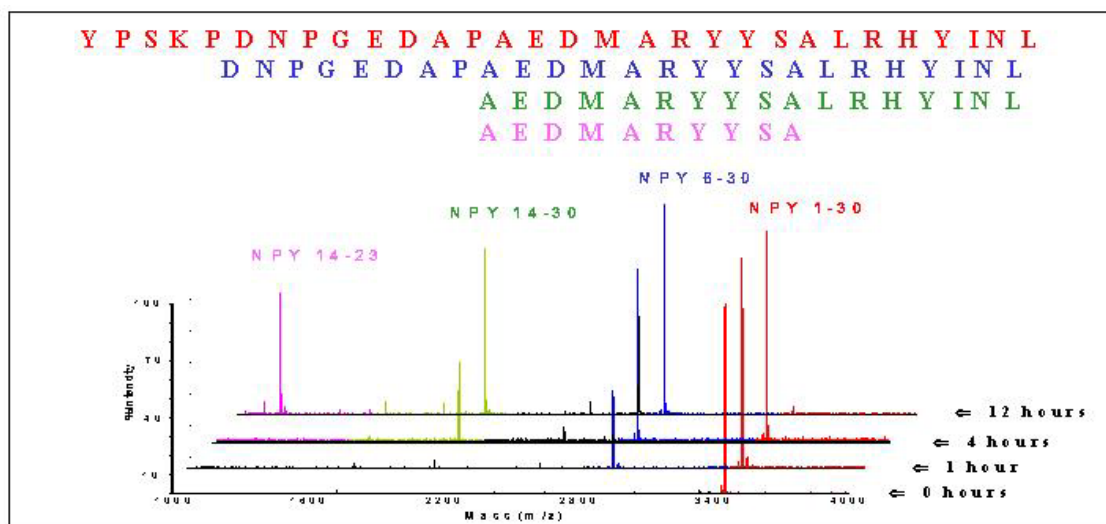


Figure 15 Representative MALDI-TOF-MS spectra of the hydrolysis of the Neuropeptide Y variant 1-30 NPY (see table 33). In green highlighted the full length original peptide peptide, residues 1-30, in yellow the first hydrolysis product, peptide residues 6-30, in red the second appearing hydrolysis product, peptide residues 14-30 and in blue the last appearing hydrolysis product 14-23.

It was demonstrated the existence of such secondary binding sites in DP4 when with the use of the hexapeptide TFTSDY it could be competitively inhibited the hydrolysis of large peptides, like glucagon, but not of the small molecular weight substrates [196]. Therefore, it should not be surprising if a similar binding pattern would be present in prolyl oligopeptidase.

Humanin is a 24 residue long peptide and like Neuropeptide Y, Humanin has multiple potential cleavage sites. Supporting the idea of the secondary binding sites in prolyl oligopeptidase, Humanin was also characterized being processed always hydrolyzing in a first term the proline closest to the amino terminal, table 34. However, the relevance of a peptide like Humanin lay rather on the unique post-cysteine cleavage site that it displays. The post-cysteine specificity of prolyl oligopeptidase was first demonstrated with this peptide [165]. In addition, Humanin offered room to characterize the reasons why its second proline cleavage site was actually not processed. In that sense, in our first approach we examined the S_3 pocket of the active site in order to find an explanation for both, the post-cysteine cleavage and the non-cleaved Pro_{19} , table 34. Previously, it was shown how the simple exchange on a lead peptide of a phenylalanine in P_3 position for a glutamate entailed a decrease by one order of magnitude on the measured specificity constant of a proline cleavage site [157]. In Humanin a phenylalanine is the P_3 residue in relation to the cysteine cleavage site while an aspartate is the P_3 residue in relation to the non-cleaved Pro_{19} . In both cases it was expected that either the post-cysteine cleavage or the proline non-cleavage to be, possibly, determined with an overwhelmed interaction of the peptides with their relative

S₃ pockets. In that sense, different Humanin variants were tested. Table 34 shows how the post-cysteine cleavage was not affected within the two Humanin variants F6A-HN and F6D-HN. The same approach was assayed for the non-cleaved Pro₁₉. The Humanin variants D17A-HN and D17F-HN were tested exchanging the Asp₁₇ for alanine and phenylalanine. Actually, neither of those Humanin variants could trigger the cleavage of the Pro₁₉.

The post-cysteine cleavage was itself such a relevant phenomenon that it was necessary to investigate further. As hallmark, the quantification of the post-cysteine hydrolysis was here achieved using short surrogates, as already outlined, but it could be still argued whether this cleavage is nothing else than a rare peculiarity. Therefore, it was required to find additional examples displaying the same post-cysteine cleavage. At first, we produced a chimeric variant of the peptide Substance P where the original Pro₄ cleavage site was exchanged for cysteine, P4C-SP, table 35. The incubation of the peptide P4C-SP with prolyl oligopeptidase was not able to reproduce the post-cysteine specificity, table 35. Interestingly, the incubation with the same peptide P4C-SP revealed, otherwise, an unexpected post-glycine specificity. Nevertheless, we persisted on our aim to identify new potential post-cysteine substrates. We found a candidate in a study of potential prolyl oligopeptidase substrates [105] isolated from pig brains. Concretely, the candidate found was VTTACHEF, a peptide derived from the precursor protein S100 calcium binding protein. As it can be appreciated in the figure 9 with this peptide we succeeded in characterizing the post-cysteine cleavage in a different peptide than Humanin. Interestingly, the primary sequence of this peptide hold two potential cleavage sites, an alanine and a cysteine. The MALDI-TOF spectra from the figure 9 shows how prolyl oligopeptidase has, even, some preference for a primary hydrolysis of the cysteine residue in front of the alanine. This correlates with the turnover rates found with the AMC derivatives, table 12, that also showed comparable hydrolytic rates for alanine and cysteine containing substrates.

As pointed above, in addition to the post-cysteine cleavage, another relevant feature of the Humanin peptide was the unique resistance towards the hydrolysis of one of its putative proline cleavage sites. We initially investigated whether the hydrolysis of the Pro₁₉ would be hindered as result of putative negative interactions of the substrate Asp₁₇ with the S₃ pocket. Actually, with the experiments noted in table 34 we could discard this possibility. The next step brought us to think whether the origin for the absence of cleavage at the Pro₁₉ site could be in the primary sequence of the amino terminal fragment of the peptide. Therefore, we shortened the original Humanin peptide from the amino terminal side, building three different length versions, see table 36. As it

is described in table 36 any of the tested substrates could be characterized with the cleavage of the proline site.

This was a surprising finding because the previous kinetic characterization of prolyl oligopeptidase did not pay much attention to the possible influence of the P_n' substrate residues over the catalysis of the enzyme. At this point it appeared to be clear that, at least in the studied case the residues on P_n' position, in relation to the proline cleavage site, were exerting an obvious inhibitory effect. In addition using the octapeptide DLPVKRRA we could measure an IC₅₀ of 34±9.9 μM that at least confirmed the binding of the resistant peptide to the active site. Then, we decided to generate different variants of the non-hydrolyzable peptide 17-24HN. The exchange of the original P₂'-P₄' residues for histidine allowed us to generate four different substrate variants, see figure 10. In this case, an alanine replacement was not used to avoid any possible misinterpretation as a result of the presence of additional cleavage sites. The MALDI-TOF spectra shown in figure 10 demonstrated how finally this last approach succeeded in clarifying the reason for the inhibition of the hydrolysis of the Pro₁₉ site. Mainly two of the P_n' positions of this model peptide were found to be responsible for the abolished hydrolysis. First, the exchange of the lysine in P₂' position for histidine rendered for the first time the detection of the proline cleavage on this peptide, figure 10A. Second, the exchange of the arginine in P₄' position for histidine rendered as well the detection of the proline cleavage, figure 10C. In that sense, a simultaneous double exchange of the arginine residues on the P₃'-P₄' positions rendered the measurement of the post-proline hydrolysis, even though not as strongly as the one found with the former, figure 10D. Finally, the single exchange of the arginine in P₃' for histidine did not ameliorate the rates of hydrolysis of the proline residue, figure 10B, compared at least to other related substrate variants. There is not available abundant data about the S_n' subsites of prolyl oligopeptidase. As pointed above, the crystal structures of prolyl oligopeptidase showed no major interactions further away from the S₃-S₂' pockets [67]. Even more, the interactions on the S₁'-S₂' subsites were found not to be determinant, as the co-crystallization of peptides with S554A variants of the enzyme did not reveal any relevant interaction. The MALDI-TOF spectra shown in figure 10 demonstrated that the hydrolysis of the studied model peptide is strongly influenced by the interaction with the residues on P₂', lysine, and P₄', arginine, positions. This is suggesting that, at least, the subsites S₂' and S₄' are not accepting basic residues on the primary sequence of the hydrolyzed substrates. In this sense, supporting this idea, it was found that in a subset of fifteen different peptides cleaved by prolyl oligopeptidase any of them were holding an arginine or lysine in P₂' position [105]. It might not be totally necessary that the existence of substrate P₂' and P₄' specificities imply a direct interaction with their

putative S₂' and S₄' pockets. For example, the co-crystallization of the octapeptide GFGPFG with prolyl oligopeptidase showed how the alpha carbon of the P₂' glycine stays close to the catalytic pair Ser⁵⁵⁴/His⁶⁸⁰. It might be argued that the lysine in P₂', as much as arginine in P₄', on the studied peptide 17-24HN, DLPVKRRA, hinder the catalysis by interfering with the construction of the tetrahedral intermediate, either by distorting the imidazolium moiety or by displacing the oxyanion conformation from a proper interaction with its partner Tyr⁴⁷³. In this sense, it has been shown in the crystal structures of dipeptidyl peptidase 4, a prolyl oligopeptidase structurally related enzyme, the conformational sensitivity of its oxyanion builder [197]. In addition, it was tested whether the "KXR" motif could exert its inhibitory role in a different peptide than Humanin. For that we chose Angiotensin, which is a well known *in vitro* prolyl oligopeptidase substrate. Angiotensin was modified by adding the studied motif "KXR", and its related variants, table 37, at the carboxy side of the proline cleavage site, placing in P₂' position the first lysine residue. The incubation of prolyl oligopeptidase with the different Angiotensin variants showed, in contrast to the peptide 17-24HN, that the modified peptides were still enzymatically processed substrates. Nevertheless, it was obvious to see how the different tested Angiotensin variants showed remarkable delays on their rates of hydrolysis in comparison to the positive control, that means Angiotensin without any of the "KXR" motifs, table 37. Examining the data shown in table 37 it is worth to notice how, in this case, the influence of the lysine at P₂' appears to be much more relevant than the one of the arginine at P₄'.

Finally, the peptide Angiotensin was used again in order to investigate the unique interactions between the substrates and the active site. In this case we investigated the coordination of the carbonyl function of the substrates P₂ residue with the side-chain of the Arg⁶⁴³. As pointed above, it has been speculated whether Arg⁶⁴³ might play a role in the catalytic mechanism of prolyl oligopeptidase, acting as enhancer of the hydrolysis. It has been suggested, but little evidence was given, that Arg⁶⁴³ might mediate in a substrate assisted catalysis mechanism. We think we could throw some light on the question with the measurement of short derivatives using the Arg⁶⁴³ variants, see tables 17 and 18. Additionally, we used here specially modified Angiotensin peptides in order to unveil the relevance of such interaction when the lack of the coordination was found in the substrate and not in the enzyme. Thus, the so-called reduced Angiotensin was a peptide lacking the carbonyl function of the peptide bond that precedes the one of the cleavable proline. On its position a reduced carbon was placed, figure 11. On the other hand, the methylated Angiotensin was a peptide that held the amine of the cleavable peptide bond methylated, figure 11. The incubation of these peptides with prolyl oligopeptidase showed how neither the reduced Angiotensin nor the methylated

Angiotensin were proteolytically processed, figure 11. The peptides remained resistant to hydrolysis at least four times longer than the positive control did. Before, it was shown in two lead peptides how the exchange of their carbonyl function for a carbon sulfide function on the P₂ substrate position entailed a relatively small increase of the K_m constant while the turnover rate constants dropped systematically one order of magnitude in comparison to the hydrolysis rates of the same peptides without any modification [198]. Therefore, it is not expected that here the binding of both Angiotensin variants, reduced and methylated, to be affected to such extent that it might be the reason why such peptides are not at all cleaved, as they still conserve unchanged the proline primary specificity.

In that sense we tested two additional fluorogenic peptide derivatives with a methylated, Dabcyl-KDRVYIHPΨ[CO-NMe]FHE-Edans, and a reduced, AlaAlaΨ[CH₂-NH]Pro-AMC, peptide bonds. Neither of these fluorogenic surrogates were useful to detect substrate turnover. As poor substrates their affinity constants could be determined, 0.33±0.01 μM for Dabcyl-KDRVYIHPΨ[CO-NMe]FHE-Edans, and 268±25 μM for AlaAlaΨ[CH₂-NH]Pro-AMC. This additionally demonstrated how, at least, the impeded step in their hydrolysis was not related to a dramatic impairment on their affinities. Therefore, it seems reasonable to think that, maybe, the lack of hydrolysis of these substrates is consequence of a mechanistic distortion of the catalysis. A distortion that specially alludes, and involves, Arg⁶⁴³ as a relevant player on the mechanism of catalysis of prolyl oligopeptidase.

4.11 Summary (Zusammenfassung).

This work has faced the kinetic characterization of some residues of prolyl oligopeptidase related to the active site: Trp⁵⁹⁵, Arg⁶⁴³, Met²³⁵, Phe¹⁷³ and Cys²⁵⁵. Although all these residues have been highlighted in the literature on the basis of crystallographic information, no concrete kinetic data are available of the possible contributions that these residues might make to the mechanism of substrate specificity used by this enzyme.

- We found here that all selected residues have an evident implication in the mechanisms of catalysis and substrate specificity of PEP. It immediately appeared to be obvious that their contributions are very dependent on the nature of the analyzed substrate.
- The Trp⁵⁹⁵ variants clearly showed that this residue is bringing the substrate to the proper conformation which allows the enzyme to achieve a feasible

nucleophilic attack. Interactions that we have shown here to have some relevant polar contributions that have been previously neglected by an overwhelmed hydrophobic interpretation of the S₁ pocket.

- Arg⁶⁴³ variants indicated that the contributions of this residue to the enzyme specificity might not be minimized to a simple binding role. The different data support the idea of an implication of this residue on the catalytic mechanism of the catalytic triad as a reinforcement element.
- Phe¹⁷³ variant revealed that the contributions of this residue might basically have relevance on the binding of the substrate.
- Variation of Met²³⁵ and Cys²⁵⁵ residues surprisingly appeared to have not a main implication on the substrate accommodation but a major role during its catalysis, a fact that can only be understood if one accepts the catalytic relevance of dynamic motions within the active site.

Furthermore, one of the hallmarks achieved within this work was the confirmation, with solid kinetic data, that the prolyl oligopeptidase specificity should be broadened, including now reduced cysteine residues as an additional primary specificity.

Additionally, we could demonstrated how the affinity of all here studied inhibitors follows the same canonical binding pattern mainly defined by the contributions made by residues Trp⁵⁹⁵ and Arg⁶⁴³.

For the first time it could be shown how relevant can be the substrate P_n' positions for the enzyme specificity. We found here that the interactions on P₂' and P₄' positions can be strongly deleterious for the hydrolytic capacity of the enzyme. In addition, our data suggest the possible existence of an extended binding pattern beyond the active site, namely second binding site, that might rule the hydrolysis of larger peptides.

German translation of the summary.

Die vorliegende Arbeit beschäftigt sich mit der kinetischen Charakterisierung einiger Reste des aktiven Zentrums der Prolyl oligopeptidase: Trp⁵⁹⁵, Arg⁶⁴³, Met²³⁵, Phe¹⁷³ und Cys²⁵⁵.

Obwohl diese Reste in der Literatur auf der Basis kristallographischer Informationen beschrieben wurden, lagen bisher keine konkreten kinetischen Daten vor, welche ihre möglichen Beiträge zum Mechanismus der Katalyse und zur Substratspezifität dieses Enzyms beschreiben.

Wir konnten nachweisen, dass alle ausgewählten Reste wichtige Beiträge zur enzymatischen Aktivität der PEP leisten, welche in starkem Maß von der Natur des analysierten Substrates abhängen.

- Die Untersuchung der Trp⁵⁹⁵-Varianten zeigt, dass dieser Rest eine Konformationsänderung bewirkt, welche dem Enzym einen zur effektiven Katalyse notwendigen nukleophilen Angriff ermöglicht. Die dabei auftretenden polaren Wechselwirkungen leisten dabei einen bedeutenden Beitrag, der bisher aufgrund einer hydrophobe Interpretation der S₁-Tasche vernachlässigt wurde.
- Durch Untersuchung der Arg⁶⁴³-Varianten konnte gezeigt werden, dass der Beitrag dieses Restes zur Enzymspezifität nicht auf eine einfache Bindungsrolle minimiert werden kann. Verschiedene Daten lassen den Schluss zu, dass dieser Rest am Mechanismus der katalytischen Triade als verstärkendes Element beteiligt ist.
- Die Analyse der Phe¹⁷³-Varianten zeigt die Bedeutung dieses Restes für die Substratbindung.
- Eine Variation der Met²³⁵- und Cys²⁵⁵-Reste scheint überraschenderweise keine Bedeutung für die Substratbindung zu haben. Ihre Hauptrolle bei der Katalyse kann nur erklärt werden, wenn man die katalytische Relevanz dynamischer Bewegungen innerhalb des aktiven Zentrums in Betracht zieht.

Ein weiteres Ergebnis dieser Arbeit ist die Bestätigung durch kinetischen Daten, dass die Prolyl oligopeptidase ebenfalls eine Spezifität für reduzierte Cysteinreste besitzt. Zudem konnte gezeigt werden, wie die Affinität aller hier untersuchten Inhibitoren dem gleichen kanonischen Bindungsmuster folgt, welches im Wesentlichen durch die Beiträge der Reste Trp⁵⁹⁵ und Arg⁶⁴³ definiert ist.

Bisher war über Relevanz der P_n'-Positionen für die Enzymspezifität wenig bekannt. Wir fanden heraus, dass sich Wechselwirkungen an P₂'- und P₄'-Position nachteilig auf die hydrolytische Kapazität des Enzyms auswirken. Zusätzlich deuten unsere Daten auf ein mögliches Vorhandensein eines ausgedehnten Bindungsmusters jenseits des aktiven Zentrums hin - einer zweiten Bindungsstelle, welche die Hydrolyse großer Peptide beeinflusst.

5.0 References.

- [1] MacArthur, M.W. & Thornton, J.M. (1991) Influence of proline residues on protein conformation. *J. Mol. Biol.*, **218**, 397-412.
- [2] Brandts, J.F., Halvorson, H.R., & Brennan, M. (1975) Consideration of the Possibility that the slow step in protein denaturation reactions is due to cis-trans isomerism of proline residues. *Biochemistry*, **14**, 4953-4963.
- [3] Ramachandran, G.N. & Mitra, A.K. (1976) An explanation for the rare occurrence of cis peptide units in proteins and polypeptides. *J. Mol. Biol.*, **107**, 85-92.
- [4] Schimmel, P.R. & Flory, P.J. (1968) Conformational energies and configurational statistics of copolypeptides containing L-proline. *J. Mol. Biol.*, **34**, 105-120.
- [5] Barlow, D.J. & Thornton, J.M. (1988) Helix geometry in proteins. *J. Mol. Biol.*, **201**, 601-619.
- [6] Chothia, C. & Janin, J. (1982) Orthogonal packing of beta-pleated sheets in proteins. *Biochemistry*, **21**, 3955-3965.
- [7] Shepherd, A.J., Gorse, D., & Thornton, J.M. (1999) Prediction of the location and type of beta-turns in proteins using neural networks. *Protein Sci.*, **8**, 1045-1055.
- [8] Zimmerman, S.S. & Scheraga, H.A. (1977) Local interactions in bends of proteins. *Proc. Natl. Acad. Sci. U. S. A.*, **74**, 4126-4129.
- [9] Hutchinson, E.G. & Thornton, J.M. (1994) A revised set of potentials for beta-turn formation in proteins. *Protein Sci.*, **3**, 2207-2216.
- [10] Williams, K.A. & Deber, C.M. (1991) Proline residues in transmembrane helices: structural or dynamic role? *Biochemistry*, **30**, 8919-8923.
- [11] Eilers, M., Hornak, V., Smith, S.O., & Konopka, J.B. (2005) Comparison of class A and D G protein-coupled receptors: common features in structure and activation. *Biochemistry*, **44**, 8959-8975.
- [12] Wess, J., Nanavati, S., Vogel, Z., & Maggio, R. (1993) Functional role of proline and tryptophan residues highly conserved among G protein-coupled receptors studied by mutational analysis of the m3 muscarinic receptor. *EMBO J.*, **12**, 331-338.
- [13] Zhao, Y., Scheuer, T., & Catterall, W.A. (2004) Reversed voltage-dependent gating of a bacterial sodium channel with proline substitutions in the S6 transmembrane segment. *Proc. Natl. Acad. Sci. U. S. A.*, **101**, 17873-17878.
- [14] Lummis, S.C., Beene, D.L., Lee, L.W., Lester, H.A., Broadhurst, R.W., & Dougherty, D.A. (2005) Cis-trans isomerization at a proline opens the pore of a neurotransmitter-gated ion channel. *Nature*, **438**, 248-252.
- [15] Kay, B.K., Williamson, M.P., & Sudol, M. (2000) The importance of being proline: the interaction of proline-rich motifs in signaling proteins with their cognate domains. *FASEB J.*, **14**, 231-241.

-
- [16] Vanhoof, G., Goossens, F., De, M., I, Hendriks, D., & Scharpe, S. (1995) Proline motifs in peptides and their biological processing. *FASEB J.*, **9**, 736-744.
- [17] Yaron, A. & Naider, F. (1993) Proline-dependent structural and biological properties of peptides and proteins. *Crit Rev. Biochem. Mol. Biol.*, **28**, 31-81.
- [18] Kalra, S.P. & Crowley, W.R. (1992) Neuropeptide Y: a novel neuroendocrine peptide in the control of pituitary hormone secretion, and its relation to luteinizing hormone. *Front Neuroendocrinol.*, **13**, 1-46.
- [19] Berglund, M.M., Hipkind, P.A., & Gehlert, D.R. (2003) Recent developments in our understanding of the physiological role of PP-fold peptide receptor subtypes. *Exp. Biol. Med. (Maywood.)*, **228**, 217-244.
- [20] Markert, Y., Koditz, J., Mansfeld, J., Arnold, U., & Ulbrich-Hofmann, R. (2001) Increased proteolytic resistance of ribonuclease A by protein engineering. *Protein Eng*, **14**, 791-796.
- [21] Frenken, L.G., Egmond, M.R., Batenburg, A.M., & Verrips, C.T. (1993) *Pseudomonas glumae* lipase: increased proteolytic stability by protein engineering. *Protein Eng*, **6**, 637-642.
- [22] Mentlein, R. (1988) Proline residues in the maturation and degradation of peptide hormones and neuropeptides. *FEBS Lett.*, **234**, 251-256.
- [23] Grandt, D., Schimiczek, M., Rascher, W., Feth, F., Shively, J., Lee, T.D., Davis, M.T., Reeve, J.R., Jr., & Michel, M.C. (1996) Neuropeptide Y 3-36 is an endogenous ligand selective for Y2 receptors. *Regul. Pept.*, **67**, 33-37.
- [24] Barrett, A.J. (1997) Nomenclature Committee of the International Union of Biochemistry and Molecular Biology (NC-IUBMB). Enzyme Nomenclature. Recommendations 1992. Supplement 4: corrections and additions (1997). *Eur. J. Biochem.*, **250**, 1-6.
- [25] Schechter, I. & Berger, A. (1967) On the size of the active site in proteases. I. Papain. *Biochem. Biophys. Res. Commun.*, **27**, 157-162.
- [26] Barrett, A.J., Rawlings, N.D., & O'Brien, E.A. (2001) The MEROPS database as a protease information system. *J. Struct. Biol.*, **134**, 95-102.
- [27] Augustyns, K., Van, d., V, Senten, K., & Haemers, A. (2005) The therapeutic potential of inhibitors of dipeptidyl peptidase IV (DPP IV) and related proline-specific dipeptidyl aminopeptidases. *Curr. Med. Chem.*, **12**, 971-998.
- [28] Walter, R., Shlank, H., Glass, J.D., Schwartz, I.L., & Kerenyi, T.D. (1971) Leucylglycinamide released from oxytocin by human uterine enzyme. *Science*, **173**, 827-829.
- [29] Venalainen, J.I., Juvonen, R.O., & Mannisto, P.T. (2004) Evolutionary relationships of the prolyl oligopeptidase family enzymes. *Eur. J. Biochem.*, **271**, 2705-2715.
- [30] Nozaki, Y., Sato, N., Iida, T., Hara, K., Fukuyama, K., & Epstein, W.L. (1992) Prolyl endopeptidase purified from granulomatous inflammation in mice. *J. Cell Biochem.*, **49**, 296-303.

-
- [31] Yoshida, K., Inaba, K., Ohtake, H., & Morisawa, M. (1999) Purification and characterization of prolyl endopeptidase from the Pacific herring, *Clupea pallasii*, and its role in the activation of sperm motility. *Dev. Growth Differ.*, **41**, 217-225.
- [32] Moriyama, A., Nakanishi, M., & Sasaki, M. (1988) Porcine muscle prolyl endopeptidase and its endogenous substrates. *J. Biochem. (Tokyo)*, **104**, 112-117.
- [33] Yoshimoto, T., Oyama, H., Koriyama, N., & Tsuru, D. (1988) Prolyl endopeptidase from bovine testis: purification, characterization and comparison with the enzymes from other tissues. *Chem. Pharm. Bull. (Tokyo)*, **36**, 1456-1462.
- [34] Yoshimoto, T., Nishimura, T., Kita, T., & Tsuru, D. (1983) Post-proline cleaving enzyme (prolyl endopeptidase) from bovine brain. *J. Biochem. (Tokyo)*, **94**, 1179-1190.
- [35] Goossens, F., De, M., I, Vanhoof, G., Hendriks, D., Vriend, G., & Scharpe, S. (1995) The purification, characterization and analysis of primary and secondary structure of prolyl oligopeptidase from human lymphocytes. Evidence that the enzyme belongs to the alpha/beta hydrolase fold family. *Eur. J. Biochem.*, **233**, 432-441.
- [36] Kalwant, S. & Porter, A.G. (1991) Purification and characterization of human brain prolyl endopeptidase. *Biochem. J.*, **276 (Pt 1)**, 237-244.
- [37] Kabashima, T., Fujii, M., Meng, Y., Ito, K., & Yoshimoto, T. (1998) Prolyl endopeptidase from *Sphingomonas capsulata*: isolation and characterization of the enzyme and nucleotide sequence of the gene. *Arch. Biochem. Biophys.*, **358**, 141-148.
- [38] Kanatani, A., Yoshimoto, T., Kitazono, A., Kokubo, T., & Tsuru, D. (1993) Prolyl endopeptidase from *Aeromonas hydrophila*: cloning, sequencing, and expression of the enzyme gene, and characterization of the expressed enzyme. *J. Biochem. (Tokyo)*, **113**, 790-796.
- [39] Li, M., Chen, C., & Wang, D. (2000) [Gene cloning and expression of prolyl endopeptidase from *Aeromonas punctata*]. *Wei Sheng Wu Xue. Bao.*, **40**, 277-283.
- [40] Yoshimoto, T., Kanatani, A., Shimoda, T., Inaoka, T., Kokubo, T., & Tsuru, D. (1991) Prolyl endopeptidase from *Flavobacterium meningosepticum*: cloning and sequencing of the enzyme gene. *J. Biochem. (Tokyo)*, **110**, 873-878.
- [41] Chevallier, S., Goeltz, P., Thibault, P., Banville, D., & Gagnon, J. (1992) Characterization of a prolyl endopeptidase from *Flavobacterium meningosepticum*. Complete sequence and localization of the active-site serine. *J. Biol. Chem.*, **267**, 8192-8199.
- [42] Vanhoof, G., Goossens, F., Hendriks, L., De, M., I, Hendriks, D., Vriend, G., Van Broeckhoven, C., & Scharpe, S. (1994) Cloning and sequence analysis of the gene encoding human lymphocyte prolyl endopeptidase. *Gene*, **149**, 363-366.

-
- [43] Shirasawa, Y., Osawa, T., & Hirashima, A. (1994) Molecular cloning and characterization of prolyl endopeptidase from human T cells. *J. Biochem. (Tokyo)*, **115**, 724-729.
- [44] Ishino, T., Ohtsuki, S., Homma, K., & Natori, S. (1998) cDNA cloning of mouse prolyl endopeptidase and its involvement in DNA synthesis by Swiss 3T3 cells. *J. Biochem. (Tokyo)*, **123**, 540-545.
- [45] Rennex, D., Hemmings, B.A., Hofsteenge, J., & Stone, S.R. (1991) cDNA cloning of porcine brain prolyl endopeptidase and identification of the active-site seryl residue. *Biochemistry*, **30**, 2195-2203.
- [46] Kimura, A. & Takahashi, T. (2000) cDNA cloning of rat prolyl oligopeptidase and its expression in the ovary during the estrous cycle. *J. Exp. Zool.*, **286**, 656-665.
- [47] Yoshimoto, T., Miyazaki, K., Haraguchi, N., Kitazono, A., Kabashima, T., & Ito, K. (1997) Cloning and expression of the cDNA encoding prolyl oligopeptidase (prolyl endopeptidase) from bovine brain. *Biol. Pharm. Bull.*, **20**, 1047-1050.
- [48] Ohtsuki, S., Homma, K., Kurata, S., & Natori, S. (1997) Molecular cloning of cDNA for Sarcophaga prolyl endopeptidase and characterization of the recombinant enzyme produced by an E. coli expression system. *Insect Biochem. Mol. Biol.*, **27**, 337-343.
- [49] Harwood, V.J., Denson, J.D., Robinson-Bidle, K.A., & Schreier, H.J. (1997) Overexpression and characterization of a prolyl endopeptidase from the hyperthermophilic archaeon *Pyrococcus furiosus*. *J. Bacteriol.*, **179**, 3613-3618.
- [50] Polgar, L. (2002) The prolyl oligopeptidase family. *Cell Mol. Life Sci.*, **59**, 349-362.
- [51] Goossens, F.J., Wauters, J.G., Vanhoof, G.C., Bossuyt, P.J., Schatteman, K.A., Loens, K., & Scharpe, S.L. (1996) Subregional mapping of the human lymphocyte prolyl oligopeptidase gene (PREP) to human chromosome 6q22. *Cytogenet. Cell Genet.*, **74**, 99-101.
- [52] Kimura, A., Yoshida, I., Takagi, N., & Takahashi, T. (1999) Structure and localization of the mouse prolyl oligopeptidase gene. *J. Biol. Chem.*, **274**, 24047-24053.
- [53] Goossens, F., De, M., I, Vanhoof, G., & Scharpe, S. (1996) Distribution of prolyl oligopeptidase in human peripheral tissues and body fluids. *Eur. J. Clin. Chem. Clin. Biochem.*, **34**, 17-22.
- [54] Daly, D.J., Maskrey, P., & Pennington, R.J. (1985) Characterization of proline endopeptidase from skeletal muscle. *Int. J. Biochem.*, **17**, 521-524.
- [55] Kato, T., Okada, M., & Nagatsu, T. (1980) Distribution of post-proline cleaving enzyme in human brain and the peripheral tissues. *Mol. Cell Biochem.*, **32**, 117-121.
- [56] Maes, M., Goossens, F., Scharpe, S., Calabrese, J., Desnyder, R., & Meltzer, H.Y. (1995) Alterations in plasma prolyl endopeptidase activity in depression, mania, and schizophrenia: effects of antidepressants, mood stabilizers, and antipsychotic drugs. *Psychiatry Res.*, **58**, 217-225.

-
- [57] Irazusta, J., Larrinaga, G., Gonzalez-Maeso, J., Gil, J., Meana, J.J., & Casis, L. (2002) Distribution of prolyl endopeptidase activities in rat and human brain. *Neurochem. Int.*, **40**, 337-345.
- [58] Bellemere, G., Vaudry, H., Mounien, L., Boutelet, I., & Jegou, S. (2004) Localization of the mRNA encoding prolyl endopeptidase in the rat brain and pituitary. *J. Comp Neurol.*, **471**, 128-143.
- [59] Dresdner, K., Barker, L.A., Orłowski, M., & Wilk, S. (1982) Subcellular distribution of prolyl endopeptidase and cation-sensitive neutral endopeptidase in rabbit brain. *J. Neurochem.*, **38**, 1151-1154.
- [60] Moreno-Baylach, M.J., Felipo, V., Mannisto, P.T., & Garcia-Horsman, J.A. (2008) Expression and traffic of cellular prolyl oligopeptidase are regulated during cerebellar granule cell differentiation, maturation, and aging. *Neuroscience*, **156**, 580-585.
- [61] Schulz, I., Zeitschel, U., Rudolph, T., Ruiz-Carrillo, D., Rahfeld, J.U., Gerhartz, B., Bigl, V., Demuth, H.U., & Rossner, S. (2005) Subcellular localization suggests novel functions for prolyl endopeptidase in protein secretion. *J. Neurochem.*, **94**, 970-979.
- [62] Ohtuski, S., Homma, K., Kurata, S., & Natori, S. (1997) Nuclear localization and involvement in DNA synthesis of Sarcophaga prolyl endopeptidase. *J. Biochem. (Tokyo)*, **121**, 1176-1181.
- [63] O'Leary, R.M. & O'Connor, B. (1995) Identification and localisation of a synaptosomal membrane prolyl endopeptidase from bovine brain. *Eur. J. Biochem.*, **227**, 277-283.
- [64] Agirregoitia, N., Irazusta, A., Ruiz, F., Irazusta, J., & Gil, J. (2003) Ontogeny of soluble and particulate prolyl endopeptidase activity in several areas of the rat brain and in the pituitary gland. *Dev. Neurosci.*, **25**, 316-323.
- [65] Tenorio-Laranga, J., Venalainen, J.I., Mannisto, P.T., & Garcia-Horsman, J.A. (2008) Characterization of membrane-bound prolyl endopeptidase from brain. *FEBS J.*, **275**, 4415-4427.
- [66] Cunningham, D.F. & O'Connor, B. (1998) A study of prolyl endopeptidase in bovine serum and its relevance to the tissue enzyme. *Int. J. Biochem. Cell Biol.*, **30**, 99-114.
- [67] Fulop, V., Bocskei, Z., & Polgar, L. (1998) Prolyl oligopeptidase: an unusual beta-propeller domain regulates proteolysis. *Cell*, **94**, 161-170.
- [68] Ollis, D.L., Cheah, E., Cygler, M., Dijkstra, B., Frolow, F., Franken, S.M., Harel, M., Remington, S.J., Silman, I., Schrag, J., & . (1992) The alpha/beta hydrolase fold. *Protein Eng*, **5**, 197-211.
- [69] Fulop, V. & Jones, D.T. (1999) Beta propellers: structural rigidity and functional diversity. *Curr. Opin. Struct. Biol.*, **9**, 715-721.
- [70] Juhasz, T., Szeltner, Z., Fulop, V., & Polgar, L. (2005) Unclosed beta-propellers display stable structures: implications for substrate access to the active site of prolyl oligopeptidase. *J. Mol. Biol.*, **346**, 907-917.

- [71] Engel, M., Hoffmann, T., Wagner, L., Wermann, M., Heiser, U., Kiefersauer, R., Huber, R., Bode, W., Demuth, H.U., & Brandstetter, H. (2003) The crystal structure of dipeptidyl peptidase IV (CD26) reveals its functional regulation and enzymatic mechanism. *Proc. Natl. Acad. Sci. U. S. A.*, **100**, 5063-5068.
- [72] Aertgeerts, K., Levin, I., Shi, L., Snell, G.P., Jennings, A., Prasad, G.S., Zhang, Y., Kraus, M.L., Salakian, S., Sridhar, V., Wijnands, R., & Tennant, M.G. (2005) Structural and kinetic analysis of the substrate specificity of human fibroblast activation protein alpha. *J. Biol. Chem.*, **280**, 19441-19444.
- [73] Strop, P., Bankovich, A.J., Hansen, K.C., Garcia, K.C., & Brunger, A.T. (2004) Structure of a human A-type potassium channel interacting protein DPPX, a member of the dipeptidyl aminopeptidase family. *J. Mol. Biol.*, **343**, 1055-1065.
- [74] Fulop, V., Szeltner, Z., & Polgar, L. (2000) Catalysis of serine oligopeptidases is controlled by a gating filter mechanism. *EMBO Rep.*, **1**, 277-281.
- [75] Szeltner, Z., Rea, D., Juhasz, T., Renner, V., Fulop, V., & Polgar, L. (2004) Concerted structural changes in the peptidase and the propeller domains of prolyl oligopeptidase are required for substrate binding. *J. Mol. Biol.*, **340**, 627-637.
- [76] Bastos, I.M., Grellier, P., Martins, N.F., Cadavid-Restrepo, G., Souza-Ault, M.R., Augustyns, K., Teixeira, A.R., Schrevel, J., Maigret, B., da Silveira, J.F., & Santana, J.M. (2005) Molecular, functional and structural properties of the prolyl oligopeptidase of *Trypanosoma cruzi* (POP Tc80), which is required for parasite entry into mammalian cells. *Biochem. J.*, **388**, 29-38.
- [77] Harris, M.N., Madura, J.D., Ming, L.J., & Harwood, V.J. (2001) Kinetic and mechanistic studies of prolyl oligopeptidase from the hyperthermophile *Pyrococcus furiosus*. *J. Biol. Chem.*, **276**, 19310-19317.
- [78] Shan, L., Mathews, I.I., & Khosla, C. (2005) Structural and mechanistic analysis of two prolyl endopeptidases: role of interdomain dynamics in catalysis and specificity. *Proc. Natl. Acad. Sci. U. S. A.*, **102**, 3599-3604.
- [79] Polgar, L. (1992) Prolyl endopeptidase catalysis. A physical rather than a chemical step is rate-limiting. *Biochem. J.*, **283 (Pt 3)**, 647-648.
- [80] Carter, P. & Wells, J.A. (1988) Dissecting the catalytic triad of a serine protease. *Nature*, **332**, 564-568.
- [81] Rawlings, N.D., O'Brien, E., & Barrett, A.J. (2002) MEROPS: the protease database. *Nucleic Acids Res.*, **30**, 343-346.
- [82] Polgar, L. (1990) Common feature of the four types of protease mechanism. *Biol. Chem. Hoppe Seyler*, **371 Suppl**, 327-331.
- [83] Blow, D.M., Birktoft, J.J., & Hartley, B.S. (1969) Role of a buried acid group in the mechanism of action of chymotrypsin. *Nature*, **221**, 337-340.
- [84] Polgar, L. & Bender, M.L. (1969) The nature of general base-general acid catalysis in serine proteases. *Proc. Natl. Acad. Sci. U. S. A.*, **64**, 1335-1342.
- [85] Jordan, F. & Polgar, L. (1981) Proton nuclear magnetic resonance evidence for the absence of a stable hydrogen bond between the active site aspartate and

- histidine residues of native subtilisins and for its presence in thiolsubtilisins. *Biochemistry*, **20**, 6366-6370.
- [86] Polgar, L. (2005) The catalytic triad of serine peptidases. *Cell Mol. Life Sci.*, **62**, 2161-2172.
- [87] Szeltner, Z., Rea, D., Juhasz, T., Renner, V., Mucsi, Z., Orosz, G., Fulop, V., & Polgar, L. (2002) Substrate-dependent competency of the catalytic triad of prolyl oligopeptidase. *J. Biol. Chem.*, **277**, 44597-44605.
- [88] Sprang, S., Standing, T., Fletterick, R.J., Stroud, R.M., Finer-Moore, J., Xuong, N.H., Hamlin, R., Rutter, W.J., & Craik, C.S. (1987) The three-dimensional structure of Asn102 mutant of trypsin: role of Asp102 in serine protease catalysis. *Science*, **237**, 905-909.
- [89] Fulop, V., Szeltner, Z., Renner, V., & Polgar, L. (2001) Structures of prolyl oligopeptidase substrate/inhibitor complexes. Use of inhibitor binding for titration of the catalytic histidine residue. *J. Biol. Chem.*, **276**, 1262-1266.
- [90] Bryan, P., Pantoliano, M.W., Quill, S.G., Hsiao, H.Y., & Poulos, T. (1986) Site-directed mutagenesis and the role of the oxyanion hole in subtilisin. *Proc. Natl. Acad. Sci. U. S. A.*, **83**, 3743-3745.
- [91] Szeltner, Z., Renner, V., & Polgar, L. (2000) Substrate- and pH-dependent contribution of oxyanion binding site to the catalysis of prolyl oligopeptidase, a paradigm of the serine oligopeptidase family. *Protein Sci.*, **9**, 353-360.
- [92] Walter, R., Shlank, H., Glass, J.D., Schwartz, I.L., & Kerenyi, T.D. (1971) Leucylglycinamide released from oxytocin by human uterine enzyme. *Science*, **173**, 827-829.
- [93] Koida, M. & Walter, R. (1976) Post-proline cleaving enzyme. Purification of this endopeptidase by affinity chromatography. *J. Biol. Chem.*, **251**, 7593-7599.
- [94] Yoshimoto, T., Orłowski, R.C., & Walter, R. (1977) Postproline cleaving enzyme: identification as serine protease using active site specific inhibitors. *Biochemistry*, **16**, 2942-2948.
- [95] Walter, R. & Yoshimoto, T. (1978) Postproline cleaving enzyme: kinetic studies of size and stereospecificity of its active site. *Biochemistry*, **17**, 4139-4144.
- [96] Polgar, L. (1988) The different mechanisms of protease action have a basic feature in common: proton transfer from the attacking nucleophile to the substrate leaving group. *Acta Biochim. Biophys. Hung.*, **23**, 207-213.
- [97] Polgar, L. (1995) Effects of ionic strength on the catalysis and stability of prolyl oligopeptidase. *Biochem. J.*, **312 (Pt 1)**, 267-271.
- [98] Polgar, L. (1991) pH-dependent mechanism in the catalysis of prolyl endopeptidase from pig muscle. *Eur. J. Biochem.*, **197**, 441-447.
- [99] Polgar, L. (1994) Prolyl oligopeptidases. *Methods Enzymol.*, **244**, 188-200.
- [100] Bunning, P. & Riordan, J.F. (1983) Activation of angiotensin converting enzyme by monovalent anions. *Biochemistry*, **22**, 110-116.

-
- [101] Yoshimoto, T., Simmons, W.H., Kita, T., & Tsuru, D. (1981) Post-proline cleaving enzyme from lamb brain. *J. Biochem. (Tokyo)*, **90**, 325-334.
- [102] Lin, L.N. & Brandts, J.F. (1983) Evidence showing that a proline-specific endopeptidase has an absolute requirement for a trans peptide bond immediately preceding the active bond. *Biochemistry*, **22**, 4480-4485.
- [103] Tsukahara, T., Ishiura, S., & Sugita, H. (1990) Regulation of prolyl endopeptidase activity by the intracellular redox state. *J. Biol. Chem.*, **265**, 21448-21453.
- [104] Szeltner, Z., Renner, V., & Polgar, L. (2000) The noncatalytic beta-propeller domain of prolyl oligopeptidase enhances the catalytic capability of the peptidase domain. *J. Biol. Chem.*, **275**, 15000-15005.
- [105] Brandt, I., Vriendt, K.D., Devreese, B., Beeumen, J.V., Dongen, W.V., Augustyns, K., Meester, I.D., Scharpe, S., & Lambeir, A.M. (2005) Search for substrates for prolyl oligopeptidase in porcine brain. *Peptides*.
- [106] Wilk, S. (1983) Prolyl endopeptidase. *Life Sci.*, **33**, 2149-2157.
- [107] Yoshimoto, T., Kado, K., Matsubara, F., Koriyama, N., Kaneto, H., & Tsuru, D. (1987) Specific inhibitors for prolyl endopeptidase and their anti-amnesic effect. *J. Pharmacobiodyn.*, **10**, 730-735.
- [108] Izquierdo, I. (1989) Mechanism of action of scopolamine as an amnesic. *Trends Pharmacol. Sci.*, **10**, 175-177.
- [109] Morain, P., Lestage, P., De Nanteuil, G., Jochemsen, R., Robin, J.L., Guez, D., & Boyer, P.A. (2002) S 17092: a prolyl endopeptidase inhibitor as a potential therapeutic drug for memory impairment. Preclinical and clinical studies. *CNS. Drug Rev.*, **8**, 31-52.
- [110] Huston, J.P. & Hasenohrl, R.U. (1995) The role of neuropeptides in learning: focus on the neurokinin substance P. *Behav. Brain Res.*, **66**, 117-127.
- [111] Di Daniel, E., Glover, C.P., Grot, E., Chan, M.K., Sanderson, T.H., White, J.H., Ellis, C.L., Gallagher, K.T., Uney, J., Thomas, J., Maycox, P.R., & Mudge, A.W. (2009) Prolyl oligopeptidase binds to GAP-43 and functions without its peptidase activity. *Mol. Cell Neurosci.*
- [112] Gould, T.D., Quiroz, J.A., Singh, J., Zarate, C.A., & Manji, H.K. (2004) Emerging experimental therapeutics for bipolar disorder: insights from the molecular and cellular actions of current mood stabilizers. *Mol. Psychiatry*, **9**, 734-755.
- [113] Williams, R.S., Eames, M., Ryves, W.J., Viggars, J., & Harwood, A.J. (1999) Loss of a prolyl oligopeptidase confers resistance to lithium by elevation of inositol (1,4,5) trisphosphate. *EMBO J.*, **18**, 2734-2745.
- [114] Williams, R.S. (2005) Pharmacogenetics in model systems: Defining a common mechanism of action for mood stabilisers. *Prog. Neuropsychopharmacol. Biol. Psychiatry*, **29**, 1029-1037.

- [115] Schulz, I., Gerhartz, B., Neubauer, A., Holloschi, A., Heiser, U., Hafner, M., & Demuth, H.U. (2002) Modulation of inositol 1,4,5-triphosphate concentration by prolyl endopeptidase inhibition. *Eur. J. Biochem.*, **269**, 5813-5820.
- [116] van Dijken, P., de Haas, J.R., Craxton, A., Erneux, C., Shears, S.B., & Van Haastert, P.J. (1995) A novel, phospholipase C-independent pathway of inositol 1,4,5-trisphosphate formation in Dictyostelium and rat liver. *J. Biol. Chem.*, **270**, 29724-29731.
- [117] Breen, G., Harwood, A.J., Gregory, K., Sinclair, M., Collier, D., St Clair, D., & Williams, R.S. (2004) Two peptidase activities decrease in treated bipolar disorder not schizophrenic patients. *Bipolar. Disord.*, **6**, 156-161.
- [118] Kimura, A., Matsui, H., & Takahashi, T. (2002) Expression and localization of prolyl oligopeptidase in mouse testis and its possible involvement in sperm motility. *Zoolog. Sci.*, **19**, 93-102.
- [119] Ohtsuki, S., Homma, K., Kurata, S., Komano, H., & Natori, S. (1994) A prolyl endopeptidase of *Sarcophaga peregrina* (flesh fly): its purification and suggestion for its participation in the differentiation of the imaginal discs. *J. Biochem. (Tokyo)*, **115**, 449-453.
- [120] Yamanaka, C., Lebrethon, M.C., Vandersmissen, E., Gerard, A., Purnelle, G., Lemaitre, M., Wilk, S., & Bourguignon, J.P. (1999) Early prepubertal ontogeny of pulsatile gonadotropin-releasing hormone (GnRH) secretion: I. Inhibitory autofeedback control through prolyl endopeptidase degradation of GnRH. *Endocrinology*, **140**, 4609-4615.
- [121] Shoji, S., Imazumi, K., Yamaoka, T., Funakoshi, T., Tanaka, J., Kambara, T., Ueki, H., & Kubota, Y. (1989) Depression of prolylendopeptidase activity in the delayed hypersensitive guinea pig skin lesion induced by bovine gamma-globulin. *Biochem. Int.*, **18**, 1183-1192.
- [122] Momeni, N., Nordstrom, B.M., Horstmann, V., Avarseji, H., & Sivberg, B.V. (2005) Alterations of prolyl endopeptidase activity in the plasma of children with autistic spectrum disorders. *BMC. Psychiatry*, **5**, 27.
- [123] Maes, M., Goossens, F., Scharpe, S., Meltzer, H.Y., D'Hondt, P., & Cosyns, P. (1994) Lower serum prolyl endopeptidase enzyme activity in major depression: further evidence that peptidases play a role in the pathophysiology of depression. *Biol. Psychiatry*, **35**, 545-552.
- [124] Van Gool, A.R., Van Ojik, H.H., Kruit, W.H., Mulder, P.G., Fekkes, D., Bannink, M., Scharpe, S., Stoter, G., Eggermont, A.M., Maes, M., & Verkerk, R. (2004) Serum activity of prolyl endopeptidase, but not of dipeptidyl peptidase IV, is decreased by immunotherapy with IFN-alpha in high-risk melanoma patients. *J. Interferon Cytokine Res.*, **24**, 411-415.
- [125] Maes, M., Monteleone, P., Bencivenga, R., Goossens, F., Maj, M., van West, D., Bosmans, E., & Scharpe, S. (2001) Lower serum activity of prolyl endopeptidase in anorexia and bulimia nervosa. *Psychoneuroendocrinology*, **26**, 17-26.
- [126] Maes, M., Libbrecht, I., Van Hunsel, F., Lin, A.H., Bonaccorso, S., Goossens, F., De, M., I, De Clerck, L., Biondi, M., Scharpe, S., & Janca, A. (1998) Lower

- serum activity of prolyl endopeptidase in fibromyalgia is related to severity of depressive symptoms and pressure hyperalgesia. *Psychol. Med.*, **28**, 957-965.
- [127] Maes, M., Lin, A.H., Bonaccorso, S., Goossens, F., Van Gastel, A., Pioli, R., Delmeire, L., & Scharpe, S. (1999) Higher serum prolyl endopeptidase activity in patients with post-traumatic stress disorder. *J. Affect. Disord.*, **53**, 27-34.
- [128] Wilk, S. & Orlowski, M. (1983) Inhibition of rabbit brain prolyl endopeptidase by n-benzyloxycarbonyl-prolyl-prolinal, a transition state aldehyde inhibitor. *J. Neurochem.*, **41**, 69-75.
- [129] Kahyaoglu, A., Haghjoo, K., Kraicsovits, F., Jordan, F., & Polgar, L. (1997) Benzyloxycarbonylprolylprolinal, a transition-state analogue for prolyl oligopeptidase, forms a tetrahedral adduct with catalytic serine, not a reactive cysteine. *Biochem. J.*, **322 (Pt 3)**, 839-843.
- [130] Bakker, A.V., Jung, S., Spencer, R.W., Vinick, F.J., & Faraci, W.S. (1990) Slow tight-binding inhibition of prolyl endopeptidase by benzyloxycarbonyl-prolyl-prolinal. *Biochem. J.*, **271**, 559-562.
- [131] Cunningham, D.F. & O'Connor, B. (1997) Proline specific peptidases. *Biochim. Biophys. Acta*, **1343**, 160-186.
- [132] Venalainen, J.I., Juvonen, R.O., Garcia-Horsman, J.A., Wallen, E.A., Christiaans, J.A., Jarho, E.M., Gynther, J., & Mannisto, P.T. (2004) Slow-binding inhibitors of prolyl oligopeptidase with different functional groups at the P1 site. *Biochem. J.*, **382**, 1003-1008.
- [133] Katsube, N., Sunaga, K., Chuang, D.M., & Ishitani, R. (1996) ONO-1603, a potential antidementia drug, shows neuroprotective effects and increases m3-muscarinic receptor mRNA levels in differentiating rat cerebellar granule neurons. *Neurosci. Lett.*, **214**, 151-154.
- [134] Venalainen, J.I., Juvonen, R.O., Forsberg, M.M., Garcia-Horsman, A., Poso, A., Wallen, E.A., Gynther, J., & Mannisto, P.T. (2002) Substrate-dependent, non-hyperbolic kinetics of pig brain prolyl oligopeptidase and its tight binding inhibition by JTP-4819. *Biochem. Pharmacol.*, **64**, 463-471.
- [135] Yoshimoto, T., Tsuru, D., Yamamoto, N., Ikezawa, R., & Furukawa, S. (1991) Structure activity relationship of inhibitors specific for prolyl endopeptidase. *Agric. Biol. Chem.*, **55**, 37-43.
- [136] Portevin, B., Benoist, A., Remond, G., Herve, Y., Vincent, M., Lepagnol, J., & De Nanteuil, G. (1996) New prolyl endopeptidase inhibitors: in vitro and in vivo activities of azabicyclo[2.2.2]octane, azabicyclo[2.2.1]heptane, and perhydroindole derivatives. *J. Med. Chem.*, **39**, 2379-2391.
- [137] Steinmetzer, T., Silberring, J., Mrestani-Klaus, C., Fittkau, S., Barth, A., & Demuth, H.U. (1993) Peptidyl ammonium methyl ketones as substrate analog inhibitors of proline-specific peptidases. *J. Enzyme Inhib.*, **7**, 77-85.
- [138] Stone, S.R., Rennex, D., Wikstrom, P., Shaw, E., & Hofsteenge, J. (1992) Peptidyl diazomethanes. A novel mechanism of interaction with prolyl endopeptidase. *Biochem. J.*, **283 (Pt 3)**, 871-876.

-
- [139] Demuth, H.U., Schlenzig, D., Schierhorn, A., Grosche, G., Chapot-Chartier, M.P., & Gripon, J.C. (1993) Design of (omega-N-(O-acyl)hydroxy amid) aminodicarboxylic acid pyrrolidides as potent inhibitors of proline-specific peptidases. *FEBS Lett.*, **320**, 23-27.
- [140] Bellemere, G., Morain, P., Vaudry, H., & Jegou, S. (2003) Effect of S 17092, a novel prolyl endopeptidase inhibitor, on substance P and alpha-melanocyte-stimulating hormone breakdown in the rat brain. *J. Neurochem.*, **84**, 919-929.
- [141] Bromme, D., Schierhorn, A., Kirschke, H., Wiederanders, B., Barth, A., Fittkau, S., & Demuth, H.U. (1989) Potent and selective inactivation of cysteine proteinases with N-peptidyl-O-acyl hydroxylamines. *Biochem. J.*, **263**, 861-866.
- [142] Toda, S., Kotake, C., Tsuno, T., Narita, Y., Yamasaki, T., & Konishi, M. (1992) Eurystatins A and B, new prolyl endopeptidase inhibitors. II. Physico-chemical properties and structure determination. *J. Antibiot. (Tokyo)*, **45**, 1580-1586.
- [143] Kamei, H., Ueki, T., Obi, Y., Fukagawa, Y., & Oki, T. (1992) Protective effect of eurystatins A and B, new prolyl endopeptidase inhibitors, on scopolamine-induced amnesia in rats. *Jpn. J. Pharmacol.*, **60**, 377-380.
- [144] Fan, W., Tezuka, Y., Ni, K.M., & Kadota, S. (2001) Prolyl endopeptidase inhibitors from the underground part of *Rhodiola sachalinensis*. *Chem. Pharm. Bull. (Tokyo)*, **49**, 396-401.
- [145] Heuermann, K. & Cosgrove, J. (2001) S-Gal: an autoclavable dye for color selection of cloned DNA inserts. *Biotechniques*, **30**, 1142-1147.
- [146] Iskakova, M.B., Szaflarski, W., Dreyfus, M., Remme, J., & Nierhaus, K.H. (2006) Troubleshooting coupled in vitro transcription-translation system derived from *Escherichia coli* cells: synthesis of high-yield fully active proteins. *Nucleic Acids Res.*, **34**, e135.
- [147] Thomas, J.G. & Baneyx, F. (1996) Protein misfolding and inclusion body formation in recombinant *Escherichia coli* cells overexpressing Heat-shock proteins. *J. Biol. Chem.*, **271**, 11141-11147.
- [148] Lottspeich F. & Zorbas H. (1998) *Bioanalytik*. Spektrum Akad. Verlag.
- [149] Lehninger A.L., Nelson D.L., & Cox M.M. (1993) *Principles of biochemistry*, Second edn. Worth Publishers.
- [150] Matayoshi, E.D., Wang, G.T., Krafft, G.A., & Erickson, J. (1990) Novel fluorogenic substrates for assaying retroviral proteases by resonance energy transfer. *Science*, **247**, 954-958.
- [151] Segel, I.H. (1993) *Enzyme Kinetics : behavior and analysis of rapid equilibrium and steady-state enzyme systems*. Wiley-interscience.
- [152] Leff, P. & Dougall, I.G. (1993) Further concerns over Cheng-Prusoff analysis. *Trends Pharmacol. Sci.*, **14**, 110-112.
- [153] Morrison, J.F. & Walsh, C.T. (1988) The behavior and significance of slow-binding enzyme inhibitors. *Adv. Enzymol. Relat Areas Mol. Biol.*, **61**, 201-301.

-
- [154] Sculley, M.J., Morrison, J.F., & Cleland, W.W. (1996) Slow-binding inhibition: the general case. *Biochim. Biophys. Acta*, **1298**, 78-86.
- [155] Winzor, D.J. & Jackson, C.M. (2006) Interpretation of the temperature dependence of equilibrium and rate constants. *J. Mol. Recognit.*, **19**, 389-407.
- [156] P.W. Atkins (1990) *Physical Chemistry*, fourth edition edn. Oxford University Press.
- [157] Szeltner, Z., Rea, D., Renner, V., Juliano, L., Fulop, V., & Polgar, L. (2003) Electrostatic environment at the active site of prolyl oligopeptidase is highly influential during substrate binding. *J. Biol. Chem.*, **278**, 48786-48793.
- [158] Szeltner, Z., Rea, D., Renner, V., Fulop, V., & Polgar, L. (2002) Electrostatic effects and binding determinants in the catalysis of prolyl oligopeptidase. Site specific mutagenesis at the oxyanion binding site. *J. Biol. Chem.*, **277**, 42613-42622.
- [159] Schilling, S., Hoffmann, T., Manhart, S., Hoffmann, M., & Demuth, H.U. (2004) Glutaminyl cyclases unfold glutamyl cyclase activity under mild acid conditions. *FEBS Lett.*, **563**, 191-196.
- [160] Ellis, K.J. & Morrison, J.F. (1982) Buffers of constant ionic strength for studying pH-dependent processes. *Methods Enzymol.*, **87**, 405-426.
- [161] Singh, S.M. & Panda, A.K. (2005) Solubilization and refolding of bacterial inclusion body proteins. *J. Biosci. Bioeng.*, **99**, 303-310.
- [162] Thomas, J.G. & Baneyx, F. (1996) Protein misfolding and inclusion body formation in recombinant *Escherichia coli* cells overexpressing Heat-shock proteins. *J. Biol. Chem.*, **271**, 11141-11147.
- [163] Polgar, L. (1992) Unusual secondary specificity of prolyl oligopeptidase and the different reactivities of its two forms toward charged substrates. *Biochemistry*, **31**, 7729-7735.
- [164] Schilling, S., Hoffmann, T., Manhart, S., Hoffmann, M., & Demuth, H.U. (2004) Glutaminyl cyclases unfold glutamyl cyclase activity under mild acid conditions. *FEBS Lett.*, **563**, 191-196.
- [165] Bar, J.W., Rahfeld, J.U., Schulz, I., Gans, K., Ruiz-Carrillo, D., Manhart, S., Rosche, F., & Demuth, H.U. (2006) Prolyl endopeptidase cleaves the apoptosis rescue peptide humanin and exhibits an unknown post-cysteine cleavage specificity. *Adv. Exp. Med. Biol.*, **575**, 103-108.
- [166] Tsuji, E., Misumi, Y., Fujiwara, T., Takami, N., Ogata, S., & Ikehara, Y. (1992) An active-site mutation (Gly633-->Arg) of dipeptidyl peptidase IV causes its retention and rapid degradation in the endoplasmic reticulum. *Biochemistry*, **31**, 11921-11927.
- [167] Polgar, L. & Patthy, A. (1992) Cleavage of the Lys196-Ser197 bond of prolyl oligopeptidase: enhanced catalytic activity for one of the two active enzyme forms. *Biochemistry*, **31**, 10769-10773.

-
- [168] Makinen, P.L., Makinen, K.K., & Syed, S.A. (1994) An endo-acting proline-specific oligopeptidase from *Treponema denticola* ATCC 35405: evidence of hydrolysis of human bioactive peptides. *Infect. Immun.*, **62**, 4938-4947.
- [169] Tyndall, J.D. & Fairlie, D.P. (1999) Conformational homogeneity in molecular recognition by proteolytic enzymes. *J. Mol. Recognit.*, **12**, 363-370.
- [170] Case, A. & Stein, R.L. (2003) Mechanistic origins of the substrate selectivity of serine proteases. *Biochemistry*, **42**, 3335-3348.
- [171] Walter, R. & Yoshimoto, T. (1978) Postproline cleaving enzyme: kinetic studies of size and stereospecificity of its active site. *Biochemistry*, **17**, 4139-4144.
- [172] Nomura, K. (1986) Specificity of prolyl endopeptidase. *FEBS Lett.*, **209**, 235-237.
- [173] Leker, R.R., Teichner, A., Grigoriadis, N., Ovadia, H., Brenneman, D.E., Fridkin, M., Giladi, E., Romano, J., & Gozes, I. (2002) NAP, a femtomolar-acting peptide, protects the brain against ischemic injury by reducing apoptotic death. *Stroke*, **33**, 1085-1092.
- [174] Polgar, L. (1999) Oligopeptidase B: a new type of serine peptidase with a unique substrate-dependent temperature sensitivity. *Biochemistry*, **38**, 15548-15555.
- [175] Polgar, L. (1991) Two forms of prolyl endopeptidase with different activities. *Biomed. Biochim. Acta*, **50**, 721-726.
- [176] Knowles, J.R. (1976) The intrinsic pKa-values of functional groups in enzymes: improper deductions from the pH-dependence of steady-state parameters. *CRC Crit Rev. Biochem.*, **4**, 165-173.
- [177] Dall'Acqua, W. & Carter, P. (2000) Substrate-assisted catalysis: molecular basis and biological significance. *Protein Sci.*, **9**, 1-9.
- [178] Brocchieri, L. & Karlin, S. (1994) Geometry of interplanar residue contacts in protein structures. *Proc. Natl. Acad. Sci. U. S. A.*, **91**, 9297-9301.
- [179] Karlin, S., Zuker, M., & Brocchieri, L. (1994) Measuring residue associations in protein structures. Possible implications for protein folding. *J. Mol. Biol.*, **239**, 227-248.
- [180] Hunter, C.A., Singh, J., & Thornton, J.M. (1991) Pi-pi interactions: the geometry and energetics of phenylalanine-phenylalanine interactions in proteins. *J. Mol. Biol.*, **218**, 837-846.
- [181] Tousignant, A. & Pelletier, J.N. (2004) Protein motions promote catalysis. *Chem. Biol.*, **11**, 1037-1042.
- [182] Antoniou, D., Caratzoulas, S., Kalyanaraman, C., Mincer, J.S., & Schwartz, S.D. (2002) Barrier passage and protein dynamics in enzymatically catalyzed reactions. *Eur. J. Biochem.*, **269**, 3103-3112.
- [183] Hammes-Schiffer, S. & Benkovic, S.J. (2006) Relating protein motion to catalysis. *Annu. Rev. Biochem.*, **75**, 519-541.

-
- [184] Daniel, R.M., Dunn, R.V., Finney, J.L., & Smith, J.C. (2003) The role of dynamics in enzyme activity. *Annu. Rev. Biophys. Biomol. Struct.*, **32**, 69-92.
- [185] Luo, J. & Bruice, T.C. (2004) Anticorrelated motions as a driving force in enzyme catalysis: the dehydrogenase reaction. *Proc. Natl. Acad. Sci. U. S. A.*, **101**, 13152-13156.
- [186] Fuxreiter, M., Magyar, C., Juhasz, T., Szeltner, Z., Polgar, L., & Simon, I. (2005) Flexibility of prolyl oligopeptidase: molecular dynamics and molecular framework analysis of the potential substrate pathways. *Proteins*, **60**, 504-512.
- [187] Sharma, V., Youngblood, B., & Reich, N. (2005) Residues distal from the active site that alter enzyme function in M.HhaI DNA cytosine methyltransferase. *J. Biomol. Struct. Dyn.*, **22**, 533-543.
- [188] Kaur, J. & Sharma, R. (2006) Directed evolution: an approach to engineer enzymes. *Crit Rev. Biotechnol.*, **26**, 165-199.
- [189] Pal, D. & Chakrabarti, P. (1998) Different types of interactions involving cysteine sulfhydryl group in proteins. *J. Biomol. Struct. Dyn.*, **15**, 1059-1072.
- [190] Edwards, P.D., Wolanin, D.J., Andisik, D.W., & Davis, M.W. (1995) Peptidyl alpha-ketoheterocyclic inhibitors of human neutrophil elastase. 2. Effect of varying the heterocyclic ring on in vitro potency. *J. Med. Chem.*, **38**, 76-85.
- [191] Kanai, K., Aranyi, P., Bocskei, Z., Ferenczy, G., Harmat, V., Simon, K., Batori, S., Naray-Szabo, G., & Hermeecz, I. (2008) Prolyl oligopeptidase inhibition by N-acyl-pro-pyrrolidine-type molecules. *J. Med. Chem.*, **51**, 7514-7522.
- [192] Taylor, P.J. & Wait, A.R. (1986) σ values for Heterocycles. *J. Chemistry society Perkin Trans.*, 1765-1770.
- [193] Cannon, W.R. & Benkovic, S.J. (1998) Solvation, reorganization energy, and biological catalysis. *J. Biol. Chem.*, **273**, 26257-26260.
- [194] Warshel, A., Aqvist, J., & Creighton, S. (1989) Enzymes work by solvation substitution rather than by desolvation. *Proc. Natl. Acad. Sci. U. S. A.*, **86**, 5820-5824.
- [195] Tsutsumi, S., Okonogi, T., Shibahara, S., Ohuchi, S., Hatsushiba, E., Patchett, A.A., & Christensen, B.G. (1994) Synthesis and structure-activity relationships of peptidyl alpha-keto heterocycles as novel inhibitors of prolyl endopeptidase. *J. Med. Chem.*, **37**, 3492-3502.
- [196] Baer, J.W. (2005) Struktur-Funktionsuntersuchungen von humaner Dipeptidylpeptidase IV und Prolylendopeptidase in Bezug auf die Hydrolyse von artifizialen und physiologischen Substraten. *Dissertation. Martin-Luther Universität Halle-Wittenberg*.
- [197] Kuhn, B., Hennig, M., & Mattei, P. (2007) Molecular recognition of ligands in dipeptidyl peptidase IV. *Curr. Top. Med. Chem.*, **7**, 609-619.
- [198] Schutkowski, M., Jakob, M., Landgraf, G., Born, I., Neubert, K., & Fischer, G. (1997) Probing substrate backbone function in prolyl oligopeptidase catalysis--large positional effects of peptide bond monothioxylation. *Eur. J. Biochem.*, **245**, 381-385.

6.0 Appendix.

All w/v and v/v were made with tridestillated water whether other is not stated.

6.1 Buffers and mediums.

6.1.1 Cloning

DNA Agarose gel electrophoresis

10X Running buffer

890mM Tris
20mM EDTA
890mM Boric acid

0.8% (w/v) Agarose gel in 1X Running buffer

LB-agar

5g/l sodium chloride
5g/l yeast extract
10g/l peptone
15g/l Agar
Autoclaved 21 minutes at 121°C

6.1.2 E. Coli expression.

LB medium

5g/l sodium chloride
5g/l yeast extract
10g/l peptone
titrated pH 7 in tridestillated water
Autoclaved 21 minutes at 121°C

Antibiotics

Chloramphenicol: In-culture solution: 30 µg/ml culture

Kanamycin: In-culture solution: 100µg/ml culture

6.1.3 Activity measurements.

PEP buffer

135.0mM Hepes
540.0mM NaCl
2.7mM EDTA
4.0mM DTT
0.03%(w/v) 35 BRIJ®
titrated at pH 7

6.1.4 Substrates and Inhibitors.

All substrates and inhibitors characterized within this work were synthesized respectively in the laboratories of peptide chemistry and medicinal chemistry of Probiobdrug AG. Only the AMC (7-Amido-4-methylcoumarin) was purchased to Bachem.

6.1.5 Protein purification.

IMAC chromatography

Regeneration buffers

Buffer A: Water

Buffer B: 100mM EDTA; pH 8

Buffer C: 100mM Nickel sulphate hexahydrate

Equilibration buffer: 50mM NaH₂PO₄/20mM Imidazol/1M NaCl; pH 7Elution buffer: 50mM NaH₂PO₄/500mM Imidazol/1M NaCl; pH 7Q sepharose chromatographyEquilibration buffer: 50mM NaH₂PO₄/1mM DTT; pH 7Elution buffer: 50mM NaH₂PO₄/1mM DTT /1M NaCl; pH 7Phenyl sepharose chromatographyEquilibration buffer: 50mM NaH₂PO₄/1mM DTT/ 30% w/v (NH₄)₂SO₄; pH 7Elution buffer: 50mM NaH₂PO₄/1mM DTT; pH 7

6.1.6 Protein characterization.

SDS-PAGE

10X Running buffer 10X

1.920M Glycine

0.250M Tris

0.034M SDS

Separating gel

2.8ml H₂O

2.8ml 1.5M Tris; pH 8.8

5.6ml Rotiophorese[®] 30 acrylamide

60µl Ammoniumpersulfate

225µl 10%(w/v) SDS

18ml Temed

Staking gel

5.6ml H₂O

2.8ml 0.5M Tris; pH 6.8

0.75ml Rotiophorese[®] 30 acrylamide

40µl Ammoniumpersulfate

125µl 10% (w/v) SDS

12µl Temed

Coomassie blue staining solution

10% (v/v) Acetic acid

40% (v/v) Methanol

40% (v/v) H₂O

0.25%(w/v) Bromophenol blue Na-salt

Coomassie blue distaining solution

10% (v/v) Acetic acid

40% (v/v) Methanol

40% (v/v) H₂O

6.1.7 MALDI-TOF-MS.

Matix solution

1%(w/v) α-cyano-4-hydroxycinnamic acid solved in 50% (v/v) Acetonitrile

Enzymatic Stop solution

0.1% (v/v) Trifluoroacetic acid; pH < 4

Zip-Tip_{C18}

Tip pre-washing acetonitrile.

Tip equilibration and unbound washing solution 0.1% (v/v) trifluoroacetic acid;
pH < 4
Elution matrix solution.

6.2 Mathematical equations.

$$A = \text{Log}(I_o/I) = \varepsilon cl \quad \text{equation 1}$$

{A} Absorbance; {Log(I_o/I)} Logarithm of the ratio of intensities of the sample incident and leaving light; {ε} Extinction coefficient constant (cm⁻¹M⁻¹); {c} Concentration (M); {l} Pathlength (cm)

$$V = V_{\max}[S]/(K_m + [S]) \quad \text{equation 2}$$

{V} Initial velocity (RFU/min); {V_{max}} Maximal initial velocity (RFU/min); {[S]} Substrate concentration (M) and {K_m} Michaelis-Menten constant (M)

$$V_{\max} = k_{\text{cat}} [E] \quad \text{equation 3}$$

{V_{max}} Maximal initial velocity (RFU/min); {k_{cat}} Turnover constant (s⁻¹); {[E]} Enzyme concentration (M)

$$V = V_{\max} [S] / (K_m (1+[I]/K_i) + [S]) \quad \text{equation 4}$$

{V} Initial velocity (RFU·min⁻¹); {V_{max}} Maximal initial velocity (RFU·min⁻¹); {[S]} Substrate concentration (M); {K_m} Michaelis-Menten constant (M); {[I]} Inhibitor concentration (M); {K_i} Inhibitor affinity constant (M)

$$K_i = IC_{50} / (1 + [S] / K_m) \quad \text{equation 5}$$

{K_i} Inhibitor affinity constant (M); {IC₅₀} Value of fifty percent of inhibition (M); {[S]} Substrate concentration (M); {K_m} Michaelis-Menten constant (M).

$$P = V_s t + (V_0 - V_s)(1 - e^{-k_{\text{obs}} t}) / k_{\text{obs}} \quad \text{equation 6}$$

{P} Products (M); {V_s} Steady-state velocity (M·s⁻¹); {t} Time (s); {V_o} Initial velocity (M·s⁻¹); {k_{obs}} Observed rate constant for the transition from initial to steady-state rates (s⁻¹)

$$k_{\text{obs}} = k_4 + k_3 [I] / (1 + [S] / K_m) \quad \text{equation 7}$$

{k_{obs}} Observed rate constant for the transition from initial to steady-state rates (s⁻¹); {k₃} Second order rate constants (s⁻¹·M⁻¹); {k₄} First order rate constants (s⁻¹); {[I]} Inhibitor concentration (M); {[S]} Substrate concentration (M); {K_m} Michaelis-Menten constant (M)

$$K_{\text{obs}} = k_{\text{off}} + k'_{\text{on}} [I] \quad \text{equation 8}$$

{K_{obs}} Observed rate constant for the transition from initial to steady-state rates (s⁻¹); {k'_{on}} Second order rate constants (s⁻¹·M⁻¹); {k_{off}} First order rate constants (s⁻¹); {[I]} Inhibitor concentration (M)

$$k_{\text{on}} = k'_{\text{on}} (1 + [S] / K_m) \quad \text{equation 9}$$

{k'_{on}} Second order rate constants (s⁻¹·M⁻¹); {k_{on}} Second order rate constants (s⁻¹ M⁻¹);
 {[S]} Substrate concentration (M); {K_m} Michaelis-Menten constant (M)

$$k_{\text{off}} = k_{\text{on}} K_i \text{ equation 10}$$

{k_{off}} First order rate constants (s⁻¹); {k_{on}} Second order rate constants (s⁻¹ M⁻¹);
 {K_i} Inhibitor affinity constant (M)

$$K = P \exp[-E_a/(RT)] \text{ equation 11}$$

{K} Rate constant (M⁻¹·s⁻¹); {P} Pre-exponential factor (M⁻¹·s⁻¹); {E_a} Activation energy (J·mol⁻¹); {R} Gas constant (8.3 J·K⁻¹ mol⁻¹); {T} Temperature (K)

$$k = \kappa (k_B T/h) K^\ddagger \text{ equation 12}$$

{k} Kinetic rate constant (s⁻¹); {κ} Transmission coefficient; {k_B} Boltzmann constant (1.38e-23 J·K⁻¹); {T} Temperature (K); {h} Planck constant (6.62e-34 J·s); {K[‡]} Equilibrium constant for the activated complex formation

$$K^\ddagger = \exp(-\Delta G^\ddagger/RT) \text{ equation 13}$$

{K[‡]} Equilibrium constant for the activated complex formation; {ΔG[‡]} Standard free energy (J·mol⁻¹); {R} Gas constant (8.3 J·K⁻¹·mol⁻¹); {T} Temperature (K)

$$\ln(k/T) = [\ln \kappa + \ln(k_B/h) + \Delta S^\ddagger/R] - \Delta H^\ddagger/(RT) \text{ equation 14}$$

$$\ln(k/T) = [\ln \kappa + \ln(k_B/h) + \Delta S^\ddagger/R] - \Delta H^\ddagger/(RT) \text{ equation 14}$$

{k} Kinetic rate constant (s⁻¹); {ΔS[‡]} Standard entropy (J·mol⁻¹·K⁻¹); {ΔH[‡]} Standard enthalpy (J·mol⁻¹); {ΔG[‡]} Standard free energy (J·mol⁻¹); {R} Gas constant (8.3 J·K⁻¹·mol⁻¹); {T} Temperature (K); {h} Planck constant (6.62e-34 J·s); {κ} Transmission coefficient; {k_B} Boltzmann constant (1.38e-23 J·K⁻¹)

$$m/z = 2eUt^2/L^2 \text{ equation 15}$$

{m} Mass of the ions (Da); {z} Charge number; {e} Elemental charge (1.6e-19C);
 {U} Voltage (V); {t} Time of flight (s); {L} Distance of flight free of electric field (m)

$$k_{\text{cat}}/K_m = k_{\text{cat}}/K_m [1/(1+10^{\text{pK}1-\text{pH}}+10^{\text{pH}-\text{pK}2})] \text{ equation 16}$$

$$k_{\text{cat}}/K_m = k_{\text{cat}}/K_m [1/(1+10^{\text{pK}1-\text{pH}}+10^{\text{pK}1+\text{pK}2-2\text{pH}}+10^{\text{pH}-\text{pK}3})] \text{ equation 17}$$

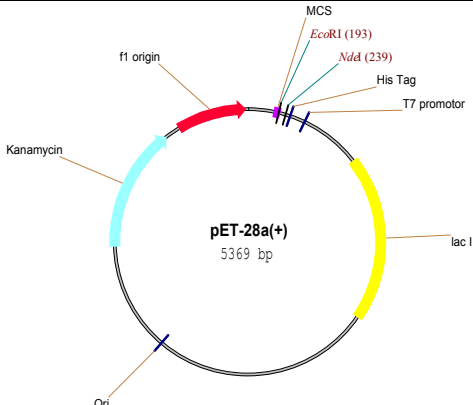
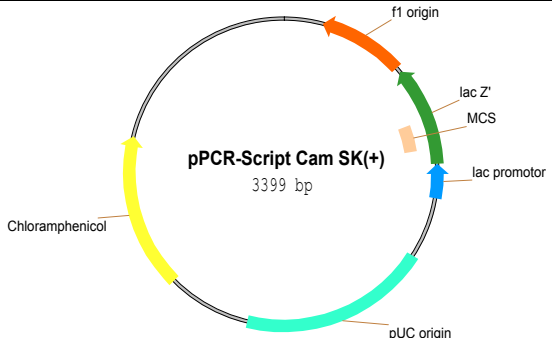
$$k_{\text{cat}}/K_m = k_{\text{cat}}/K_{m1} [1/(1+10^{\text{pK}1-\text{pH}}+10^{\text{pH}-\text{pK}2})] + k_{\text{cat}}/K_{m2} [1/(1+10^{\text{pK}2-\text{pH}}+10^{\text{pH}-\text{pK}3})] \text{ equation 18}$$

{k_{cat}/K_m} specificity constant (M⁻¹sec⁻¹); {pK_x} pK_a of the catalytically relevant residues; {pH} pH

6.3 Chemicals.

Sodium Chloride (Roth); Yeast extract (Duchefa); Peptone (Duchefa); Kanamycin (Sigma); Chloramphenicol (Sigma); 35 BRIJ[®] (Sigma); DTT (Roth); Hepes (Roth); EDTA (Sigma); Ammoniumpersulfate (BioRad), Roptiphorese[®] 30 Acrylamide (Roth); SDS (Roth); Temed (Roth); α -cyano-4-hydroxycinnamic acid (Aldrich); Agar (Roth); Agarose (PeqLab); Tris (Roth); Boric acid (Roth); Agar (Roth); Glycine (Roth); Acetic acid (Roth); Methanol (Roth); Ethanol (Roth); Trifluoroacetic (Merck); Acetonitrile (Merck); Sodium dihydrogenphosphate dihydrate (Roth), Nickel sulfate hexahydrate (Merck); Imidazol (Merck); Ammonium sulfate (Merck); DMSO (Fluka); DMF (Fluka) Bromophenol blue Na-salt (Serva); 7-Amido-4-methylcoumarin (Bachem); paranitro aniline (Bachem); Bradford reagent (Sigma-Aldrich); TRIZOL (GibcoBRL); X-gal (Duchefa), MES (Sigma); N-Ethylmorpholine (Fluka).

6.4 Vectors.

Vector	Plasmid features
 <p>pET-28a(+) 5369 bp</p>	<p>Size: 5.4kba Resistance: Kanamycin Cloning sites: EcoR I and Nde I Type: Expression vector Promotor: Lac I Provider: Novagen</p>
 <p>pPCR-Script Cam SK(+) 3399 bp</p>	<p>Size: 3.4kba Resistance: Chloramphenicol Cloning site: Srf I Type: Sub-cloning vector Promotor: Lac I Provider: Stratagene</p>

Tab 39 Summary table of the plasmids used for the cloning and expression of the human prolyl oligopeptidase coding sequence. On top, the schematic representation of the vector pET-28a(+). On the bottom, schematic representation of the cloning vector pPCR-Script Cam(+).

6.5 Chromatograms of the prolyl oligopeptidase purification.

Representative chromatograms of the prolyl oligopeptidase purification

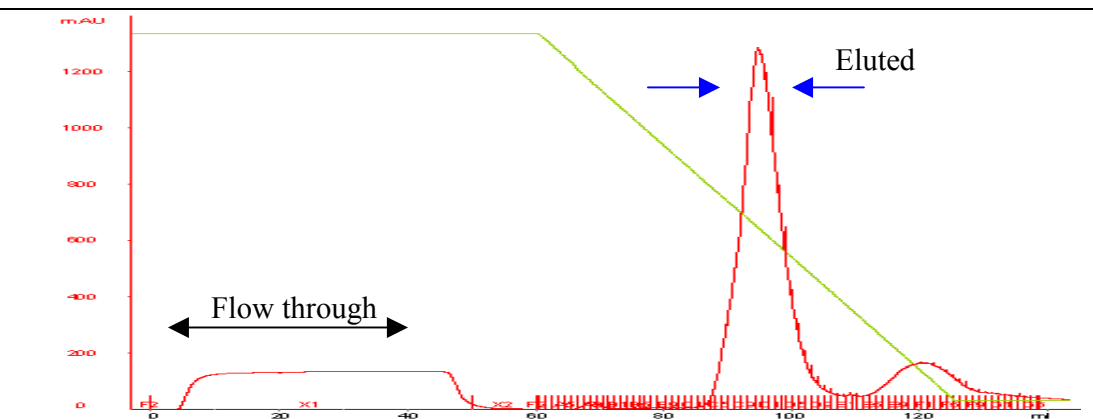
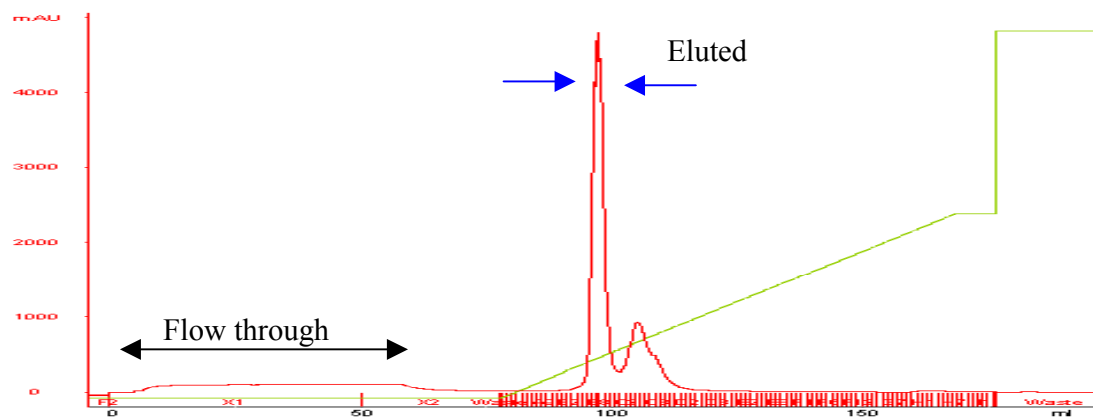
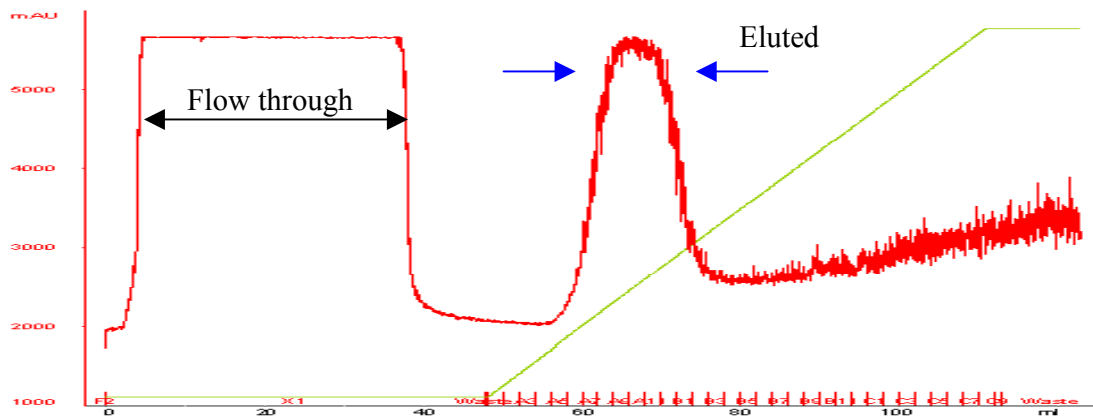


Table 40 Representative chromatograms obtained with the purification of the overexpressed recombinant human prolyl oligopeptidase. On top, chromatogram of a chelating sepharose, on the middle, a chromatogram of a Q sepharose and, on the bottom, a chromatogram of a phenyl sepharose. The profiles show increase of absorbance measured at 220nm. The main peaks, marked with blue arrows, are indicating the elution of the purified target protein. Flow through is stated as not adsorbed protein.

6.6 List of oligoprimers.

List of prolyl oligopeptidase gene specific primers		
Feature	Name	sequence
Cloning	hPEPEcoRI3'	5'AGAATTCATGGAATCCAGTCGACGTTTC3'
Cloning	hPEPNdeI5'	5'CTAGCTAGCATGCTGTCTTTCCAGTACC3'
mutagenesis	PEP-W595Y5'	5'TCGGCCATGCTTACACCACTG 3'
mutagenesis	PEP-W595Y3'	5'CAGTGGTGTAAGCATGGCCGA 3'
mutagenesis	PEP-W595F5'	5'TCGGCCATGCTTTACCACTG3'
mutagenesis	PEP-W595F3'	5'CAGTGGTGAAAGCATGGCCGA3'
mutagenesis	PEP-W595A5'	5'TCGGCCATGCTGCCACCAC3'
mutagenesis	PEP-W595A3'	5'GTGGTGGCAGCATGGCCGA3'
mutagenesis	PEP-R643K5'	5'TGACCATGATGACAAAAGTGGTCCC3'
mutagenesis	PEP-R643K3'	5'GGGACCACTTTGTCATCATGGTCA3'
mutagenesis	PEP-R643A5'	5'TGACCATGATGACGCCGTGGTCCC3'
mutagenesis	PEP-R643A3'	5'GGGACCACGGCGTCATCATGGTCA3'
mutagenesis	PEP-M235I5'	5'TCCTGATGAACCTAAATGGATCGGTG3'
mutagenesis	PEP-M235I3'	5'CACCGATCCATTTAGGTTTCATCAGGA3'
mutagenesis	PEP-M235A5'	5'ATGAACCTAAATGGGCCGGTGG3'
mutagenesis	PEP-M235A3'	5'CCACCGGCCCATTTAGGTTTCAT3'
mutagenesis	PEP-F173A5'	5'TGCTTGAAAGAGTCAAGGCCAGCTG3'
mutagenesis	PEP-F173A3'	5'CAGCTGGCCTTGACTCTTTCAAGCA3'
mutagenesis	PEP-C255A5'	5'ATCAATAAGGGAAGGAGCTGATCCAGTAAACC3'
mutagenesis	PEP-C255A3'	5'GGTTTACTGGATCAGCTCCTTCCCTTATTGAT3'

Table 41 Table that lists the sequences of the different oligoprimers used for the cloning and the site directed mutagenesis approaches.

6.7 Molecular structure of the ammonium methyl ketone analogue molecules.

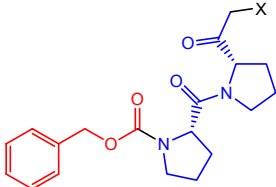
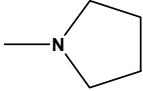
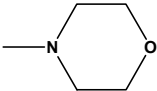
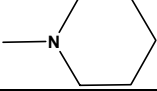
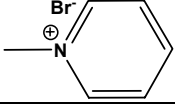
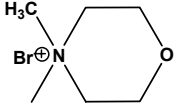
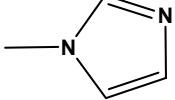
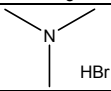
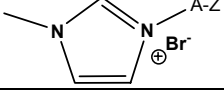
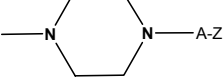
Ammonium methyl ketone molecules	
	
Code	X moiety
AH683	-N ⁺ Me ₃ Br ⁻
AH684	
AH685	-NMe ₂
AH686	
AH687	
AH688	
AH673	-OH
AH689	
AH690-3	
AH681	-N ⁺ Et ₃ Br ⁻
AH685	
AH690-4	
AH691	

Table 42 Derivatization of the ammonium methyl ketone inhibitor, AMK, scaffold. On top the main core molecular structure of the inhibitors. In red the benzyloxycarbonyl (Z) and in blue the L-Pro-L-Pro-CH₂ sequence (A). It follows the molecular structures (X) of the different moieties used for the derivatization. All molecules were synthesized in the medicinal chemistry department of Probiobdrug AG (Germany). X stands in AH683 for methyl ammonium; in AH684 for pyrrolidine; in AH686 for morpholine; in AH687 for piperidine; in AH688 for pyridinium; in AH689 for methyl morpholinium; in AH690-3 for imidazole; in AH681 for ethyl ammonium; in AH690-4 for imidazolium and in AH691 in piperazine. All compounds were generated as salt form.

6.8 Molecular structure of the heteroaryl ketone analogue molecules.

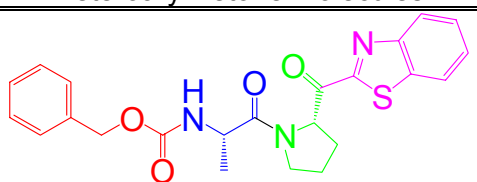
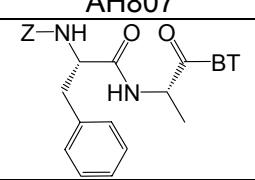
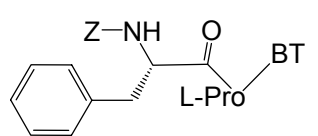
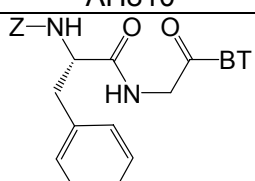
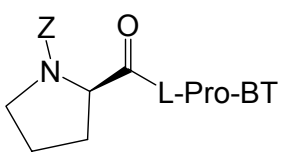
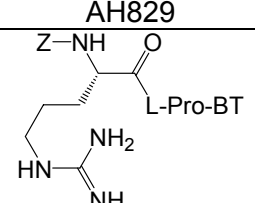
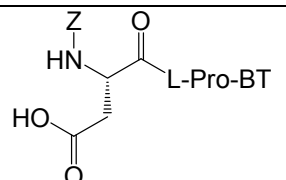
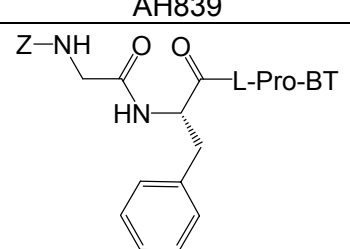
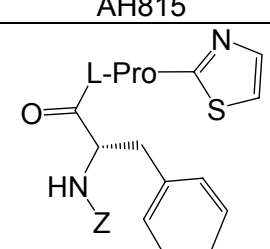
Heteroaryl ketone molecules	
	
AH807	ZW215
	
AH810	AH817
	
AH829	AH831
	
AH839	AH815
	
AH851	
Z-L-Pro-BT	

Table 43 Derivatization of the heteroaryl ketone, HAK, scaffold. On top the core molecular structure of the inhibitor AJN118. In red the benzyloxycarbonyl moiety (Z), in blue L-Alanine (L-Ala), in green L-Proline (L-Pro), and in pink benzothiazole (BT). AH807 Z-L-Phe-L-Ala-BT; ZW215 Z-L-Phe-L-Pro-BT; AH810 Z-L-Phe-Gly-BT; AH817 Z-L-Pro-L-Pro-BT; AH829 Z-L-Arg-L-Pro-BT; AH831 Z-L-Asp-L-Pro-BT; AH839 Z-L-Gly-L-Phe-L-Pro-BT; AH815 Z-L-Gly-L-Phe-L-Pro-Thiazole; AH851 Z-L-Pro-BT.

6.9 Molecular structure of the diketone analogue molecules.

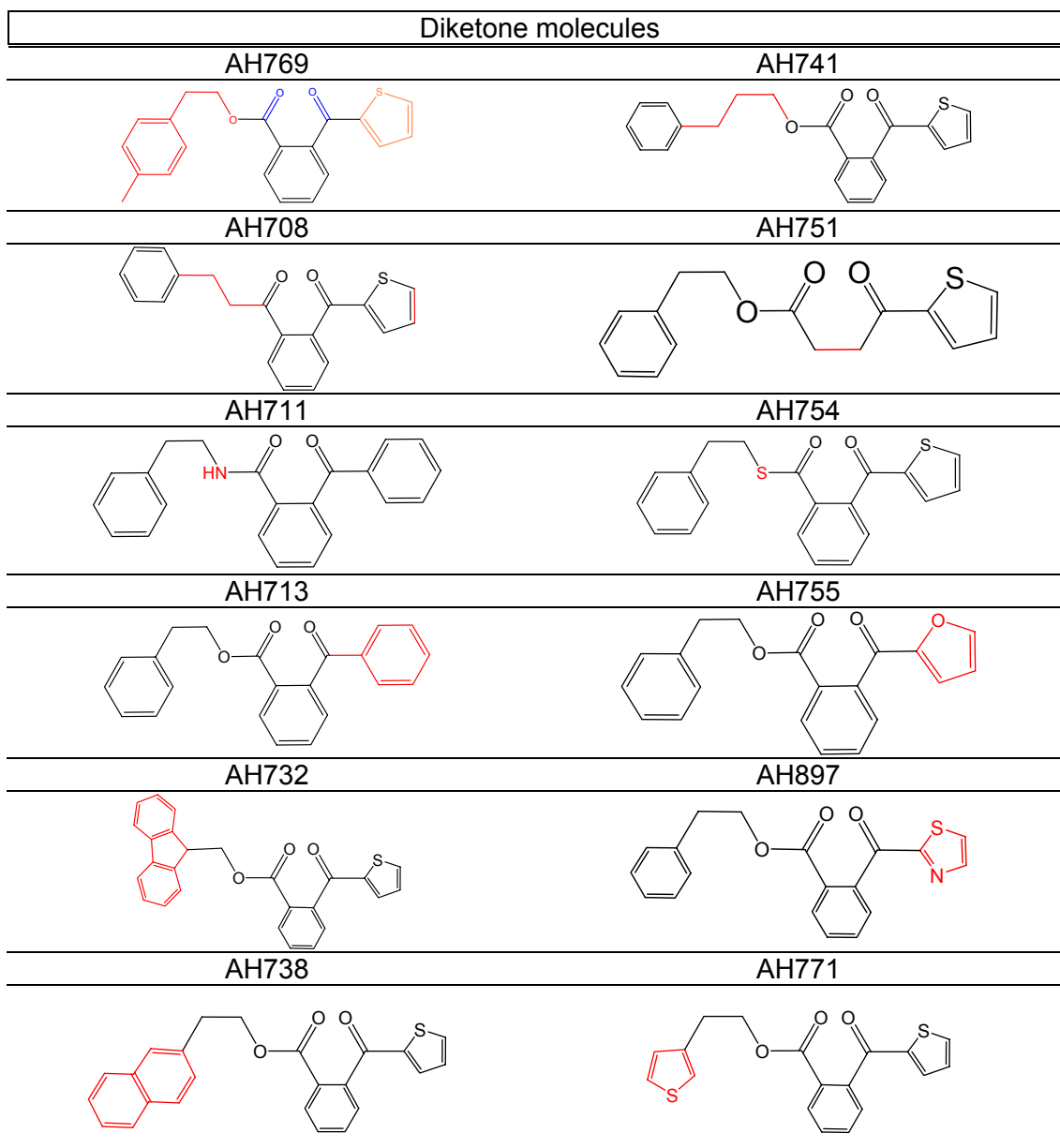


Table 44 Derivatization of the diketone, DK/AH769, inhibitor scaffold. Highlighted in red the moiety object of the derivatization. All molecules were synthesized in the medicinal chemistry department of Probiobdrug AG (Germany). AH707 2-(Phenyl-ethyl-oxycarbonyl)-phenylthienon; AH741 2-(Phenyl-propyl-oxycarbonyl)-phenylthienon; AH708 2-(Phenyl-propyl-carbonyl)-phenylthienon; AH751 Phenethyl-4-oxo-4-(thiophen-2-yl)butanoate; AH711 2-(Phenylethyl-amincarbonyl)-benzophenon; AH754 2-(Phenyl-ethyl-thiocarbonyl)-phenylthienon; AH713 2-(Phenyl-ethyl-oxycarbonyl)-benzophenon; AH755 2-(Phenyl-ethyl-oxycarbonyl)-(furan-2-yl)(phenyl)methanone; AH732 2-(Fluorenyl-methyl-oxycarbonyl)-phenylthienon; AH897 2-(Phenyl-ethyl-oxycarbonyl)-phenyl(thiazol-2-yl)methanone; AH738 2-(2-Naphthenyl-ethyl-oxycarbonyl)-phenylthienon; AH771 2-(3-Thiophenyl-ethyl-oxycarbonyl)-phenylthienon.

6.10 Miscellaneous.

Devices	Manufacturer
Avanti J-20 and Avanti J-30I	Beckman
Agarose gels viewer UV-system	iNTAS
Äktapurifier	Amershan Biosciences
Autoclave Hiclave HV-110L	HMC
Biodoc-it Imagin System	UVP
DNA-Gelelectrophoresis GEB1A-UVT	Hybaid AGS
Electrophoresis powerstation E143	CONSORT
Electrophoresis powerstation Pac 300	BioRad
Fluorescence 96-well plate reader Fluostar Optima	BMG Labtech
French Press	Spectronic instruments
Gelectrophoresis Mini-Protean 2-D Cell	BioRad
Ice machine	Ziegler
MALDI-TOF-MS Voyager DE™ PRO	Applied biosystems
PCR thermocycler Mastercycler gradient	Eppendorf
PCR thermocycler Sprint	Hybaid AGS
pH-meter MP220	Mettler Toledo
Plate Incubator B15	Heraeus
Shacker incubator-HT Unitron	INFORS-HT
Shacker incubator-TH15/-TH30	E. Bühler
Spectrophotometer SmartSpec 3000	Bio-Rad
Spectropolarimeter Jasco J710	Jasco
Tabletop centrifuge Allegra X-22R	Beckman
Tabletop centrifuge Biofuge fresco	Heraeus
Tabletop centrifuge Biofuge pico	Heraeus
Thermomixer	Eppendorf
Thermomixer compact	Eppendorf
Vacuum pump	KnF neuberger
Vortex Genie 2	Scientific industries
Water purifier PURELAB PLUS UV	USF SERAL
Waterbath P5	HAAKE

Enzyme	Provider
EcoRI endonuclease	New England Biolabs
MMLV reverse transcriptase Rnase H mutant	Invitrogen
NedI endonuclease	New England Biolabs
Pfu DNA polymerase	Promega
Recombinant human prolyl oligopeptidase and its variants	Probiobdrug AG
SrfI endonuclease	Stratagene
Taq DNA polymerase	Promega
T4 DNA ligase	Promega

Molecular Biology Kits	Provider
JET quick DNA Clean-up Spin kit	Genomed
JET quick DNA Gelextraction Spin kit	Genomed
JET quick DNA PCR purification Spin kit	Genomed
JET quick DNA Plasmid Miniprep Spin kit	Genomed
PCR-script™ Cam cloning kit	Stratagene
Superscript™ II Reverse Transcriptase	Invitrogen
TRIzol® Reagent	Invitrogen/GibcoBRL

Computer software	Provider
Chem office 2004	Scientific solutions SA
Grafit 4.03	Erithacus software
Maldi protein mass analysis GPMW	Lighthouse Data
Office suite	Microsoft
Prism 3.02	Graphpad
Pymol	DeLano scientific
Reference manager 10	Adept scientific
Vector NTI suite 6	Infomax

Miscellaneous laboratory material	Manufacturer
C18-Zip-Tips	Millipore
Dialysis membrane Visking 14kDa cut -off	Roth
Filtration microfiber filters	Whatman
Filtration nitrocellulose membrane 0.8 μ M	Millipore
ViVASPIN 20 ml concentrator 30kDa cut-off	Vivascience
96 well plates (Dabcyl/Edans and pNA derivatives)	BMG Labtechnologies
96 well plates (AMC derivatives)	NUNC

List of Figures and Tables

Figure 1 Sagittal section of a human brain.....	8
Figure 2 Representation of the three dimensional structure of the porcine prolyl oligopeptidase.....	10
Figure 3 Schematic representation of the catalytic mechanism followed by prolyl oligopeptidase.....	13
Figure 4 Cellular pathways where prolyl oligopeptidase have been indicated to be implicated.....	18
Figure 5 SDS-PAGE gel of the soluble fraction of a prolyl oligopeptidase expression.....	40
Figure 6 SDS-PAGE gel after performing the purification of the recombinant human prolyl oligopeptidase according to the established protocol detailed in table 11.....	42
Figure 7 Eyring and Arrhenius plots of the PEP catalyzed substrate hydrolysis.....	46
Figure 8 Porcine prolyl oligopeptidase active site related residues on stick representation from the published crystal structure with PDB id 1u0o.....	48
Figure 9 MALDI-TOF-MS spectra of the time depending hydrolysis of the peptide VTTACHEF with prolyl oligopeptidase.....	64
Figure 10 MALDI-TOF-MS spectra of the time depending hydrolysis of the variants of the lead peptide DLPVKRRA by prolyl oligopeptidase.....	65
Figure 11 MALDI-TOF-MS spectra of the time depending cleavage of the angiotensin peptide variants.....	67
Figure 12 SDS-PAGES of the different variants of prolyl oligopeptidase purified within this work.....	68
Figure 13 Plots of the prolyl oligopeptidase hydrolysis initial rates against substrate concentration of the FRET derivatives.....	75
Figure 14 pH-rate profiles of the prolyl oligopeptidase hydrolysis of AlaAlaProAMC and Angiotensin I.....	78
Figure 15 Representative MALDI-TOF-MS spectra of the hydrolysis of the Neuropeptide Y variant 1-30NPY.....	95
Table 1 Table summarizing the molecular structure of the most relevant synthetic prolyl oligopeptidase inhibitors.....	21
Table 2 Synthesis of the primary cDNA pool.....	23
Table 3 Amplification of the coding sequence of the PREP gene by PCR.....	24
Table 4 Schematic description of the established protocol for DNA precipitation.....	24
Table 5 Cloning reaction performed following the recommendations indicated in the protocol of the pPCR-Script Cam cloning Kit.....	25
Table 6 Plasmid restriction reaction used for the direct cloning of the prolyl oligopeptidase coding sequence into the commercial vector pET28a(+).	25
Table 7 Ligation reaction of the DNA fragments for the direct cloning of the prolyl oligopeptidase coding sequence into the commercial vector pET28a(+).	26
Table 8 Summary of the basic parameters established for the performance of the IMAC chromatography.....	28
Table 9 Summary of the basic parameters established for the performance of the Q sepharose chromatography.....	29
Table 10 Summary of the basic parameters established for the performance of the phenyl sepharose chromatography.....	29
Table 11 Purification table of the isolation of the recombinant prolyl oligopeptidase expressed in <i>Escherichia coli</i>	42
Table 12 Kinetic parameters of the recombinant human prolyl oligopeptidase determined with the AMC derivatives.....	43
Table 13 Kinetic parameters of the wild type recombinant human prolyl oligopeptidase determined with internally quenched substrates.....	44
Table 14 Kinetic parameters of the recombinant wild type human prolyl oligopeptidase determined with internally quenched NAP based substrates.....	45

List of Figures and Tables

Table 15-A Summary table of the thermodynamic parameters inferred from the Eyring plots shown in figure 7.....	46
Table 15-B Summary table of the parameters inferred from the Arrhenius plots shown in figure 7.....	47
Table 16 Summary table of the parameters obtained from the measured pH-dependencies of the catalyzed turnover of the indicated substrates.....	47
Table 17 Kinetic parameters of the recombinant human R643A prolyl oligopeptidase variant with AMC derivatives.....	49
Table 18 Kinetic parameters of the recombinant human R643K prolyl oligopeptidase variant with AMC derivatives.....	49
Table 19 Kinetic parameters of the recombinant human W595A prolyl oligopeptidase variant with AMC derivatives.....	50
Table 20 Kinetic parameters of the recombinant human W595F prolyl oligopeptidase variant with AMC derivatives.....	51
Table 21 Kinetic parameters of the recombinant human W595Y prolyl oligopeptidase variant with AMC derivatives.....	52
Table 22 Kinetic parameters of the recombinant human F173A prolyl oligopeptidase variant with AMC derivatives.....	53
Table 23 Kinetic parameters of the recombinant human M235A prolyl oligopeptidase variant with AMC derivatives.....	54
Table 24 Kinetic parameters of the recombinant human M235I prolyl oligopeptidase variant with AMC derivatives.....	55
Table 25 Kinetic parameters of the recombinant human C255A prolyl oligopeptidase variant with AMC derivatives.....	56
Table 26 On the table's head the molecular structure of the ammonium methyl ketone inhibitor, AMK, is shown.....	56
Table 27 On the table's head the molecular structure of the heteroarylketone inhibitor, HAK, is shown.....	57
Table 28 On the table's head the molecular structure of the diketone inhibitor, DK, is shown.....	58
Table 29 Constants of the PEP-inhibition determined with different ammonium methyl ketone derivatives.....	59
Table 30 Constants of the PEP-inhibition determined with different heteroaryl ketone derivatives.....	59
Table 31 Constants of the PEP-inhibition determined with different diketone inhibitor derivatives.....	60
Table 32 Inhibition constants of the PEP-inhibition determined with different diketone Slow-tight binding inhibitor	61
Table 33 Summary table of the cleavage pattern of the Neuropeptide Y peptide variants by prolyl oligopeptidase.....	62
Table 34 Summary table of the cleavage pattern of the Humanin peptide variants, HN, by prolyl oligopeptidase.....	63
Table 35 Summary table of the cleavage pattern of the Substance P peptide variants, P4C-SP, by prolyl oligopeptidase.....	63
Table 36 Summary table of the hydrolysis pattern of the Humanin variants, 13-24HN, 15-24HN, 17-24HN, by prolyl oligopeptidase.....	64
Table 37 Summary table of the hydrolysis pattern of the variants of the lead peptide Angiotensin II, DRVYIHPF	66
Table 38 Kinetic parameters obtained with the prolyl oligopeptidase hydrolysis of the chromogenic substrate Z-GlyPro-pNA.....	69
Table 39 Summary table of the plasmids used for the cloning and expression of the human prolyl oligopeptidase coding sequence.....	120
Table 40 Representative chromatograms obtained with the purification of the overexpressed recombinant human prolyl oligopeptidase.....	121

List of Figures and Tables

Table 41 Table that lists the sequences of the different oligoprimers used for the cloning and the site directed mutagenesis approaches.....	122
Table 42 Derivatization of the ammonium methyl ketone inhibitor, AMK, scaffold....	123
Table 43 Derivatization of the heteroaryl ketone, HAK, scaffold.....	124
Table 44 Derivatization of the diketone, DK/AH769, inhibitor scaffold.....	125
Scheme 1 Schematic depiction of the catalytic mechanism followed by prolyl oligopeptidase.....	31
Scheme 2 Representation of the binding mechanism of a competitive inhibitor to an enzyme in presence of the substrate.....	33
Scheme 3 Formulation of the Michaelis-Menten steady-state constants as function of the single rate limiting constants of the reaction described in scheme 1.....	70

List of publications.

Manuscript: Subcellular localization suggests novel functions for prolyl endopeptidase in protein secretion Schulz, I., Zeitschel, U., Rudolph, T., Ruiz-Carrillo, D., Rahfeld, J.U., Gerhartz, B., Bigl, V., Demuth, H.U., & Rossner, S. (2005). *J. Neurochem.*, **94**, 970-979.

Poster: Prolyl endopeptidase cleaves the apoptosis rescue peptide humanin and exhibits an unknown post-cysteine cleavage specificity Bar, J.W., Rahfeld, J.U., Schulz, I., Gans, K., Ruiz-Carrillo, D., Manhart, S., Rosche, F., & Demuth, H.U. (2006). *Adv. Exp. Med. Biol.*, **575**, 103-108.

Poster: Kinetic Mapping of the Active Site of Prolyl Oligopeptidase David Ruiz Carrillo, Jens-Ulrich Rahfeld, Andre Niestroj, Nadine Jänckel, Raik Wolf, Susanne Manhart and Hans-Ulrich Demuth. 3rd International Conference on Dipeptidyl Peptidase and Related Proteins Antwerp, Belgium, April 23-25, 2008.

Poster: Structural characterization of the bacterial glutaminyl cyclase from *Zymomonas mobilis* Ruiz Carrillo D., Parthier C., Stelter M., Grandke J., Jaenckel N., Schilling S., Neumann P., Demuth H-U., Stubbs M.T., Rahfeld J., *Acta Cryst.* (2008) A64 C379-380.

Poster: Structural examination of two different glutaminyl cyclases, a mammal from mouse and a bacterial from *Myxococcus xanthus*. Ruiz Carrillo D., Parthier C., Jänckel N., Böhme M., Wermann., Schilling S., Demuth H-U., Stubbs M-T., Rahfeld J-U. VIII European symposium of the Protein Society June 14-18, P372 (2009).

Manuscript: Kinetic and structural characterization of the bacterial glutaminyl cyclases from *Zymomonas mobilis* and *Myxococcus xanthus*. Ruiz Carrillo D., Parthier P., Stelter M., Jänckel N., Grandke J., Schilling S., Neumann P., Wolf R., Demuth¹ H-U., Stubbs M-T. and Rahfeld J-U. Submitted to the Journal of structural Biology (2009).

Oral Presentations: Winter schools Proteases and their inhibitors in Tiers, 2006 to 2009 (Italy).

Acknowledgments

In first place i would like thank Prof. Dr. H.-U. Demuth and PD Dr. K. Glund for giving me the opportunity to carry out the theme of my PhD work at Probiodrug AG.

I want as well to express my gratitude to Prof. Dr. M. T. Stubbs for his supervision of my PhD work in the Halle-Wittenberg Martin Luther University and for the friendly and helpful collaboration i found in his working group, specially on Dr. Christoph Partier.

I want to sincerely thank my direct supervisor and mentor at Probiodrug AG Dr. J.-U. Rahfeld for his support on the daily laboratory work and his constant attendance for constructive discussions.

In the medicinal chemistry department of Probiodrug AG i want to express my gratitude to Dr. A.J. Niestroj for the synthesis of the different inhibitors and for the fruitful discussions.

In the mass spectrometry department of Probiodrug AG i would like to thank Dr. R. Wolf for the invaluable support on the measurements performed with the MALDI-TOF-MS.

I want sincerely to thank in the cell culture department of Probiodrug AG Dr. I. Schulz for the friendly attendance for constructive discussions about prolyl oligopeptidase.

In the peptide chemistry department of Probiodrug AG i would specially like to thank Dr. S. Manhart and H.-H. Ludwig for the supply of all peptide derivatives.

In the molecular biology department of Probiodrug AG i would like to warmly thank N. Jänckel for her professionalism. As well, i would like to thank specially L. Wagner for her incessant and friendly support in many different aspects of my work and my life. As well, I want to thank sincerily S.Treichel for her indispensable support in the cloning work. In addition, i would not like to forget to thank the rest of the "Mobi" group for the friendly working atmosphere.

Also, i want to thank the rest of Probiodrug AG co-workers for the helpful and friendly working atmosphere they offered me.

Finalmente quisiera dar las gracias a mi esposa Jialing, a mis padres y a toda mi familia por su constante derroche de amor que siempre hizo que todo tuviera sentido.

Erklärung

Hiermit erkläre ich, dass ich die vorliegende Arbeit selbständig und ohne fremde Hilfe verfasst, andere als die angegebenen Quellen und Hilfsmittel nicht benutzt, und die den benutzten Werken wörtlich oder inhaltlich entnommenen Stellen als solche kenntlich gemacht habe.

Declaration

I hereby declare the present thesis to be written independently without external assistance other than the sources and aids being cited in this dissertation. Therefore any extracts of external works used literally or figuratively in the present thesis are outlined and cited accordingly.

David Ruiz Carrillo
Halle an der Saale
June 30 2009

Biography

Name	David Ruiz Carrillo
Date of birth	May the 17 th , 1974
Place of birth	Figueres (Spain)
Status	Married
1979 – 1990	Primary school at “Col.legi públic Pompeu Fabra”, Llançà (Spain)
1990 – 1995	Secondary school at “Institut IES Narcís Monturiol”, Figueres (Spain)
1995 – 1996	Year of preparation for university studies at “ Institut IES Ramón Muntaner” Figueres (Spain)
1996 - 1999	Six semesters of chemistry at University of Girona, Girona (Spain)
1999 - 2001	Four semesters of biochemistry at University Complutense of Madrid, Madrid (Spain)
2001	Graduated in Biochemistry by the University Complutense of Madrid
2002 to date	Research associate in the molecular biology department of Probiodrug AG and PhD applicant in the Martin-Luther University Halle-Wittenberg, Halle an der Saale (Germany)